Accurate Predictions of Molecular Structures and Properties

by

Jing Kong

Submitted in partial fulfilment of the requirements

for the degree of Doctor of Philosophy

at

Dalhousie University

Department of Chemistry

Halifax, Nova Scotia

May, 1996

ISBN 0-612-15970-1

Canada

Name Jing Kong

Dissertation Abstracts International and *Masters Abstracts International* are arranged by broad, general subject categories. Please select the one subject which most nearly describes the content of your dissertation or thesis. Enter the corresponding four-digit code in the spaces provided.

Physical Chemistry
SUBJECT TERM

0494
SUBJECT CODE

UMI

Subject Categories

THE HUMANITIES AND SOCIAL SCIENCES

COMMUNICATIONS AND THE ARTS
Architecture 0729
Art History 0377
Cinema 0900
Dance 0378
Fine Arts 0357
Information Science 0723
Journalism 0391
Library Science 0399
Mass Communications 0708
Music 0413
Speech Communication 0459
Theater 0465

EDUCATION
General 0515
Administration 0514
Adult and Continuing 0516
Agricultural 0517
Art 0273
Bilingual and Multicultural 0282
Business 0688
Community College 0275
Curriculum and Instruction 0727
Early Childhood 0518
Elementary 0524
Finance 0277
Guidance and Counseling 0519
Health 0680
Higher 0745
History of 0520
Home Economics 0278
Industrial 0521
Language and Literature 0279
Mathematics 0280
Music 0522
Philosophy of 0998
Physical 0523
Psychology 0525
Reading 0535
Religious 0527
Sciences 0714
Secondary 0533
Social Sciences 0534
Sociology of 0340
Special 0529
Teacher Training 0530
Technology 0710
Tests and Measurements 0288
Vocational 0747

LANGUAGE, LITERATURE AND LINGUISTICS
Language
- General 0679
- Ancient 0289
- Linguistics 0290
- Modern 0291

Literature
- General 0401
- Classical 0294
- Comparative 0295
- Medieval 0297
- Modern 0298
- African 0316
- American 0591
- Asian 0305
- Canadian (English) 0352
- Canadian (French) 0355
- English 0593
- Germanic 0311
- Latin American 0312
- Middle Eastern 0315
- Romance 0313
- Slavic and East European 0314

PHILOSOPHY, RELIGION AND THEOLOGY
Philosophy 0422
Religion
- General 0318
- Biblical Studies 0321
- Clergy 0319
- History of 0320
- Philosophy of 0322

Theology 0469

SOCIAL SCIENCES
American Studies 0323
Anthropology
- Archaeology 0324
- Cultural 0326
- Physical 0327

Business Administration
- General 0310
- Accounting 0272
- Banking 0770
- Management 0454
- Marketing 0338

Canadian Studies 0385
Economics
- General 0501
- Agricultural 0503
- Commerce-Business 0505
- Finance 0508
- History 0509
- Labor 0510
- Theory 0511

Folklore 0358
Geography 0366
Gerontology 0351
History
- General 0578
- Ancient 0579
- Medieval 0581
- Modern 0582
- Black 0328
- African 0331
- Asia, Australia and Oceania 0332
- Canadian 0334
- European 0335
- Latin American 0336
- Middle Eastern 0333
- United States 0337

History of Science 0585
Law 0398
Political Science
- General 0615
- International Law and Relations 0616
- Public Administration 0617

Recreation 0814
Social Work 0452
Sociology
- General 0626
- Criminology and Penology 0627
- Demography 0938
- Ethnic and Racial Studies 0631
- Individual and Family Studies 0628
- Industrial and Labor Relations 0629
- Public and Social Welfare 0630
- Social Structure and Development 0700
- Theory and Methods 0344

Transportation 0709
Urban and Regional Planning 0999
Women's Studies 0453

THE SCIENCES AND ENGINEERING

BIOLOGICAL SCIENCES
Agriculture
- General 0473
- Agronomy 0285
- Animal Culture and Nutrition 0475
- Animal Pathology 0476
- Food Science and Technology 0359
- Forestry and Wildlife 0478
- Plant Culture 0479
- Plant Pathology 0480
- Plant Physiology 0817
- Range Management 0777
- Wood Technology 0746

Biology
- General 0306
- Anatomy 0287
- Biostatistics 0308
- Botany 0309
- Cell 0379
- Ecology 0329
- Entomology 0353
- Genetics 0369
- Limnology 0793
- Microbiology 0410
- Molecular 0307
- Neuroscience 0317
- Oceanography 0416
- Physiology 0433
- Radiation 0821
- Veterinary Science 0778
- Zoology 0472

Biophysics
- General 0786
- Medical 0760

EARTH SCIENCES
Biogeochemistry 0425
Geochemistry 0996
Geodesy 0370
Geology 0372
Geophysics 0373
Hydrology 0388
Mineralogy 0411
Paleobotany 0345
Paleoecology 0426
Paleontology 0418
Paleozoology 0985
Palynology 0427
Physical Geography 0368
Physical Oceanography 0415

HEALTH AND ENVIRONMENTAL SCIENCES
Environmental Sciences 0768
Health Sciences
- General 0566
- Audiology 0300
- Chemotherapy 0992
- Dentistry 0567
- Education 0350
- Hospital Management 0769
- Human Development 0758
- Immunology 0982
- Medicine and Surgery 0564
- Mental Health 0347
- Nursing 0569
- Nutrition 0570
- Obstetrics and Gynecology 0380
- Occupational Health and Therapy 0354
- Ophthalmology 0381
- Pathology 0571
- Pharmacology 0419
- Pharmacy 0572
- Physical Therapy 0382
- Public Health 0573
- Radiology 0574
- Recreation 0575
- Speech Pathology 0460
- Toxicology 0383

Home Economics 0386

PHYSICAL SCIENCES
Pure Sciences
Chemistry
- General 0485
- Agricultural 0749
- Analytical 0486
- Biochemistry 0487
- Inorganic 0488
- Nuclear 0738
- Organic 0490
- Pharmaceutical 0491
- Physical 0494
- Polymer 0495
- Radiation 0754

Mathematics 0405
Physics
- General 0605
- Acoustics 0986
- Astronomy and Astrophysics 0606
- Atmospheric Science 0608
- Atomic 0748
- Electronics and Electricity 0607
- Elementary Particles and High Energy 0798
- Fluid and Plasma 0759
- Molecular 0609
- Nuclear 0610
- Optics 0752
- Radiation 0756
- Solid State 0611

Statistics 0463

Applied Sciences
Applied Mechanics 0346
Computer Science 0984
Engineering
- General 0537
- Aerospace 0538
- Agricultural 0539
- Automotive 0540
- Biomedical 0541
- Chemical 0542
- Civil 0543
- Electronics and Electrical 0544
- Heat and Thermodynamics 0348
- Hydraulic 0545
- Industrial 0546
- Marine 0547
- Materials Science 0794
- Mechanical 0548
- Metallurgy 0743
- Mining 0551
- Nuclear 0552
- Packaging 0549
- Petroleum 0765
- Sanitary and Municipal 0554
- System Science 0790

Geotechnology 0428
Operations Research 0796
Plastics Technology 0795
Textile Technology 0994

PSYCHOLOGY
General 0621
Behavioral 0384
Clinical 0622
Developmental 0620
Experimental 0623
Industrial 0624
Personality 0625
Physiological 0989
Psychobiology 0349
Psychometrics 0632
Social 0451

To My Wife

Table of Contents

List of Figures

List of Tables

Abstract

Finding the conditions under which quantitatively reliable hyperfine structures can be obtained is one of the challenges of theoretical chemistry. The hyperfine structure of the $^{14}NH_2$ radical is investigated by means of multireference single and double configuration interaction techniques. Particular attention is paid to the dependence of the coupling constants on the reference space, the configuration selection energy threshold and the basis set. It has been found that the convergence can be reached at a high level of theory and excellent agreement with experiment is obtained. In order to reduce the computational cost with the minimum loss of accuracy, the basis set contraction is explored with respect to the hyperfine structure. Three popular contraction schemes are examined and it is found that all three contraction schemes yield convergence to the uncontracted one with a triple-zeta contraction, whereas the atomic natural orbital approach provides the smoothest and fastest convergence. Density functional theory calculations of isotropic couplings of the atoms B to O are also carried out with a variety of functional forms and basis sets. It is shown that the atomic isotropic coupling constants are very dependent on the functional form, the auxiliary basis set and the orbital basis set.

A great deal of attention has been paid experimentally and theoretically to alkaline-earth hydroxides (MOH). Previous studies have stressed the ionic bonding between the metal and the hydroxide group as an ligand. By means of high-level theoretical calculations, it is shown that another structure, HMO, exists. It has two low-lying electronic states: $^2\Pi$ and $^2\Sigma^+$. The studies have been carried out at several levels with a basis set of at least triple-zeta plus double polarization quality. Analysis of the electronic structures suggests that HBeO has two polarized covalent bonds formed from the *sp* hybrids of Be; HMgO has one covalent bond (between H and Mg) and one ionic bond and can be viewed as $(HMg)^+O^-$; HCaO has two ionic bonds represented by H^- $Ca^{2+}O^-$.

The thesis concludes with a general proof that it is possible to achieve $O(N^2)$ time scaling formally with respect to the size of the molecule (N), as opposed to $O(N^4)$ with the conventional self-consistent-field methods.

List of Symbols

Ψ	wave function
$\hat{H}$	Hamiltonian operator
t	time
h	Planck's constant (6.62618×10^{-34} J·s)
$\hbar$	Planck's constant divided by 2π
E	energy
$\hat{T}$	kinetic energy operator
$\hat{V}$	Coulomb energy operator
q	point charge
Z	nuclear charge
$\hat{M}_z$ and $\hat{M}^2$	angular momentum operators
l	angular momentum quantum number
$\hat{S}_z$, $\hat{S}^2$	electron spin operators
s, m_s	electron spin quantum numbers
α, β	electron spin states ($m_s = \frac{1}{2}, -\frac{1}{2}$)

$\langle\ ,\ \rangle$	Dirac bracket notation
$\delta_{ij},\ \delta(ij)$	Kronecker delta
δ	variation
$\hat{P}_{ij}$	permutation operator
ψ_i	molecular orbital, the spatial orbital for an electron
ϵ_{ij}	Lagrange undetermined multiplier
ϵ_i	orbital energy
$\det[\cdots]$	Slater determinant
$\hat{F}$	Fock operator
$\hat{J}$	Coulomb operator
$\hat{K}$	exchange operator
Ψ_i^a	singly-excited configuration
$\rho(\bar{r},\cdots)$	density
$\rho(\bar{r}',\cdots,\bar{r},\cdots)$	density matrix
$\rho_s(\bar{r})$	spin density
$\hat{\rho}_s(\bar{r})$	spin density operator
ν	frequency

$\boldsymbol{P}$	orbital density matrix
$\boldsymbol{S}$	overlap matrix of basis functions
B_{AB}	bond order between atoms A and B
I	moment of inertia
$\hat{L}$	rotational angular momentum
$\hat{H}_r$	Hamiltonian operator for molecular rotation
$\hat{H}_v$	Hamiltonian operator for molecular vibration
k_i	vibrational force constant
v_i	vibrational quantum number
T_E	energy threshold for selection of configurations
ΔE	energy difference
A_{iso}	isotropic hyperfine coupling constant
A_{ani}	anisotropic hyperfine coupling constant

List of Abbreviations

ANO	atomic natural orbital
AO	atomic orbital
BP	Becke's exchange potential with Perdew's correlation functional
CASSCF	complete active space SCF
CCA	coupled cluster approximation
CCD	coupled cluster with double substitutions
CC-PVTZ	correlation-consistent-polarized-valence-triple-zeta
CCSD	coupled cluster with single and double substitutions
CI	configuration interaction
CID	CI wave function with double excitations
CIS	CI wave function with single excitations
CISD	CI wave function with single and double excitations
CPF	coupled−pair functional
DFT	density functional theory
ESR	electron spin resonance
FORS	fully-optimized reaction space
GTO	Gaussian-type orbital
GVB	general valence bond
HF	Hartree-Fock

HFS	hyperfine structure
ICC	isotropic hyperfine coupling constant
KS	Kohn-Sham
LCGTO-DFT	linear combination of GTOs version of DFT
LDA	local spin density approximation
LMO	localized molecular orbital
MBPT	many-body perturbation theory
MCSCF	multiconfiguration SCF
MO	molecular orbital
MPn	*n*th-order Møller-Plesset perturbation theory
MRCISD	multireference CISD
NMR	nuclear magnetic resonance
PNO-CI	paired natural orbital CI
PWP	Perdew and Wang exchange functional with the correlation correction by Perdew
ROHF	restricted open-shell HF
RS	Rayleigh-Schrödinger
SCF	self-consistent-field
STO	Slater-type orbital
TZP	triple-zeta plus polarization
TZV	triple-zeta valence
UHF	unrestricted-HF

VB	valence bond

Acknowledgements

First and foremost, I wish to thank my supervisor, Professor Russell J. Boyd. I thank him for his excellent guidance, exceptional patience, constant support and strong motivation during my four years of study. I also thank him for the opportunity to work in this department and university, in this city and country. I could not have asked for more.

I would like to thank Dr. Leif Erikkson, with whom I started the project of hyperfine structure calculations. I would also like to thank Drs. M. Li and J. Coxon, who stimulated the study of the alkaline-earth hydroxides.

The people in Dr. Boyd's group have all been supportive. George Heard and Stacey Wetmore proofread most of this thesis, which, as far as I know, is not a very pleasant job. I had some stimulating discussions with Dr. Jiahu Wang. Kent Worsnop helped me to setup the PC and answer many of my PC questions.

I consider myself very fortunate to have been associated with the people who have been in this group: Drs. Jaime Martell, Zheng Shi, Mimi Lam, Jian Wang and Natalie Cann. These people have helped to make my new life here much easier and more pleasant. I sincerely wish them good luck.

Special thanks go to my next door neighbours Drs. Klaus Eichele and Roderick Wasylishen, from whom I have obtained a great deal of free and valuable advice during my coffee breaks. Drs. Klaus Eichele and Mike Lumsden answered almost all of my questions regarding to the use of WordPerfect 5.2.

The graduate scholarships from the I.W. Killam Memorial Trust Fund and Dalhousie University are much appreciated.

My last word is reserved for my family: my wife Wei Lin and son Nathan. Wei Lin's companionship is the most precious blessing I have ever had. Nathan's smile is like sunshine and is my daily meal. I simply feel that they are part of this thesis.

Chapter 1.

Introduction

Chemistry is about molecules. Molecules are composed of atoms, and atoms are composed of electrons and nuclei. Electrons and nuclei have substructures which usually do not change during a chemical process which typically involves the rearrangement of atoms. Physicists early in this century have found the natural laws - *quantum mechanics* - governing the interactions among electrons and nuclei. Thus, from the divide-and-conquer point of view, the chemistry is already well understood as we know the exact behaviour of a system composed of two particles, either electrons or nuclei or one of each kind. But nature does not give up that easily; no one has found the way to solve analytically the equations that the physicists have provided for a system which has more than two particles, i.e. we cannot, predict with infinite precision the behaviour of a molecule (the system composed of many electrons and nuclei), let alone its changes.

The branch of science dealing with this problem is *quantum chemistry*. Its goal is to develop a quantum mechanical theory which not only is able to predict molecular properties and chemical processes with the desired accuracy, but also provides a clear physical picture and concepts to make the quantities and their changes meaningful. With many years of development, the role of quantum chemistry has grown enormously, from one of explanation to one of quantitative prediction. A system of theories from rough approximation to rigid calculations is being established so that chemists can use these

tools to predict, verify or explain experimental results with increasing confidence.

This thesis reflects my learning experience in quantum*96Xchemistr€hapter 2 introduces the fundamental principles on which this thesis is based. Chapter 3 describes the major methods of quantum chemistry. Efforts have been made to present not only the mathematical formulae but also the physical concepts and pictures the formulae stand for. Although the computational quantum chemistry software packages are becoming more and more automatic, a fundamental understanding of concepts and theories is still crucial if meaningful results are desired.

Chapters 4 and Chapter 5 are composed of my work in this field. Chapter 4 deals with one of the major difficulties in quantum chemistry - quantitative prediction of the spin polarization effect. The conditions for obtaining converged results are explored with a vigorous theoretical treatment. Chapter 5, on the other hand, shows the power of the state-of-the-art theoretical methodologies. A new series of isomers of the alkaline earth monohydroxides has been predicted and their structural and electronic properties are discussed.

In Chapter 6, a new theoretical method is proposed to obtain the wave function for a large molecular system in a much more efficient and physically more meaningful way than by means of current standard methods. Chapter 7 concludes the thesis by outlining the directions of future work.

Chapter 2.

The Basics of Quantum Mechanics

2.1. The Schrödinger Equation

Quantum mechanics postulates that the state of any system is completely determined by its *wave function* Ψ, which is the solution of the *Schrödinger equation*:

$$\hat{H}\Psi = i\hbar\frac{\partial \Psi}{\partial t} \tag{1}$$

where $\hat{H}$ is the *Hamiltonian operator*, t is the time and $\hbar$ is Planck's constant divided by 2π. For most problems in chemistry including those in this thesis, $\hat{H}$ is independent of time and the Schrödinger equation can be rewritten as an *eigenvalue* problem:

$$\hat{H}\Psi = E\Psi \tag{2}$$

where E, the eigenvalue of the Hamiltonian operator, is the total energy of the system under study. The corresponding state of the time-independent Hamiltonian, the *eigenfunction* Ψ, is called a *stationary state*. Usually the wave function is *normalized* to unity: $\int \Psi^* \Psi d\tau = 1$.

Chemistry problems involve two kinds of particles: electrons and nuclei. In the absence of an external field, the total energy is the sum of the *kinetic energy* of the electrons and nuclei, and the *Coulomb energy* between the electrons and the nuclei. The corresponding Hamiltonian operator can be written as:

$$\hat{H} = \hat{T}_N + \hat{T}_e + \hat{V}(r_{ee}) + \hat{V}(r_{eN}) + \hat{V}(r_{NN}) \tag{3}$$

where $\hat{T}$ represents the operator for kinetic energy and has the form $-\frac{\hbar^2}{2m}\nabla^2$ for each particle with the mass m. $\hat{V}$, the operator for Coulomb energy, has the form $\frac{q_i q_j}{r_{ij}}$ which depends on the distance r_{ij} between the two particles and their charges q_i, q_j. The subscripts N and e stand for the nuclei and the electrons, respectively.

Since electrons are much lighter and thus move much faster than nuclei, one can assume (*Born-Oppenheimer approximation*) that the nuclei do not move when the electrons are studied. Thus $\hat{T}_N$ can be neglected and $\hat{V}_N$ becomes a constant. The Hamiltonian for the electrons in the *atomic units*[a] becomes:

---

[a] Atomic units are used throughout this thesis. In atomic units, $\hbar$, m and q are all equal to 1. The atomic unit of energy is the hartree and the unit of length is the bohr. One hartree equals $4.359\,14 \times 10^{-18}$ J and one bohr equals $5.291\,67 \times 10^{-11}$ m.

$$\hat{H} = -\frac{1}{2}\sum_{i\in e}(\nabla_i^2 - \sum_{a\in N}\frac{Z_a}{r_{ia}}) + \sum_{i<j\in e}\frac{1}{r_{ij}} + \sum_{a,b\in N}\frac{Z_a Z_b}{r_{ab}} \qquad (4)$$

where i , j are the indices for electrons, a, b the indices for nuclei, and Z is the nuclear charge. The first term is the single electron contribution which contains no electron-electron interaction and is usually abbreviated as $\sum_{i\in e}\hat{h}_i$.

One of the most important consequences of Equation (2) is that the change of the state can be scattered, i.e. $\Psi = \Psi_1, \Psi_2, \cdots$. The discrete states usually exist for the systems in which the particles are limited in space. The boundary conditions for the wave function make it dependent on discrete numbers. These numbers are called *quantum numbers*. The electrons in an atom or molecule can only move around the nuclei due the attraction of the latter and therefore have discrete states. This explains atomic and molecular spectroscopy and leads to the molecular orbital model which is the basis of quantum chemistry.

The physical interpretation of the wave function is that $\Psi(\bar{r}_1,\bar{r}_2,\cdots)\Psi^*(\bar{r}_1,\bar{r}_2,\cdots)d\bar{r}_1\bar{r}_2\cdots$ is the probability of finding particle 1 in $(\bar{r}_1, \bar{r}_1 + d\bar{r})$, particle 2 in $(\bar{r}_2, \bar{r}_2 + d\bar{r})$, etc. In quantum chemistry, the concept of electron density is used more frequently. It is proportional to the probability of finding an electron around a point in space.

2.2. Observables and Operators

In addition to the discrete states, quantum mechanics takes a different view of the physical world. Unlike classical mechanics which allows one to easily visualize the dynamics of a system defined by the coordinates and momenta of the particles, from which physical properties of the system can be directly obtained, a quantum state is completely defined by a wave function. The properties have to be obtained by "observing" the wave. That is, measurable physical properties, called *observables*, are obtained by applying the corresponding operators to the wave function.

When an operator $\hat{O}$ for the observable O is applied to a normalized wave function Ψ, two situations can occur. If the wave function is an eigenfunction of the operator, the eigenvalue will be the observed quantity for every measurement at different times. If not, then one may obtain different values that are the eigenvalues of $\hat{O}$ when measuring at different times and the ideal average or the *expectation value* of the measurements will be:

$$\overline{O} = \int \Psi^* \hat{O} \Psi d\tau = \langle \Psi | \hat{O} | \Psi \rangle \tag{5}$$

In the last equality, the *Dirac bracket notation* is used to symbolize the integration. The condition for two operators being able to share the same eigenfunction is that they must *commute*:

$$[\hat{A}, \hat{B}] = \hat{A}\hat{B} - \hat{B}\hat{A} = 0 \tag{6}$$

The probability of obtaining each eigenvalue of $\hat{O}$ can be calculated; the formula will be given in the next section.

Quantum mechanics states that an operator for an observable is linear and *Hermitian*. When an operator is Hermitian, for any function φ, it has the property:

$$\langle \varphi | \hat{O} | \varphi \rangle = \langle \varphi | \hat{O} | \varphi \rangle^* \tag{7}$$

The immediate result of Equation (7) is that any eigenvalue of $\hat{O}$ is real, as required since it is an observable. The Hamiltonian operator defined in Equation (4) is an example of a linear Hermitian operator whose eigenvalues, the energies, are always real. Two other important properties of a linear Hermitian operator are: (i) its eigenfunctions, ϕ_i, are orthogonal to each other:

$$\langle \phi_i | \phi_j \rangle = \delta_{ij} \tag{8}$$

and (ii) the eigenfunctions form a *complete linear space*. That means any well-behaved function f can be expanded as a linear combination of the eigenfunctions :

$$f = \sum_i \langle \phi_i | f \rangle \phi_i \tag{9}$$

where $\langle \phi_i | f \rangle$ is the expansion coefficient. δ_{ij} in Equation (8) is the *Kronecker delta*, sometimes also denoted as $\delta(ij)$. It is equal to 1 when $i = j$ and 0 otherwise.

2.3. The Principle of Superposition

The uncertainty due to the fact that each measurement to the same system may be different is "completely opposed to classical ideas, according to which the result of any observation is certain" (Dirac[1]). In quantum mechanics, a state A may be formed by a linear combination of states B and C, and the result of an observation on A can be either B or C with a finite probability. This principle is called the *principle of superposition*, which "forms the foundation of quantum mechanics" (Dirac[1]). This principle gives the physical meaning to Equation (9).

The probability of a given result can be calculated. Suppose the set of ϕ_i are the eigenfunctions of a linear Hermitian operator $\hat{O}$ with eigenvalues o_i and f is the normalized wave function of a state which is a linear combination of the ϕ_i:

$$f = \sum_i c_i \phi_i \qquad (10)$$

then one can derive from Equations (5), (8) and (9) that the probability of obtaining o_i is:

$$p(o_i) = c_i c_i^* = |c_i|^2 \qquad (11)$$

Since f is normalized, $|c_i| \leq 1$.

In quantum chemistry, the concept of state superposition has been widely used to interpret the molecular wave function.

2.4. Variation Principle

Due to the completeness of a Hermitian operator (Equation (9)), any well-behaved function can be the function f in Equation (10). If we take Ψ in Equation (5) as f in Equation (9), we can obtain the expectation value $\langle \Psi | \hat{O} | \Psi \rangle$ as:

$$\langle \Psi | \hat{O} | \Psi \rangle = \sum_i |c_i|^2 o_i = |c_{\min}|^2 o_{\min} + \cdots + |c_i|^2 o_i + \cdots + |c_{\max}|^2 o_{\max} \qquad (12)$$

The direct result of the above equation is that the expectation value of any function to an Hermitian operator is between the smallest and the largest eigenvalues of the operator. Since the Hamiltonian is Hermitian, this conclusion leads to the *variation principle*: the expectation value of any normalized trial function is an upper bound to the exact ground state energy. The *ground state* is the state with the lowest energy. That is:

$$\langle \Psi | \hat{H} | \Psi \rangle \geq E_0 \tag{13}$$

The variation principle is the mathematical foundation of quantum chemistry. Most chemical processes, as other things in nature, occur in the electronic ground state of the system. The best approximation of the wave function can thus be obtained by varying the parameters of a trial function to minimize the energy expectation value (referred to hereafter as simply the energy).

In the following section, several important properties pertaining to atomic and molecular systems will be introduced.

2.5. Some Important Operators

2.5.1. Angular momentum and spin

In addition to energy, *angular momentum* M due to the distribution of particles in space is another basic observable. The commutation rules for $\hat{M}_x$, $\hat{M}_y$, $\hat{M}_z$, $\hat{M}^2$ are:

$$[\hat{M}_x, \hat{M}_y] = i\hbar\hat{M}_z \tag{14}$$

$$[\hat{M}^2, \hat{M}_z] = 0 \tag{15}$$

In addition:

$$[\hat{H}, \hat{M}_z] = 0 \tag{16}$$

$$[\hat{H}, \hat{M}^2] = 0 \tag{17}$$

The possible eigenvalues of $\hat{M}_z$ and $\hat{M}^2$ can be derived from the above relationships:

$$\hat{M}^2 \varphi_{lm} = l(l+1)\hbar^2 \varphi_{lm} \qquad (l = 0, \frac{1}{2}, 1, \frac{3}{2}, \cdots) \tag{18}$$

$$\hat{M}_z \varphi_{lm} = m\hbar \varphi_{lm} \qquad (m = -l, -l+1, \cdots, l-1, l) \tag{19}$$

where l is the *angular momentum quantum number* and m the *magnetic quantum number*. Since $\hat{M}_z$, $\hat{M}^2$ and $\hat{H}$ commute with each other, for each energy and angular momentum magnitude, there are $2l + 1$ states with different m, i.e. $2l + 1$ *degenerate* states with the same energy and magnitude of the angular momentum. These quantum numbers are particularly useful for defining the state of an atom. For example, the energy of the hydrogen atom is determined by the principal quantum number n. For each n, l can be 0, 1, ... n-1, and the degree of degeneracy is n^2. The

eigenfunctions for $\hat{M}_z$ and $\hat{M}^2$ can be shown to be the spherical harmonics $Y_l^m(\theta,\phi)$. Therefore, the angular momentum operators provide a great deal information about the wave function even before the Schrödinger equation is solved.

2.5.2. Spin

The electron itself has an intrinsic angular momentum S, called *spin*. In nonrelativistic quantum mechanics, electron spin is introduced by means of a postulate. The spin operators $\hat{S}_z$, $\hat{S}^2$ have exactly the same commutation rules as $\hat{M}_z$ and $\hat{M}^2$. A single electron only has two possible states, usually denoted as α and β, with magnetic quantum numbers $m_s = \frac{1}{2}$ or $-\frac{1}{2}$ and the angular momentum quantum number, called the *spin quantum number*, $s = \frac{1}{2}$. As in the case of the eigenfunctions of other Hermitian operators, α and β are orthogonal to each other and assumed to be normalized.

Generally speaking, one more term will arise in Equation (3) due to the interaction between the angular momentum of an electron system and the spins of the electrons, but it is very small and usually treated as a perturbation. Thus, a wave function will be a simple product of two parts - the spatial part and the spin part - to make itself an

eigenfunction of both the Hamiltonian and the spin operators.

In a many-electron system, most of the electrons have opposite spins. The total S_z of the system is the sum of the S_z for each electron. That is:

$$\hat{S}_z = \sum_i \hat{S}_{zi} \tag{20}$$

The calculation of the total S^2 for the system is a bit more involved, but can be done by using the commutation relationship for the angular momentum. A system whose S is zero is called a *closed-shell* system. Otherwise, it is called an *open-shell* system.

2.5.3. Antisymmetry of electron systems

When one observes the state of a quantum system composed of the same kind of particles, such as electrons in a molecule, the observation, (or the operator,) is made on the wave function, i.e. the system as a whole, not each individual particle. Therefore, each individual particle is not distinguishable from the others. That is to say that the Hamiltonian commutes with the permutation operator $\hat{P}_{ij}$ which exchanges the positions of particles i and j.

$\hat{P}_{ij}$ has two possible eigenvalues 1 and -1. An electron system is found to be the -1 state. That is the wave function $\Psi(\cdots,\vec{r}_i,\cdots,\vec{r}_j,\cdots)$ for an atom or molecule should have the

following property:

$$\Psi(\cdot\cdot,\vec{r}_i,\cdot\cdot,\vec{r}_j,\cdot\cdot) = -\Psi(\cdot\cdot,\vec{r}_j,\cdot\cdot,\vec{r}_i,\cdot\cdot) \tag{21}$$

which is also a general expression for the *Pauli principle*.

Chapter 3.

The Foundations of Quantum Chemistry

Quantum chemistry applies quantum mechanics to a molecular environment. It has two goals: one is to build up a system of concepts to interpret observations or to provide foundations for chemical concepts, the other is to predict quantitatively physical and chemical properties.

There are two major difficulties in quantum chemistry. Qualitatively, since molecules are made of atoms, it is natural to attempt to understand chemical phenomena in terms of the properties of atoms. But as far as quantum mechanics is concerned, electrons in a molecule are not distinguishable and thus belong to all the atoms. This implies that there are no clear boundaries among the atoms in a molecule.

Quantitatively, the general mathematical procedure to solve a multidimensional problem like Equation (2) is to break it down into one-dimensional problems. But unfortunately, this approach cannot be used without making an additional approximation because $\frac{1}{r_{12}}$ is not separable. Therefore, quantum chemistry, by nature, is approximate.

Its development can be seen as the efforts to define the dominant factors affecting the chemical and physical properties of a system so that these properties can be understood and calculated.

The theories and mathematical formulae this thesis is based on are part of so-called *ab initio* methods which do not include any empirical parameters, as opposed to semi-empirical methods that include parameters chosen on the basis of experimental data. In *ab initio* methods, the parameters of a trial wave function are obtained by the optimization of the energy according to the variation principle (Equation (13)). The trial function is usually a linear combination of some limited one-electron and multi-electron basis functions.

Hartree-Fock theory is central to quantum chemistry and will be covered in detail in the following sections. Special attention has been given to the restricted open-shell method which is usually not covered in detail in standard quantum chemistry textbooks. Major correlation methods are also presented with the emphasis on the configuration interaction and multiconfiguration self-consistent-field algorithms upon which the research in this thesis is based.

3.1. Molecular Orbitals and Self-Consistent Field Methods

3.1.1. Unrestricted Hartree-Fock method

The simplest approximation for a wave function is to assume that the function for each electron is independent and the total wave function is the product of one-electron wave functions. Since electrons have spin, the one-electron function is a product of a spatial part $\psi(\vec{r})$ and a spin part, which is either α or β. Thus, the one-electron

function can be represented as $\psi(\bar{r})\alpha$ or $\psi(\bar{r})\beta$ (see Section 2.5.2). A trial function for a many-electron system then becomes:

$$\Psi = \psi_1(1)\alpha(1)\psi_2(2)\beta(2)\psi_3(3)\alpha(3)\cdots \tag{22}$$

The spatial function is called an *orbital*, or *molecular orbital* (MO) if the system under study is a molecule, and the one-electron function is called a *spin-orbital*. The numbers of α and β spin orbitals are determined by the total spin of the system.

According to the antisymmetry principle (Section 2.5.3), the wave function should change sign when two electrons exchange their positions. A *Slater determinant*[2] has this property and can be represented as:

$$(n!)^{-1/2}\begin{vmatrix} \psi_1(1)\alpha(1) & \psi_2(1)\beta(1) & \cdots & \psi_n(1)\alpha(1) \\ \psi_1(2)\alpha(2) & \psi_2(2)\beta(2) & \cdots & \psi_n(2)\alpha(2) \\ & & \vdots & \\ \psi_1(n)\alpha(n) & \psi_2(n)\alpha(n) & \cdots & \psi_n(n)\alpha(n) \end{vmatrix} \tag{23}$$

where $(n!)^{-1/2}$ is the normalization factor and n is the total number of electrons. Equation (23) is often abbreviated as $\det[\psi_1(1)\alpha(1)\ \psi_2(2)\beta(2)\cdots\psi_n(n)\alpha(n)]$.

For mathematical convenience, the spin-orbitals are usually assumed to be orthogonal to each other. That means that since the spins α and β are orthogonal to each other, the orbitals associated with the same spin are constrained to the following condition:

$$\langle \psi_i | \psi_j \rangle = \delta_{ij} \qquad (m_{s_i} = m_{s_j}) \tag{24}$$

where m_{s_i} and m_{s_j} are the spin quantum numbers. The energy of the trial function $\langle \Psi | \hat{H} | \Psi \rangle$ (see Section 2.1 for the expression of the Hamiltonian) under the orthogonal conditions then is:

$$E = \langle \Psi | \hat{H} | \Psi \rangle = \sum_i \langle \psi_i | \hat{h} | \psi_i \rangle + \frac{1}{2} \sum_{i,j} \{ (\psi_i \psi_j | \psi_i \psi_j) - \delta(m_{s_i} m_{s_j}) (\psi_i \psi_j | \psi_j \psi_i) \} \tag{25}$$

where

$$(\psi_a \psi_b | \psi_c \psi_d) = \iint \frac{\psi_a^*(1) \psi_b(2)^* \psi_c(1) \psi_d(2)}{r_{12}} d\tau_1 d\tau_2 \tag{26}$$

In Equation (25), the first term is the one-electron part that includes the kinetic energy of the electrons and the potential energy of attraction to the nuclei. In the second summation, $(\psi_i \psi_j | \psi_i \psi_j)$ is the repulsion energy between electrons in orbitals ψ_i and ψ_j. The $(\psi_i \psi_j | \psi_j \psi_i)$ term is due to the antisymmetry requirement which does not have any classical interpretation. Because the integration is over spins, $(\psi_i \psi_j | \psi_j \psi_i)$ will vanish if the i th and j *th* spin-orbitals have different spins. The nuclear repulsion energy (the third term in Equation (4)) is omitted because it is a constant and will disappear during the variation procedure.

According to the variation principle, the best approximation to the exact wave function for the ground state can be obtained by varying the orbitals ψ_i under the orthogonal constraint (Equation (24)). This is an optimization problem and can be solved using *Lagrange's method* of *undetermined multipliers*:

$$\delta(E - \sum_{i,j\in\alpha} \epsilon_{ij}\langle\psi_i|\psi_j\rangle - \sum_{i,j\in\beta} \epsilon_{ij}\langle\psi_i|\psi_j\rangle) = 0 \qquad (27)$$

where the ϵ_{ij} are the undetermined multipliers. (Please note δ in the above equations means variation). By substituting Equation (25) into Equation (27), the optimization problem becomes:

$$\begin{aligned} 0 = \sum_i \{\langle\delta\psi_i|\hat{h}|\psi_i\rangle + \sum_j \{(\delta\psi_i\psi_j|\psi_i\psi_j) - \delta(m_{s_i}m_{s_j})(\delta\psi_i\psi_j|\psi_j\psi_i)\} \\ - \sum_j \epsilon_{ij}\delta(m_{s_i}m_{s_j})\langle\delta\psi_i|\psi_j\rangle\} \end{aligned} \qquad (28)$$

Since each $\delta\psi_i^*$ is independent of all others, the above equation leads to the following n simultaneous equations for the orbitals with spins α and β:

$$(\hat{h} + \sum_{j\in\alpha\vee\beta} \hat{J}_j - \sum_{j\in\alpha} \hat{K}_j)|\psi_i\rangle = \hat{F}^\alpha|\psi_i\rangle = \sum_{j\in\alpha} \epsilon_{ij}|\psi_j\rangle \qquad (i \in \alpha) \qquad (29)$$

and

$$(\hat{h} + \sum_{j\in\alpha\vee\beta} \hat{J}_j - \sum_{j\in\beta} \hat{K}_j)|\psi_i\rangle = \hat{F}_i^{\beta}|\psi_i\rangle = \sum_{j\in\beta} \epsilon_{ij}|\psi_j\rangle \qquad (i \in \beta) \qquad (30)$$

in which $\hat{F}_i^{\alpha}$ and $\hat{F}_i^{\beta}$ are called *Fock operators*. The *Coulomb operator* $\hat{J}_j$ and the *exchange operator* $\hat{K}_j$ are defined as follows:

$$\hat{J}_j(1)\psi_i(1) = \int \frac{\psi_j^*(2)\psi_j(2)}{r_{12}} d\tau_2 \psi_i(1) \qquad (31)$$

$$\hat{K}_j(1)\psi_i(1) = \int \frac{\psi_j^*(2)\psi_i(2)}{r_{12}} d\tau_2 \psi_j(1) \qquad (32)$$

The Coulomb operator $\hat{J}_j$ is the Coulomb potential from the electron in orbital ψ_j. The exchange operator $\hat{K}_j$, arising from the antisymmetry requirement, does not operate locally like $\hat{J}_j$, but rather it is defined in terms of the function upon which it operates.

Similarly, there is another set of equations which are conjugates to Equations (29) and (30) arising from varying Equation (27) by $\delta\psi_i^*$. The two equations are as follows:

$$\langle\psi_i|\hat{F}^{\alpha} = \sum_{j\in\alpha} \epsilon_{ji}\langle\psi_j| \qquad (i \in \alpha) \qquad (33)$$

and

$$\langle \psi_i | \hat{F}^{\beta} = \sum_{j \in \beta} \epsilon_{ji} \langle \psi_j | \qquad (i \in \beta) \tag{34}$$

Since the Hamiltonian is Hermitian, one can show that the Fock operators are Hermitian. By taking the conjugate of Equations (33) and (34) and comparing the new equations with Equations (29) and (30), one can find that the solutions of Equations (33) and (34) guarantee that the matrix $[\epsilon_{ij}]$ is Hermitian:

$$\epsilon_{ij} = \epsilon^*_{ji} \tag{35}$$

In order to solve Equations (29), (30) and (35), two observations should be noted. First, Equations (29) and (30) involve only the ϵ_{ij} with i and j belonging to the same spin. Therefore the ϵ_{ij} with i and j belonging to different spins can be assumed to be zero and the matrix can be divided into two diagonal blocks, one for each spin. Diagonalization of $[\epsilon_{ij}]$ then can be done within each block. Secondly a determinant has the property that adding one column to another results in no change. That means a unitary transformation of the orbitals within each spin does not change the trial wave function and, thus, the Fock operators do not change. Therefore, it is always possible to transform the orbitals so that $[\epsilon_{ij}]$ becomes diagonal and thus to write Equations (29) and (30) in a form similar to the eigenvalue problem:

$$\hat{F}^{\omega}|\psi_i\rangle = \varepsilon_{ii}|\psi_i\rangle \qquad (i \in \omega = \alpha \text{ or } \beta) \tag{36}$$

Since the Fock operators depend on their eigenfunctions, an iterative calculation process must be carried out until the Fock operators have the same eigenfunctions as those from which the operators are formed. The eigenvalue ε_{ii}, commonly denoted as ε_i, is real since it is Hermitian. It has the unit of energy and is interpreted as the *orbital energy*. In addition to the *occupied orbitals*, the eigenfunctions which are used to construct the Fock operators, there are many other eigenfunctions that are solutions of Equation (36). These eigenfunctions are called *unoccupied orbitals* or *virtual orbitals*. The orbital energies of the occupied orbitals are always lower than those of the virtual orbitals in order to ensure the minimum total energy.

The concept of an orbital originated from Bohr's study of the hydrogen atom, which helped to shape the quantum mechanics. Hartree[3] first proposed the simple product of one-electron functions (similar to Equation (22) but without the spin) as a trial function for the study of atoms. Later Fock[4] and Slater[5] independently introduced antisymmetry into the product of orbitals and established the Hartree-Fock (HF) method. In the HF method, an electron moves in a time-averaged electric field produced by all the other electrons as expressed by the Coulomb and exchange operators. The function or orbital for the electron is the eigenfunction of an effective Hamiltonian (the Fock operator). The eigenvalue of the effective Hamiltonian becomes the energy of taking a electron from the orbital to infinity, i.e. the ionization energy (Koopmans' theorem[6]).

Since the average field and the orbitals depend on each other, the final orbitals should yield a field that will produce themselves. This method is called the *self-consistent-field* (SCF) method.

Despite its simplicity (or due to its simplicity, depending on the point of view), the HF method, or the orbital model, is the core of quantum chemistry for both qualitative analyses and quantitative predictions. Although the orbitals change whenever there is a change of physical or chemical conditions, the variations have often been found to be small and the orbitals can be assumed to remain the same for qualitative analysis or even semiquantitative calculations such as frontier MO analysis. Quantitatively, it can be easily shown that a determinant which is formed by substituting an occupied orbital with a virtual orbital will not interact with the ground state determinant (Brillouin's theorem):

$$\langle \Psi_i^a | \hat{H} | \Psi \rangle = 0 \tag{37}$$

where Ψ_i^a, called a *singly-excited configuration*, is the normalized determinant with the i th occupied orbital replaced by the a th virtual orbital. Brillouin's theorem leads to the conclusion that the HF wave function is correct to the first-order if it is taken as the zeroth-order approximation for a perturbation treatment[7].

The equations given so far belong to the *unrestricted-HF* (UHF) method, formulated by Pople and Nesbet[8]. For a closed-shell system, the numbers of α and β electrons are the same and may lead to the same $\hat{F}_i^\alpha$ and $\hat{F}_i^\beta$. This in turn results in the

same set of orbitals for the α and β electrons, or in other words, all the orbitals are *doubly occupied* by two electrons with opposite spins. In an open-shell system, however, $\hat{F}_i^{\alpha}$ and $\hat{F}_i^{\beta}$ are not the same, resulting in different spatial distributions of α and β orbitals, i.e. all the orbitals are *singly-occupied*. Because of this, the UHF method can describe the spin-polarization effect which will be discussed in the next chapter.

3.1.2. Restricted open-shell Hartree-Fock method

A UHF wave function for an open-shell system generally is not an eigenfunction of the spin operator $\hat{S}^2$. A single determinant trial function is an eigenfunction of $\hat{S}^2$ only when all the occupied orbitals are either doubly occupied, or singly occupied by the electrons with the same spin. This observation leads to the establishment of the restricted open-shell HF (ROHF) method. In the ROHF method, a trial wave function is composed of two types of orbitals. The closed-shell orbitals are doubly occupied and can be shown to have zero contribution to S^2. The open-shell orbitals are singly occupied by either an α or a β electron. The open-shell part may contain more orbitals than electrons. For example, it is commonly known that the electronic configuration of the ground state of the boron atom is $(1s)^2(2s)^2(2p)^1$. $(1s)^2(2s)^2$ is the closed-shell part. The $2p$ shell has three orbitals $2p_x$, $2p_y$ and $2p_z$, from which six determinants or

configurations can be constructed:

$$\begin{aligned}
\Psi_1 &= \det[1s(1)\alpha(1)1s(2)\beta(2)2s(3)\alpha(3)2s(4)\beta(4)2p_x(5)\alpha(5)] \\
\Psi_2 &= \det[\quad \cdots \quad \textit{closed-shell} \quad \cdots \quad 2p_y(5)\alpha(5)] \\
\Psi_3 &= \det[\quad \cdots \quad \textit{closed-shell} \quad \cdots \quad 2p_z(5)\alpha(5)] \\
\Psi_4 &= \det[\quad \cdots \quad \textit{closed-shell} \quad \cdots \quad 2p_x(5)\beta(5)] \\
\Psi_5 &= \det[\quad \cdots \quad \textit{closed-sehll} \quad \cdots \quad 2p_y(5)\beta(5)] \\
\Psi_6 &= \det[\quad \cdots \quad \textit{closed-shell} \quad \cdots \quad 2p_z(5)\beta(5)]
\end{aligned} \tag{38}$$

Since an atom has spherical symmetry, the two trial functions corresponding to the two spin states should be:

$$\begin{aligned}
\Psi_{\frac{1}{2}} &= 3^{-\frac{1}{2}}(\Psi_1 + \Psi_2 + \Psi_3) \\
\Psi_{-\frac{1}{2}} &= 3^{-\frac{1}{2}}(\Psi_4 + \Psi_5 + \Psi_6)
\end{aligned} \tag{39}$$

where the subscripts indicate the S_z value of the functions. It is obvious that the two functions will give the same energy:

$$\begin{aligned}
E = &\sum_{i\in C} 2\langle\psi_i|\hat{h}|\psi_i\rangle + \sum_{i\in O}\frac{1}{3}\langle\psi_i|\hat{h}|\psi_i\rangle + \frac{1}{2}\sum_{i,j\in C}\{4(\psi_i\psi_j|\psi_i\psi_j) \\
&- 2(\psi_i\psi_j|\psi_j\psi_i)\} + \frac{1}{6}\sum_{i\in C,\, j\in O}\{2(\psi_i\psi_j|\psi_i\psi_j) - (\psi_i\psi_j|\psi_j\psi_i)\}
\end{aligned} \tag{40}$$

Compared with the energy expression for an UHF wave function (Equation (25)), the energy expression for the ROHF wave function has a few main differences. First, the ROHF energy expression is more conveniently divided into the closed-shell part and open-shell part and the interactions between them, as opposed to dividing the UHF one

into different spins. Secondly, the coefficients of the one-electron and two-electron terms depend on the type of orbitals in ROHF, rather than being the same for all the orbitals. Unlike a UHF trial function where all the orbitals are singly occupied, the orbitals in an ROHF trial function can have occupancies of 2, 1 or a fraction. As shown in the above equation, the Coulomb energy between doubly occupied closed-shell orbitals is four times that of two singly occupied orbitals. The exchange energy, on the other hand, is two times since only the interactions between the electrons with opposite spin are included. When a doubly occupied orbital interacts with a singly occupied orbital, both the Coulomb part and the exchange part are half the value of those in the case of two doubly occupied orbitals. Since the occupancy for the three p orbitals is one-third, i.e. the unpaired electron is shared equally among the three orbitals, the coefficients 1/3 and 1/6 appear for the one-electron part and the Coulomb and exchange parts.

This unsymmetrical representation of the orbitals in the energy expression reflects the fact that an ROHF Slater determinant will be changed by a unitary transformation that mixes closed-shell and open-shell orbitals. For example, a unitary transformation between $2s$ and $2p_x$ orbitals in the determinant Ψ_1 will result in a new determinant $\det[closed\text{-}shell\cdot 2p_x\alpha 2p_x\beta 2s\alpha]$ which will yield a different energy expression when Equation (40) is applied. This means the Fock operators for an ROHF wave function will change under a unitary transformation and an eigenequation (Equation (36)) cannot be assumed. However, it is desirable to transform the problem to an eigenvalue equation since the methods of solving these equations have been well developed.

The standard method to solve this problem originated with Roothaan[9]. He

realized that a unitary transformation within the open-shell orbitals does not change the energy expression in most cases and a diagonalization can be assumed within the open-shell and closed-shell, respectively. The cross terms then can be cast into the Fock operators to obtain a pseudo-eigenequation. In many cases, the energy expression for an open-shell system can be written as:

$$\begin{aligned} E = & 2\sum_{k}\langle\psi_k|\hat{h}|\psi_k\rangle + \sum_{k,l}(2\langle\psi_k|\hat{J}_l|\psi_k\rangle - \langle\psi_k|\hat{K}_l|\psi_k\rangle) \\ & + f[2\sum_{m}\langle\psi_m|\hat{h}|\psi_m\rangle + f\sum_{m,n}(2a\langle\psi_m|\hat{J}_n|\psi_m\rangle - b\langle\psi_m|\hat{K}_n|\psi_m\rangle) \\ & + 2\sum_{k,m}\langle\psi_k|\hat{J}_m|\psi_k\rangle - \langle\psi_k|\hat{K}_m|\psi_k\rangle)] \qquad (k,l \in C,\ m,n \in O) \end{aligned} \tag{41}$$

where a, b and f are numerical constants depending on the specific case. f is the occupation fraction, e.g. it is $\frac{1}{2}$ when the open shell is half-full. a and b are chosen so that the trial function is an eigenfunction of $\hat{S}_z$ and $\hat{S}^2$ and has the symmetry of the system. For example, in the case of the boron atom, $a = b = 0$, and $f = \frac{1}{6}$.

By virtue of the variation principle and Lagrange multiplier method, optimizing the trial function is equivalent to solving the following variational problem:

$$\delta(E - \sum_{i,j\in C+O} 2\epsilon_{ij}\langle\psi_i|\psi_j\rangle) = 0 \tag{42}$$

which results in the simultaneous equations:

$$(\hat{h} + \sum_l (2\hat{J}_l - \hat{K}_l) + f\sum_n (2\hat{J}_n - \hat{K}_n)|\psi_k\rangle = \hat{F}_C|\psi_k\rangle - \sum_l \epsilon_{kl}|\psi_l\rangle + \sum_m \epsilon_{km}|\psi_m\rangle \tag{43}$$

$$f(\hat{F}_C + f\sum_n (2a\hat{J}_n - b\hat{K}_n)|\psi_m\rangle = \hat{F}_O|\psi_m\rangle - \sum_l \epsilon_{kl}|\psi_l\rangle + \sum_m \epsilon_{km}|\psi_m\rangle \tag{44}$$

and the Hermitian condition for the multipliers ϵ_{ij}:

$$\epsilon_{ij} = \epsilon^*_{ji} \tag{45}$$

$\hat{F}_C$ and $\hat{F}_O$ are the Fock operators for the closed-shell orbitals and open-shell orbitals, respectively.

So far, this procedure is similar to the one for an UHF trial function (Equations (27) to (35)). But since the energy generally will change with a unitary transformation of the orbitals, the Fock operators will change accordingly and the matrix $[\epsilon_{ij}]$ cannot be assumed to be diagonal without modification of the Fock operators. Therefore, the Equations (43), (44) and (45) cannot be simply reduced to an eigenvalue problem like Equation (36). However, one can assume that $[\epsilon_{ij}]$ is partially diagonalized within the closed-shell orbitals or open-shell orbitals and Equations (43) and (44) become:

$$\hat{F}_C|\psi_k\rangle = \epsilon_k|\psi_k\rangle + \sum_m \epsilon_{km}|\psi_m\rangle \tag{46}$$

$$\hat{F}_O|\psi_m\rangle = \sum_k \varepsilon_{mk}|\psi_k\rangle + \varepsilon_m|\psi_m\rangle \tag{47}$$

Here one can see that:

$$\varepsilon_{mk} = \langle\psi_k|\hat{F}_O|\psi_m\rangle \tag{48}$$

$$\varepsilon_{km} = \langle\psi_m|\hat{F}_C|\psi_k\rangle \tag{49}$$

Then the Hermitian condition (Equation (45)) results in:

$$\varepsilon_{mk} = \varepsilon^*_{km} = \langle\psi_m|\hat{F}_O|\psi_k\rangle^* = \langle\psi_k|\hat{F}_O|\psi_m\rangle \tag{50}$$

Upon combining this equation with Equation (46) one obtains:

$$\hat{F}_C|\psi_k\rangle = \varepsilon_k|\psi_k\rangle + \sum_m |\psi_m\rangle\langle\psi_m|\hat{F}_O|\psi_k\rangle \tag{51}$$

which can be rewritten as a pseudo-eigenequation:

$$(\hat{F}_C - \sum_m |\psi_m\rangle\langle\psi_m|\hat{F}_O)|\psi_k\rangle = \varepsilon_k|\psi_k\rangle \tag{52}$$

It can be easily shown that the Hermitian condition of $[\varepsilon_{ij}]$ is satisfied. To make the left side of the above equation Hermitian, one can add a zero term and change it to:

$$[\hat{F}_C - \sum_m (\hat{F}_O|\psi_m\rangle\langle\psi_m| + |\psi_m\rangle\langle\psi_m|\hat{F}_O)]|\psi_k\rangle = \hat{F}'_C|\psi_k\rangle = \varepsilon_k|\psi_k\rangle \tag{53}$$

Similarly one can obtain a pseudo-eigenequation for the open-shell orbitals:

$$(\hat{F}_O - \sum_k (\hat{F}_C|\psi_k\rangle\langle\psi_k| + |\psi_k\rangle\langle\psi_k|\hat{F}_C)]|\psi_m\rangle = \hat{F}'_O|\psi_m\rangle = \epsilon_m|\psi_m\rangle \qquad (54)$$

The problem has thus been changed to an eigenvalue one by absorbing the cross terms into the diagonal terms using the projection operators $\sum_i |\psi_i\rangle\langle\psi_i|$ for the closed-shell and open-shell orbitals. Equations (53) and (54) can be solved by an iterative procedure similar to the case of UHF and the method described is therefore a SCF method.

There are many ways to write the pseudo-eigenequations. In fact, it is possible to make the pseudo-operators $\hat{F}'_C$ and $\hat{F}'_O$ the same[9]. It should be noted however that Brillouin's and Koopmans' theorems do not apply to the ROHF solutions.

The energy expression of an ROHF wave function in Equation (41) is applicable to most cas Davidson[10] has proposed a more general energy expression:

$$E = \sum_i n_i\langle\psi_i|\hat{h}|\psi_i\rangle + \frac{1}{2}\sum_{i,j} n_i n_j\{\langle\psi_i|\hat{J}_j|\psi_i\rangle - \frac{1}{2}\langle\psi_i|\hat{K}_j|\psi_i\rangle\} + \frac{1}{4}\sum_{i,j>K} \beta_{ij}\langle\psi_i|\hat{K}_j|\psi_i\rangle \qquad (55)$$

The trial wave function is written as a linear combination of Slater determinants of orthogonal orbitals:

$$\Psi = \sum c_p \det\{\psi_1\alpha\psi_1\beta\cdots\psi_K\beta,\psi_{K+1}\chi_{1,p}\cdots\psi_{K+L}\chi_{L,p}\} \qquad (56)$$

n_i is the orbital occupation number. The last term in Equation (55) adjusts the exchange

energy according to the distribution of spins among the open-shell orbitals of all determinants:

$$\beta_{ij} - \beta_{ji} - 1 - 2\sum_{p,q} c_p^* c_q \langle \chi_{ip} | \chi_{jq} \rangle \prod_{l \neq i,j} \langle \chi_{lp} | \chi_{lq} \rangle \qquad (57)$$

The $[\varepsilon_{ij}]$ pertaining to those open-shell orbitals among which β_{ij} is -1 can be assumed to be diagonalized and the orbitals are grouped into diagonal sets. The cross terms between the sets were handled in the same fashion as Roothaan's method.

Davidson's method covers most open-shell cases. Most generally, the energy expression[11] for an arbitrary linear combination of Slater determinants can be written as:

$$E - \sum_{i,j} (\omega_{ij} \langle \psi_i | \hat{h} | \psi_j \rangle + \sum_{k,l} (\alpha_{ij}^{kl} (\psi_i \psi_j | \psi_k \psi_l) - \beta_{ij}^{kl} (\psi_i \psi_k | \psi_j \psi_l)) \qquad (58)$$

where the parameters are decided by the specific state and the symmetry of the system under study. A general form of the pseudo-eigenequation can be given using projection operators.

So far, we have seen that solving a ROHF problem is much more complicated than a UHF one. Davidson[12] pointed out, however, that it is actually possible to obtain an ROHF solution for many systems by using the UHF procedure. It is because for these systems, such as the atoms B to F, the open-shell orbitals have different symmetry, i.e. belong to different symmetry representations from the closed-shell orbitals. The

orthogonal conditions between the closed-shell and open-shell orbitals thus become redundant and can be removed. The ε_{ij} connecting them can be assumed to be zero. Under this circumstance, the variation of the orbitals will be in the same symmetry representation and no mixture with the closed-shell orbitals, which belong to a different symmetry representation, will occur.

Consider the case of the boron atom as an example. If the Ψ_1 configuration is used as a trial function for a UHF procedure, the resulting energy E_1 will be the same as E_4 when Ψ_4 is used as a UHF trial function. In addition, the resulting α orbitals and β orbitals in Ψ_1 will be the same as the β orbitals and α orbitals, respectively, in Ψ_4. When the spin of the electron in the p_x orbital of Ψ_1 changes from α to β without a change of the orbitals, the resulting energy will be higher because the two orbitals in each closed-shell are not equal to each other, although the configuration is the same as Ψ_4. If $\frac{1}{2}(E_1 + E_4)$ is optimized instead of E_1 and E_4 separately, the α and β orbitals in the two determinants will be averaged to the same set, resulting in an ROHF representation.

Obviously, the equivalence of orbitals can be treated in the same way. Using the same example, we know that the three orbitals $2p_x$, $2p_y$ and $2p_z$ are equivalent due to the spherical symmetry. Equivalence can be achieved by averaging all six configurations which would give the same energy under the UHF scheme.

3.2. LCAO Method and Basis Sets

The HF equations are a set of integro-differential equations and can be in principle solved exactly by numerical methods and the energy obtained is called the *HF limit*. The calculations of the HF limit are mainly for the purpose of calibration and are too computationally demanding to implement for most cases. In this section, methods which lead to approximate solutions of the HF equations by the techniques of linear algebra are introduced.

3.2.1. Roothaan equations

The contemporary methods for solutions of the SCF equations are rooted in Roothaan's study[13] in 1951 in which he suggested that the SCF equations be solved in the space of a finite basis set.

Suppose that an orbital ψ_i is a linear combination of a set of basis functions $\{\phi_\mu\}$:

$$\psi_i = \sum_{\mu}^{N} c_{\mu i}\phi_\mu \tag{59}$$

where N is the number of basis functions. A pseudo-eigenequation then becomes a

secular equation:

$$\sum_{\nu} (F_{\nu\mu} - \epsilon_i S_{\nu\mu}) c_{\nu i} = 0 \qquad (60)$$

where $F_{\nu\mu}$ is the Fock matrix $\langle \phi_\nu | \hat{F} | \phi_\mu \rangle$ and $S_{\nu\mu}$ is the overlap matrix $\langle \phi_\nu | \phi_\mu \rangle$.

The Roothaan equations (Equation (60)) define the main theme of quantum chemistry in which the Schrödinger equation is solved approximately by the methods of linear algebra.

3.2.2. Basis set functions

The Roothaan equations are not necessarily approximations to the original HF eigenvalue equations. They are accurate if the space of the basis function set is complete. Unfortunately, a complete set usually has an infinite number of functions and is generally not applicable. Instead, a great deal of effort has been spent on searching for efficient finite basis sets which yield as little loss of accuracy as possible.

It is natural to choose atom-centred functions for two reasons. First, a molecule is composed of atoms and can only be dissociated into them in a chemical process. It would make a qualitative explanation easier if a wave function of a molecule is made of atomic functions too. Secondly, it has been found that the total atomization energy of a molecule is a very small fraction of the total energy. Therefore using atomic functions can yield a good quantitative approximation.

The exact wave function for the simplest atomic system - the hydrogen atom - has been found to have the form $R_{nl}(r)Y_m^l(\theta,\phi)$. $R_{nl}(r)$ is expressed as follows:

$$R_{nl} \propto r^l e^{-\frac{r}{n}} \sum_{i=0}^{n-l-1} c_i r^i \tag{61}$$

where n, l and m are the principal and angular momentum quantum numbers (see Section 2.5.1). Slater proposed that an analogous type of function should be the trial function for atomic orbitals of other atoms:

$$S_{nlm} \propto r^{n-1} e^{-\zeta r} Y_l^m(\theta,\phi) \tag{62}$$

where ζ is to be determined by a variational procedure. This type of orbital function is called a *Slater-type orbital* (STO).

Each STO is characterized by the quantum numbers n, l and m. The orbitals with the same n are in the same *shell*. In each shell, there are $2l + 1$ orbitals with the same l which form a subshell. The subshells are named conventionally as s, p, d, f... for l equal to 0, 1, 2, 3, etc. The exponential factor ζ controls the decay of the radial function. The inner shells - the shells that have small n and are closer to the nucleus - have larger ζ and therefore lower orbital energies. The outer shells have smaller ζ and higher orbital energies. The differences between a STO and a wave function of hydrogen

are that the radial function of the former does not possess the nodal property of the latter and that the subshells of a many-electron atom yield different orbital energies (the larger the l, the higher the orbital energy). A STO can also be expressed in Cartesian coordinates. $Y_l^m(\theta,\phi)$ is a polynomial of $\sin\theta$, $\cos\theta$ and $\cos\phi$ and can be transformed into x^i, y^j and z^k or their linear combinations by multiplying by r^l. That is:

$$S_{nijk} \propto x^i y^j z^k r^{n-l} e^{-\zeta r} \tag{63}$$

where $i + j + k = l$.

The following are some examples of atomic STOs for $1s$, $2p$ and $3d$ shells:

$$S_{1s} \propto re^{-\zeta_{1s} r} \tag{64}$$

$$S_{2p_x} \propto xe^{-\zeta_{2p} r} \tag{65}$$

$$S_{3d_{x2}} \propto x^2 e^{-\zeta_{3d} r} \tag{66}$$

These real functions are not the eigenfunctions of $\hat{M}_z$ and $\hat{M}^2$, but their linear combinations are. This change is allowed for energy calculations because the states with the same m are degenerate and their energy will not be changed by a unitary

transformation within them. In the above representation, there are six d functions with $S_{3d_{z^2}} + S_{3d_{y^2}} + S_{3d_{z^2}}$ equivalent to S_{3s}. This is redundant and, thus, five linear combinations of these d functions are often used instead: d_{xy}, d_{xz}, d_{yz}, $d_{x^2}-d_{y^2}$ and $d_{2z^2}-d_{x^2}-d_{y^2}$.

STOs closely resemble the atomic orbitals and are able to yield results near those obtained from the numerical HF method. The problem is that the multicentre integrals are extremely hard to evaluate. The Fock matrix for a closed-shell system has the following form:

$$F_{\nu\mu} = \langle\phi_\nu|\hat{h}|\phi_\mu\rangle + \sum_{\sigma,\lambda\, j} c_{j\sigma}^* c_{j\lambda}[2(\nu\mu|\sigma\lambda) - (\nu\lambda|\sigma\mu)] \qquad (67)$$

When the basis functions are from different atoms, the integral $(\nu\mu|\sigma\lambda)$ becomes too complicated to calculate analytically. Despite tremendous efforts to develop methods for the evaluation of these integrals, the use of STOs is primarily restricted to the study of diatomic or linear molecules.

The *Gaussian-type orbital* (GTO), proposed by Boys[14] is almost exclusively the choice of basis function type for *ab initio* quantum chemistry calculations. A GTO has the following form:

$$G_{ijk} \propto x^i y^j z^k e^{-\zeta r^2} \qquad (68)$$

in which the exponents are obtained usually by optimizing the atomic HF wave function of the ground state of an atom.

The advantage of the Gaussian function is that a multi-centre integral can be reduced to a two-centre integral which can be calculated analytically. This has great importance for the application of quantum chemistry methods as it makes calculations on polyatomic molecules feasible. Please note that GTOs do not include the shell numbers because they do not have the preexponential part as in STOs. Instead, each atomic shell is reflected by its exponential factor.

On a one-to-one basis, the performance of a GTO does not match that of a STO. In particular, a GTO does not possess the *cusp* of a true wave function, i.e. a true wave function has a slope proportional to the function value at the nucleus whereas a GTO gives zero slope at the nucleus. GTOs are competitive, however, because a STO or an atomic orbital can be well fitted by a number of GTOs. Although less efficient than STOs in terms of the number of functions, GTOs have made quantum mechanical calculations feasible for polyatomic systems. The inefficiency incurred by the increase in the number of basis functions can also be reduced by *basis set contraction*, i.e., the GTOs are grouped together in a linear combination:

$$\phi_\mu = \sum_\lambda c_{\lambda\mu} g_\lambda \qquad (69)$$

where the ϕ_μ are the basis functions to be used in the formation of MOs as in Equation (59). These functions are also called *contracted Gaussian functions* as opposed to the *uncontracted Gaussian functions* g_λ (also called *primitive Gaussians*). The contraction coefficients are taken from HF atomic orbitals.

3.2.3. Basis set contractions

The basis set contraction is an important concept. As mentioned above, a single GTO does not converge well to the true orbital and thus more Gaussian functions are needed, which increases the size of basis sets. From Equation (38) one can see that the construction of a Fock matrix element involves four basis functions, which means the computing time for the SCF part is proportional to N^4. When the basis functions are used for a molecule which contains K identical atoms, the time scales as $(KN)^4$. Therefore, it is very important to limit the number of basis functions while minimizing the loss of accuracy.

The concept of basis set contraction also makes physical sense. When atoms form a molecule, the atomic orbitals are deformed or polarized by the molecular environment, but are not destroyed completely. The closed-shell atomic orbitals, in fact, remain largely unchanged so that the atoms are still distinguishable in a molecule. It has been found in calculations with uncontracted primitive Gaussians that the primitives are divided into several groups and the ratios of the coefficients in a group remain relatively constant. Also, the dissociation energy is usually only a few percent of the total energy, indicating that the atomic functions do not change much in a molecule.

Dunning[15] proposed some rules-of-thumb for the contraction of primitive Gaussians. First, functions of greatest importance in regions between the nuclei should be left uncontracted. This is because these GTOs are in the valence region and they take part in bonding. As a result, flexibility is obtained which is needed to describe the

molecular environment. Secondly, functions spanning two different orbital spaces (e.g. 1*s* and 2*s* orbitals of an atom) should also be allowed to vary freely because their contributions to the atomic orbitals may change with the molecular environment. These rules have guided the development of basis sets.

3.2.4. Additional basis functions

When the basis sets are used for molecular calculations, some extra considerations must be taken into account. In a molecular environment, the atom is no longer in its ground state. Instead, its "state" can be understood as the superposition of the atomic ground state and excited states. Therefore, using the basis functions optimized in the atomic ground state may cause large quantitative errors. To correct this deficiency, additional functions, whose exponents are usually obtained by HF calculations for atomic excited states, are added to the basis set.

One type of additional function is the *polarization function*. A polarization function has a higher angular quantum number than that of the occupied orbitals of the ground state of the atom, e.g. a *d* function for the nitrogen atom. Polarization functions are designed to help describe the distortion of the atomic orbitals in a molecular environment. A well-known example is the NH_3 molecule, which is predicted to be planar if a large (*s*, *p*) set is used. The addition of *d* functions to the N basis set corrects the problem.

Diffuse functions, which have extra small exponents, are sometimes added to a

basis set. They are particularly important for anions which generally have diffuse electron clouds. The charge distribution in a molecule is not even among the atoms. Some atoms may have more electrons around them than when they are separated, i.e. they become "larger" by attracting electrons from other atoms.

Recent advances in the development of basis sets will be discussed in the next chapter.

3.3. Atomic Charges and Bond Orders

With the exception of core orbitals, the molecular orbitals obtained through the HF equations generally do not belong to a particular atom or to a pair of atoms. Instead they are *delocalized*, i.e. spread around the whole molecule. A chemist, however, would like to think of a molecule in terms of the properties of the atoms and the bonds between them. One of the popular concepts is that of *atomic charge*. The atoms are said to gain or lose electrons in a molecule.

The atomic charge is not an observable and therefore its definition is arbitrary. The most widely used definition is due to Mulliken. He proposed that the total number of electrons can be formally decomposed into the sum of the contributions from each atom in the following way:

$$N = \sum_{i}^{occupied} p_i \langle \psi_i | \psi_i \rangle = \sum_{i}^{occupied} p_i \sum_{\sigma,\lambda} c_{\sigma i} c_{\lambda i} \langle \phi_\sigma | \phi_\lambda \rangle$$
$$= \sum_{\sigma,\lambda} \sum_{i}^{occupied} p_i c_{\sigma i} c_{\lambda i} \langle \phi_\sigma | \phi_\lambda \rangle = \sum_{\sigma,\lambda} P_{\sigma\lambda} S_{\sigma\lambda} = \sum_{\sigma} (PS)_{\sigma\sigma} \tag{70}$$

where $\boldsymbol{P}$ is called *orbital density matrix*[a] and $\boldsymbol{S}$ is the *overlap matrix of basis functions*. We therefore can take $\sum_{\sigma \in A} (PS)_{\sigma\sigma}$ as the number of electrons belonging to the atom $\boldsymbol{A}$ and the atomic charge then can be defined as:

$$q_A = Z_A - \sum_{\sigma \in A} (PS)_{\sigma\sigma} \tag{71}$$

Another useful concept is *bond order*. For a diatomic molecule, a *single bond* is formed when two valence electrons form an orbital, such as in a H_2 molecule. This is also called σ *bond* because it does not change when the axis system rotates along the bond. A double bond is also possible if two p electrons from each atom form a π *bond* which changes sign when the axis system rotates 180°. Similar to the definition of the atomic charge, the definition of the bond order is arbitrary too. The one used in this thesis is due to Mayer[16]:

$$B_{AB} = \sum_{\sigma \in A, \lambda \in B} (PS)_{\sigma\lambda} (PS)_{\lambda\sigma} \tag{72}$$

---

[a] This density matrix is referred to in the context of basis functions. The density matrix for the total wave function will be introduced later in this chapter.

It can be shown that this bond order has integer values equal to those predicted by the classical valence picture in the specific case of some homonuclear diatomics treated at the minimal basis level.

3.4. Electron Correlation

Although the HF theory and molecular orbital model provide a simple and clear explanation of the electronic wave function, it is only an approximation. The energy difference between the exact solution and the HF limit is called the *correlation energy* and the associated effect is called *the correlation effect.*

$$(\hat{H} - E_{HF})|\Phi\rangle = E_{corr}|\Phi\rangle \tag{73}$$

The correlation energy is a very small fraction of the total energy, but so are the dissociation energy and other energies associated with chemical processes. Furthermore, many molecular properties depend mainly or even solely on the correlation effect.

Qualitatively speaking, the HF method overestimates the probability that two electrons with opposite spins are close to each other. This happens because the electrons are formally assumed to be independent of one another. It can be understood through a probability interpretation of the wave function. For example, for a two-electron closed-shell system, the probability of finding an electron at position $\vec{r}$ with a HF wave function is:

$$p(\bar{r}) = \psi^*(\bar{r})\psi(\bar{r}) \tag{74}$$

where ψ is the only occupied orbital. The probability of finding the two electrons at points $\bar{r}_1$ and $\bar{r}_2$ respectively is:

$$p(\bar{r}_1,\bar{r}_2) = \Phi^*(\bar{r}_1,\bar{r}_2)\Phi(\bar{r}_1,\bar{r}_2) = \psi^*(\bar{r}_1)\psi(\bar{r}_1)\psi^*(\bar{r}_2)\psi(\bar{r}_2) = p(\bar{r}_1)p(\bar{r}_2) \tag{75}$$

which means the probability distribution of the electron 2 does not depend on the position of electron 1 . But in reality two electrons tend to stay away from each other because of the Coulomb repulsion between them and it should be less probable to find other electrons close to each other. Therefore each electron creates a hole, called the *Coulomb hole*, around itself.

In the next few sections, the methods of obtaining the correlation effect, variational and nonvariational, will be introduced. All these methods are based on the logical extension of the molecular orbital model by including many configurations instead of just one. The nonvariational methods are more efficient but they may lead to overestimation of the correlation energy.

3.4.1. Configuration interaction

Given a set of N basis functions for an n-electron system, C_n^{2N} distinct determinants or configurations can be formed. The HF configuration is only one of them

and it is the one with the lowest possible energy for a single configuration. Since the HF orbitals, including both occupied and virtual, are just a unitary transformation of the basis functions, we can use the HF orbitals as the reference to index the configurations. A new configuration can be formed by moving or "exciting" a certain number of electrons from the occupied orbitals to the virtual orbitals. Thus, the singly-excited configurations Ψ_i^a are formed by exciting one electron from an occupied orbital i to a virtual orbital a. The *doubly-excited configurations*, Ψ_{ij}^{ab}, are constructed by exciting two electrons. This process can be repeated until the number of excited electrons or the number of virtual orbitals is exhausted. The configurations constructed this way are then transformed to become the eigenfunctions of the spin operator, which is called *spin-adaption*. A trial wave function is then expanded in the space of these configurations:

$$\Phi = c_0\Psi + \sum_{i,a} c_i^a \Psi_i^a + \sum_{i<j,a<b} c_{ij}^{ab} \Psi_{ij}^{ab} + \sum_{i<jk,a<b<c} c_{ijk}^{abc} \Psi_{ijk}^{abc} \cdots = \sum_m c_m \Psi_m \quad (76)$$

A secular equation is obtained by the virtue of the variation principle under the normalization condition $\langle\Phi|\Phi\rangle=1$:

$$\sum_n (H_{mn} - Ec_n) = 0 \quad (77)$$

The last equation is also the Schrödinger eigenvalue equation in a linear space and can be solved by diagonalizing the *Hamiltonian matrix* $H_{mn} = \langle\Psi_m|\hat{H}|\Psi_n\rangle$. An element

of the Hamiltonian matrix has a form similar to Equation (58). Since the base vectors are many-electron functions, each eigenfunction whose eigenvalue is above the lowest one is an approximation to an *excited state*.

The method described above is called *configuration interaction* (CI). In a CI wave function, the orbitals are no longer formally independent of each other and an electron cannot be viewed as moving in the average potential field of the other electrons. Instead, the electrons, or the orbitals, are correlated. The CI expansion which includes all possible configurations with the proper space and spin symmetries is called *full-CI*. The completeness of a full-CI wave function is only limited by the completeness of the basis functions. The maximum recovery of correlation energy for a given basis set is the difference between the full-CI energy and the HF energy.

The CI method is conceptually simple and its energy is a vigourous upper-bound to the true wave function. Its drawback is that the number of configurations increases very rapidly with the excitation level. Even with today's computing power, a full-CI calculation is only possible for a system with a few electrons and a moderately-sized basis set. Progress needs to be made in two obvious directions: (i) solving the CI problem efficiently, and (ii) reducing the dimensionality by choosing only the important configurations.

Formally, the solution of Equation (77) involves the following steps: (i) obtaining HF orbitals, (ii) transforming the atomic orbital integrals into molecular orbital integrals as defined in Equation (58), (iii) selecting configurations and making the configurations symmetry and spin adapted, (iv) constructing the Hamiltonian matrix elements, and (v)

solving the eigenvalue problem. This creates two major computational bottlenecks for the CI method - the storage of the matrix elements and the solution of the eigenvalue problem.

The Hamiltonian matrix is usually very large (the square of the number of configurations can easily exceed hundreds of thousands) and the direct diagonalization is impossible in practice. On the other hand, only the few eigenfunctions (also called *roots*) with the lowest eigenvalues (low-lying electronic states) are normally of interest. Nesbet[17] showed that the burden of finding the lowest roots is far less than that of finding all the roots. His approach, which does not contain explicit diagonalization, is based on the minimization of *Rayleigh quotient*:

$$q(C) = \frac{C^T H C}{C^T S C} \tag{78}$$

It is stationary if, and only if, the vector C is an eigenfunction of the matrix H. An iterative optimization procedure is designed such that a trial vector is corrected for each step until $q(C)$ does not change. Davidson[18] proposed that a partial diagonalization can be used to accelerate convergence. Both of the Nesbet and Davidson's algorithms have been widely used in various CI methods.

The effort of calculating and storing the Hamiltonian matrix elements can be reduced because it has been noted very early that most of the Hamiltonian matrix elements are zero due to the fact that configurations that differ by three orbitals yield zero. The number of non-zero elements is reduced further by symmetry. Therefore,

the storage requirement for the Hamiltonian matrix elements is not as great as it appears to be. Furthermore, Roos[19] argued that the Hamiltonian matrix elements do not have to be calculated explicitly. After all, all that is need is the calculation of $\boldsymbol{HC}$, which needs only the storage proportional to the number of configurations as opposed to the square and can be evaluated, in principle, directly from the molecular integrals since the matrix elements themselves are a combination of these integrals. The coupling constants have been given[20] for the direct calculation of $\boldsymbol{HC}$ for *CI wave functions with single and double excitations* (CISD) with different spin states. The calculations of these coupling constants can be further simplified and generalized using the graphical unitary group approach[21], which gives tremendous insights into the Hamiltonian matrix.

The most convenient way to limit the number of configurations is to truncate the CI expansion at a certain excitation level. Since the reference HF configuration is already optimized and correct to the first-order (Brillouin theorem), it has been postulated that the highly excited configurations make only a negligible contribution. In reality, the CI expansion in most studies includes only the single and double excitations, i..e at the CISD level. The CISD energy accounts for more than 90% of the full-CI correlation energy for small molecules[22] and gives significant improvement over the HF energy. The problem with the CISD method is that it is not *size-consistent*, which arises when molecular dissociation is studied. A CISD treatment for the separated fragments implies quadruple excitations for the system as a whole whereas the CISD wave function for the bound molecule does not include any excitations beyond doubles. This problem also leads to the decreasing effectiveness of the CISD method with the increasing size of the

system. It has been found that at least quadruple excitations have to be included to obtain near-zero size-inconsistency.

Another way of limiting the CI expansion is to exclude some molecular orbitals from the excitations. Commonly, the doubly occupied core orbitals are not included if a valence property is desired. Also, the virtual orbitals with the highest orbital energies are often excluded from excitations because they are usually the antibonding orbitals for the core-shell orbitals.

On the other hand, it is often desirable to go beyond the CISD level. Since including the excitations higher than doubles is prohibitive, one way to include some higher excitations is to use configurations other than the HF one as the references. This approach is called the multireference CISD (MRCISD) method. A triple excitation is included in a MRCISD wave function by a double excitation from a singly-excited configuration and a quadruple excitation is obtained by a double excitation from a doubly-excited configuration. If the reference configurations are chosen properly, the most important triple and quadruple excitations can be included. More importantly, the full-CI limit can be approached by systematically expanding the reference space. The development of this method will be discussed in the next chapter.

3.4.2. Natural orbitals

A CI wave function can be qualitatively analyzed by using the coefficient of each configuration as a measure of its significance. The cost of this multiconfiguration picture

is that the simple single electron picture, the molecular orbital model in which the orbitals are either occupied or unoccupied, does not exist any more. Instead, every orbital included in the excitations is occupied at least once but not all the time. Its contribution is represented indirectly from the coefficients of the configurations which depend on the orbitals.

In their classic paper[23], Shull and Löwdin proposed the concept of a *natural spin orbital* as an optimized one-electron function for a correlated wave function. The natural spin orbitals are obtained by diagonalizing the electron density matrix. The definition of the density matrix is as follows:

$$\rho(\bar{r}_1\sigma_1,\bar{r}_1'\sigma_1') = N\sum_{\sigma_2\sigma_3}\int\Phi(\bar{r}_1\sigma_1,\bar{r}_2\sigma_2,\cdots)\Phi^*(\bar{r}_1'\sigma_1',\bar{r}_2\sigma_2,\cdots)d\bar{r}_2d\bar{r}_3\cdots \qquad (79)$$

Since the wave function is a linear combination of Slater determinants which are products of HF spin orbitals, the *first-order density matrix* can be expressed in terms of these spin orbitals $\psi_i(\bar{r})$[a]:

$$\rho(\bar{r},\bar{r}') = \sum\psi_i(\bar{r})\gamma_{ij}\psi_j^*(\bar{r}') \qquad (80)$$

It can be shown that the matrix γ_{ij} is Hermitian and can be diagonalized so that Equation (80) is written in a diagonal form:

---

[a] The subscript on $\bar{r}$ is dropped because the electrons are not distinguishable.

$$\rho(\vec{r},\vec{r}') = \sum n_i \eta_i(\vec{r})\eta_i^*(\vec{r}') \qquad (81)$$

The one-electron functions η_i are called natural spin orbitals and the n_i are the occupation numbers of the natural spin orbitals and are between 0 and 1. If the sum in Equation (81) is over spin variables, the spinless natural orbitals will be obtained, which are also known simply as the *natural orbitals* which possess occupation numbers between 0 and 2.

The concept of natural orbitals provides a simple physical picture of correlated electronic structures. One only needs to imagine that the occupation numbers are no longer integers in a more accurate theoretical treatment.

The concept also has a quantitative advantage. For a two-electron system, it can be shown that the number of configurations for a full-CI wave function with N spin-orbitals can be reduced from $\frac{N(N+1)}{2}$ to N. For many-electron systems, it has been verified by many calculations that the CI wave function with natural orbitals as one-electron basis functions converges faster than HF MOs. Based on this observation, Bender and Davidson[24] proposed an iterative CI calculation scheme which uses the natural orbitals from a truncated CI calculation as the basis for the next step of a CI calculation until convergence is reached. 88.7% of the correlation energy was recovered from a CI wave function of 45 configurations out of 270,000. Another method explicitly based on the natural orbital concept is the *paired natural orbital CI* (PNO-CI) method[25]. The natural orbitals are also used in almost all other correlation methods implicitly,

mainly for faster convergence and for choosing the important orbitals.

3.4.3. Multi-configuration SCF method

The Hartree-Fock method was originally used for atomic systems because of their high symmetry. A different formula was used for the first qualitatively satisfactory quantum-mechanical study of H_2 by Heitler and London in 1927. Their trial function was based on the simple intuitive idea that the trial wave function should be composed of the atomic wave functions since a molecule is composed of atoms:

$$\Psi = c_1\psi_a(1)\psi_b(2) + c_2\psi_a(2)\psi_b(1) \tag{82}$$

where ψ_a and ψ_b are the wave functions of the ground state of the hydrogen atom on atoms a and b, respectively. c_1 and c_2 are the variables to be determined by the variation principle. Due to the symmetry of the system, the solution is obvious:

$$\Psi = C(\psi_a(1)\psi_b(2) + \psi_a(2)\psi_b(1))(\alpha(1)\beta(2) - \alpha(2)\beta(1)) \tag{83}$$

where C is the normalization factor. The total energy can be expressed as:

$$E - 2E_{atom} = \frac{J + K}{1 + S^2} \tag{84}$$

where S is the overlap integral, J is the total Coulomb energy and K is the exchange energy. The Heitler-London method gives the explanation of the origin of chemical bonding and the correct dissociation behaviour. At a short distance, e.g. around the equilibrium bond length, the electrons gain energy by moving in a larger area due to the exchange effect. In addition, each of them is attracted by the nucleus of the other atom. At infinity, J, K and S become zero and the trial function becomes the exact wave function of two infinitely separated hydrogen atoms, assuming ψ_a and ψ_b are the exact wave function of the ground state of the hydrogen atom. The H-H chemical bond is formed through the coupling of the electron from each atom and the identities of the atoms are maintained through the atomic valence orbitals shown in the final wave function.

In contrast, a molecular orbital model would give a different picture. If the HF method is used with the basis functions ψ_a and ψ_b, a doubly occupied orbital will be obtained:

$$\psi_1 = \psi_a + \psi_b \tag{85}$$

and the spatial part of the wave function becomes (with the spin function omitted since

it is the same as in Equation (83)[a]):

$$\Psi = C(\psi_a(1)\psi_b(2) + \psi_a(2)\psi_b(1) + \psi_a(1)\psi_a(2) + \psi_b(1)\psi_b(2)) \qquad (86)$$

Compared with the Heitler-London wave function (Equation (83)), the HF wave function has two more terms corresponding to the H^-H^+ state of the two atoms. At infinite separation, it leads to an equal superposition of HH and H^-H^+, resulting in the wrong dissociation behaviour. The reason for this problem is not hard to understand: the HF method for a closed-shell system requires the two electrons to remain in the same orbital which is contrary to the reality of two separated atoms.

If Equation (83) is rewritten in terms of the virtual HF orbital $\psi_2 = \psi_a - \psi_b$, its spatial part becomes:

$$\Psi = C(\frac{1}{1-S^2}\psi_1(1)\psi_1(2) - \frac{1}{1+S^2}\psi_2(1)\psi_2(2)) \qquad (87)$$

---

[a] A false impression may arise that the spin function for a two-electron system is not important since it is separable from the spatial part and thus does not contribute to the evaluation of energy. Although a UHF-like trial function $\det[\psi_a\alpha\psi_b\beta]$ would lead to the correct dissociation behaviour, it does not have the right symmetry because the spin-orbitals on the two atoms are different. In fact, a symmetry adapted UHF procedure, as pointed out in Section 3.1.1, will always lead to a spin-restricted result for a system with equal numbers of α and β electrons. On the other hand, the Heitler-London wave function can be obtained using the ROHF method. In the ROHF method, the system has two open-shell orbitals (ψ_a and ψ_b) and zero total spin. To start, one can make the product $\psi_a(1)\alpha(1)\psi_b(2)\beta(2)$ the eigenfunction of $\hat{S}^2$ and obtain $\psi_a(1)\psi_b(2)(\alpha(1)\beta(2) - \alpha(2)\beta(1))$. To make it antisymmetric with respect to the exchange of the two electrons, one adopts the form of Equation (83).

One can see that the Heitler-London wave function is a superposition of two HF configurations. The first one represents the attracting or *bonding* tendency of the two atoms and the second corresponds to the repulsive or *antibonding* tendency of the atoms. At a short distance, the overlap integral S is large and the bonding configuration is dominant, resulting in a chemical bond. At infinity, S vanishes and the wave function becomes an equal sum of the two configurations with the opposite effects, resulting in two equivalent valence orbitals. According to the principle of superposition (Section 2.3), the bonding and antibonding states exist at the same time and their probabilities of happening depend on the distance between the two atoms. The molecular orbital model fails at the dissociation limit because it includes only the bonding configuration and cannot dissociate into two valence orbitals.

To generalize the Heitler-London treatment of the hydrogen molecule, one can see that a chemical bond is formed from a pair of valence orbitals from different atoms involving electrons possessing opposite spins. This extended Heitler-London theory is called *valence-bond theory* (VB). The mathematical aspect of that theory is the general valence bond (GVB) theory[26]. A GVB trial wave function is similar to a HF one, closed-shell or open-shell, except that it involves one pair-function for each chemical bond with the form $\psi_{ia}\psi_{ib}(\alpha\beta - \alpha\beta)$ instead of a simple product of a one-electron function. For mathematical convenience, an orthogonal form similar to Equation (87) is usually taken, leading to the following form of a trial function:

$$\Psi = \det[\{core\}\{(c_{11}\psi_{11}\psi_{11} - c_{12}\psi_{12}\psi_{12})\alpha\beta(c_{21}\psi_{21}\psi_{21} - c_{22}\psi_{22}\psi_{22})\alpha\beta\cdots\}\{open\}] \quad (88)$$

The molecule orbital ψ_i, which is a linear combination of basis functions, and the coefficients in the pair functions need to be optimized simultaneously. This is done by a SCF procedure. The energy expression of the above trial function is similar to Equation (41), only that the coefficients a, b and f contain variables c_{p1} and c_{p2}. Thus, the orbitals can be obtained in a similar fashion to the ROHF methods and then c_{p1} and $_{p2}$ are optimized for each pair while the other orbitals remain unchanged. The whole process is repeated until self-consistency is reached.

A GVB wave function (Equation (88)) can be expanded as a linear combination of determinants. Unlike a HF configuration where all the doubly occupied orbitals remain occupied all the time, there are more orbitals designated for double occupancy than the number of paired-electrons, from which the configurations corresponding to the dissociated states are chosen. In such a wave function, unlike a HF wave function, the orbitals are not formally independent of each other any more. Instead, they are correlated.

The GVB method is a special case of a correlation theory known as multiconfiguration SCF (MCSCF). Similar to a CI wave function, an MCSCF wave function is a linear combination of a number of configurations. The difference is that the orbitals and the coefficient of each configuration in an MCSCF wave function are optimized simultaneously. Obviously, the MCSCF procedure will yield a lower energy

than the CI method at the same length of configuration expansion but the procedure will take a longer time because each step of it involves a CI calculation. The basic assumption of MCSCF theory is that most of the important chemical and physical aspects of interaction in a given system can be represented by a wave function consisting of a few terms when the single HF configuration is not adequate. It often happens that the HF methods do not give a qualitatively correct picture because the multiconfiguration nature of the chemical bond as described by valence-bond theory. One dramatic example is the F_2 molecule. The one-configuration restricted HF method predicts that the energy of F_2 is higher than the sum of two F atoms. The two configuration MCSCF wave function of Das and Wahl[27] reverses that conclusion.

Although there have been numerous MCSCF studies, selecting the few most important configurations for an MCSCF wave function is still more or less an art and a great deal of insight into the particular system is needed[28]. It is also quite possible that the significance of the configurations changes with the molecular rearrangements. On the other hand, from the valance-bond analysis we know that the low-lying states of a molecule can always be described as the coupling of atomic valence electronic structures. In other words, valence orbitals and valence electrons are dominant during molecular rearrangements. Based on this point of view, Roos et al[29] and Ruedenberg et al[30] proposed independently that a full-CI expansion in the space of the valence orbitals of all the atoms be used as an MCSCF wave function. The advantage of this approach is that it allows the free interaction of all configurations which may become significant during molecular rearrangements so that all pertinant changes can be reflected without

bias in the calculations. This method is known as the *complete active space SCF* (CASSCF) or *fully-optimized reaction space* (FORS) method.

3.5. Nonvariational Post-HF Methods

3.5.1. Perturbation theories

Since the correlation energy is only a small fraction of total energy, it can be naturally treated as a perturbation to the HF solution with the hope that it will cost less than the variational treatment.

All quantum chemistry perturbation methods are based on Rayleigh-Schrödinger (RS) perturbation theory. In the RS theory, the configurations are organized by the magnitude of their contributions in proportion to the magnitude of the perturbation term in the Hamiltonian operator. Suppose that the total Hamiltonian $\hat{H}$ is the sum of the unperturbed Hamiltonian $\hat{H}_0$ and the perturbation $\hat{V}$. We can rewrite the Schrödinger equation as:

$$(\hat{H}_0 + \lambda \hat{V})|\Phi\rangle = E|\Phi\rangle \tag{89}$$

where the parameter λ is introduced to represent the magnitude of the perturbation. If the (2) were solved exactly, one would obtain the exact eigenfunctions and eigenvalues

as a Taylor series in λ:

$$E = E^{(0)} + \lambda E^{(1)} + \lambda^2 E^{(2)} + \cdots \tag{90}$$

$$|\Phi\rangle = |\Phi^{(0)}\rangle + \lambda|\Phi^{(1)}\rangle + \lambda^2|\Phi^{(2)}\rangle + \cdots \tag{91}$$

By substituting Equations (90) and (91) into Equation (89) and expanding the perturbation functions $|\Phi^{(i)}\rangle$ with the unperturbated eigenfunctions $|\Phi_j^{(0)}\rangle$, one obtains the following perturbation energies and functions for the ground state by equating the terms with the same power of λ:

$$E^{(1)} = \langle\Phi_0^{(0)}|\hat{V}|\Phi_0^{(0)}\rangle \tag{92}$$

$$\Phi^{(1)} = \sum \frac{\langle\Phi_i^{(0)}|\hat{V}|\Phi_0^{(0)}\rangle}{E_0^{(0)} - E_i^{(0)}} \tag{93}$$

$$E^{(2)} = \sum \frac{\langle\Phi_0^{(0)}|\hat{V}|\Phi_l^{(0)}\rangle\langle\Phi_l^{(0)}|\hat{V}|\Phi_0^{(0)}\rangle}{E_0^{(0)} - E_l^{(0)}} \tag{94}$$

. . .

The most widely used quantum chemistry perturbation method to recover the correlation effect originated from Møller and Plesset's work[7] in 1934. They took the sum of the Fock operators for each occupied orbital as the zeroth-order approximation:

$$\hat{H}_0 = \sum \hat{F}(i) = \langle \Phi_0^{(0)} | \sum_{i<j} \frac{1}{r_{ij}} | \Phi_0^{(0)} \rangle \qquad (95)$$

where the second term takes away the double-count of Coulomb interactions between the occupied orbitals. Then the perturbation term becomes:

$$\hat{V} = \hat{H} - \hat{H}_0 \qquad (96)$$

This method is well known as *Møller-Plesset perturbation theory*, denoted as MPn in which n stands for the perturbation level. One important feature of the RS perturbation theory is that the energy obtained at any perturbation level is size consistent. This becomes obvious in terms of cluster expansions which are discussed in the next section.

3.5.2. Cluster expansions

The wave function of a supersystem consisting of two noninteractive subsystems is the multiplication of the wave functions of the two subsystems. A double excitation on the subsystems will result in a quadruple excitation of the supersystem. This type of excitation is called an *unlinked cluster* whose expansion coefficient is obtained by the

multiplication of the coefficients of the two separate double excitations. Now, if we let the subsystems interact with each other, the unlinked clusters should still exist and the total excitations should be the sum of the unlinked clusters and *linked clusters*. The latter vanish when the supersystem is separated.

If we use the concept of linked and unlinked clusters to analyze the CI expansion at the level of double excitation (CID), we can see that the reason that it is not size-consistent is that it does not contain unlinked quadruple excitations which are the simultaneous double excitations for the separated system. If we simply add the unlinked quadruple excitations to the expansion, the trial wave function becomes:

$$\Phi = c_0\Psi + \frac{1}{2}\sum c_{ij}^{ab}\Psi_{ij}^{ab} + \frac{1}{32}\sum \hat{P}_{ijkl}^{abcd} c_{ij}^{ab} c_{kl}^{cd} \Psi_{ijkl}^{abcd} \qquad (97)$$

where $\hat{P}_{ijkl}^{abcd}$ is the antisymmetry operator over the MO indexes. The above wave function contains nonlinear terms and is very difficult to optimize variationally. Instead, in the *coupled cluster approximation* (CCA), Equation (73) is integrated successively by Ψ, Ψ_{ij}^{ab} and Ψ_{ijkl}^{abcd} for both sides and the correlation energy and the expansion coefficients are obtained iteratively. Since the CCA equations are usually solved non-variationally, it is possible to obtain more than 100% of the correlation energy.

The approximation of excluding the linked quadruple excitations makes physical sense. The Hartree approximation assumes that the probability of finding one electron at a specific position is independent of the positions of the other electrons:

$$p(\bar{r}_1,\bar{r}_2,\bar{r}_3,\bar{r}_4,\cdots) = p_1(\bar{r}_1)p_2(\bar{r}_2)p_3(\bar{r}_3)p_4(\bar{r}_4)\cdots \quad (98)$$

so that the trial wave function has the form of a Slater determinant. The next logical improvement in the approximation is that the probability is dependent on the position of one of the other electrons, i.e. the correlation is paired:

$$p(\bar{r}_1,\bar{r}_2,\bar{r}_3,\bar{r}_4,\cdots) = p_{12}(\bar{r}_1,\bar{r}_2)p_{34}(\bar{r}_3,\bar{r}_4)\cdots \quad (99)$$

Furthermore, the pair functions or orbitals can be written as a correction to the independent functions:

$$\phi(\bar{r}_1,\bar{r}_2) = \phi_1(\bar{r}_1)\phi_2(\bar{r}_2) + u_{12}(\bar{r}_1,\bar{r}_2) \quad (100)$$

By applying the antisymmetric operator to the paired products and expanding $u_{ij}(\bar{r}_i,\bar{r}_j)$ in the MO space, one can obtain a function which includes all the unlinked clusters as the products of double excitations. The particular truncation in Equation (97) is called coupled clusters with doubles (CCD).

3.6. Density Functional Theory

All the quantum chemistry methods discussed in the previous sections are based on the orbital model. Since we know that an electron in an orbital does not have a

precise position at any time and an orbital is not a trajectory but rather extends everywhere in space, a picture of an electron cloud is probably more appropriate. The mathematical representation of such a cloud is the electron density.

A *reduced nth-order density matrix*, which contains spin variables, is defined as[a]:

$$\rho(1',2',\cdots,n',1,2\cdots,n) = C_n^N \int\int\cdots\int \Phi^*(1',2',\cdots,n,n+1',\cdots,N)\Phi(1,2,\cdots,n,n+1,\cdots,N)d(n+1)d\cdots dN \quad \textbf{(101)}$$

Obviously, a lower-order density matrix can be derived from a higher-order density matrix. When i is set to equal to i', the density matrix becomes the *density* with n variables, which is also the probability for simultaneously finding n electrons at the specified positions and spins according to the probability interpretation of the wave function (Section 2.1). For example, we can write symbolically the probability of finding one electron at position and spin 1 and another at position and spin 2 as a second-order density $\rho(1,2,1,2)$ or simply $\rho(1,2)$. We have also seen the first-order density matrix in Section 3.4.2.

As introduced in Chapter 2, the Hamiltonian with the Born-Oppenheimer approximation for an electronic system is composed of the kinetic energy operator $\hat{T} = \sum_i \hat{t}_i$, the electron-electron interaction $\hat{V}_{ee} = \sum_{i<j} r_{ij}^{-1}$ and an external electric field

---

[a] Note that the numbers 1, 2, etc are used here to symbolize the space and spin coordinates of the electrons $\bar{r}_1\sigma_1$, $\bar{r}_2\sigma_2$, etc. Please also note that the integration over the spin coordinates is actually summation.

$v(\vec{r})$, typically the Coulomb potential due to the nuclei. Equation (4) can be rewritten as follows:

$$\hat{H} = \hat{T} + \hat{V}_{ee} + \hat{v}(\vec{r}) = \sum_i \hat{t}_i + \sum_{j>i} r_{ij}^{-1} + \hat{v}(\vec{r}) \tag{102}$$

The energy expression can then be written in terms of the reduced density matrix[a]:

$$\begin{aligned} E &= \langle \Psi | \sum_i \hat{t}(i) + \sum_{j>i} r_{ij}^{-1} + \hat{v}(\vec{r}) | \Psi \rangle \\ &= N \langle \Psi | \hat{t}(1) | \Psi \rangle + C_N^2 \langle \Psi | r_{12}^{-1} | \Psi \rangle + N \langle \Psi | v(r) | \Psi \rangle \\ &= \int (\hat{t}(1) \rho(1',1))_{1'=1} d1 + \int r_{12}^{-1} \rho(1,2,1,2) d1 d2 + \int v(1) \rho(1,1) d1 \end{aligned} \tag{103}$$

Although from the above equation it appears that the second-order density matrix is all that is needed, it turns out that such a matrix has to be derivable from the wave function. This condition, called *N-representability*, is yet not known and one still has to obtain the wave function for an accurate solution.

However, Hohenberg and Kohn[31] were able to prove that none of the density matrices are needed to determine formally the energy of the ground state of an electronic system in an external field. The energy is determined only by the first-order electronic density (defined as the density hereafter) of the system. They found that the external field has a one-to-one mapping to the density of the ground state. Since the external field determines the Hamiltonian, the latter is decided by the density and the variation

[a] The first equal sign in Equation (103) is due to the indistinguishability of electrons.

principle can be written as:

$$E(\rho) \geq E_0(\rho_0) \tag{104}$$

in which ρ_0 is the exact density of the ground state. These conclusions are called *the Hohenberg-Kohn theorems*, which form the basis of the *density functional theory* (DFT) which will be discussed in this section.

Despite the fact that the proof of the Hohenberg-Kohn theorems is almost trivial, they are truly remarkable because any well-behaved density function is N-representable. As evidenced from the discussions in the preceding sections in this Chapter, so much effort has been spent on obtaining the accurate many-body wave function, but all that is actually needed is an accurate density, which is a one-particle function.

The major challenge for DFT is to obtain the energy from the density. Although the density is ultimately the only variable needed, the energy expression in Equation (103) shows that the calculation of the kinetic energy depends on the first-order density matrix and that of the electron-electron interaction energy on the second-order density. Only the energy due to interaction with the external field can be calculated directly from the density. It is not yet known how to obtain the exact N-representable first-order density matrix and second-order density from an exact ground state density although a one-to-one map between the two does exist. Therefore, approximations have to be made.

In order to find a way to approximate the relationship between these quantities, the Slater determinant, the simplest trial wave function with the antisymmetry, should be

considered. One can show that the second-order density of a unrestricted Slater wave function is determined by the first-order density matrix:

$$\rho(1,2,1,2) = \frac{1}{2}(\rho(1,1)\rho(2,2) - \rho(1,2)\rho(2,1)) \tag{105}$$

where the first-order density matrix is expressed in terms of spin-orbitals:

$$\rho(1',1) = \sum \psi^*(1')\psi(1) \tag{106}$$

V_{ee} then becomes:

$$V_{ee} = \frac{1}{2}\int \rho(1,1) r_{12}^{-1} \rho(2,2) d1d2 - \frac{1}{2}\int \rho(1,2) r_{12}^{-1} \rho(2,1) d1d2 = J + E_x \tag{107}$$

Comparing with the UHF energy expression in Equation (25), the quantity J is the Coulomb energy between electrons and E_x is the exchange energy. This can be seen by realizing that in the expression for the first-order density matrix (Equation (106)), $\rho(1,2)$ is zero if the two electrons have different spins. Now the total energy can be written formally as the sum of the HF energy and the correlation energy E_c using the density as the variable:

$$E(\rho) = T(\rho) + V_{ee}(\rho) + \int v\rho d\vec{r} = T(\rho) + J(\rho) + E_x(\rho) + E_c(\rho) + \int v\rho d\vec{r} \quad (108)$$

One approach is to approximate all the terms in the above equation by the density so that the energy is expressed in terms of the density only. This idea was pioneered by Thomas[32], Fermi[33] and Dirac[34] in the 1920's and 1930's. Their approach is to approximate the electrons in an atom in the configuration space of a many noninteractive electron gas system. The result is that the kinetic energy, and also the total energy, may be assumed to be continuous and an approximate first-order density matrix is obtained in terms of the density. The problems with this model are the accuracy and the applicability to molecules. The early calculations showed that the energies of atoms are as much as 20% different from the HF results and the errors are mainly caused by the approximate kinetic energy functional. The least computational cost is obtained by using the density as the variable and, therefore, this area is still pursued vigorously[35].

The mainstream approach of DFT is to use the first-order density matrix as the variable, as first suggested by Kohn and Sham[36]. Instead of using the density as the variable, they loosened the requirement a bit and used the first-order density matrix, or the one-electron orbital as in Equation (106). By analogy with a many-electron system (such as atoms or molecules) to a non-interactive system with an effective field on each electron, it can be shown that it is possible in principle to obtain the exact kinetic energy with a Slater determinant composed of the orbitals. In DFT, these orbitals are called the *Kohn-Sham (KS) orbitals*. The KS orbitals are N-representable because they are

derivable from a Slater determinant. Comparing Equation (106) with the natural spin orbital expansion (Equation (81)) the occupation for each KS orbital is one.

To obtain the KS orbitals, the variation principle is applied to the energy expression as in Equation (108):

$$0 = \sum_i \left(\frac{\partial T(\rho)}{\partial \rho} + \frac{\partial J(\rho)}{\partial \rho} + \frac{\partial E_x(\rho)}{\partial \rho} + \frac{\partial E_c(\rho)}{\partial \rho} + v\right)\frac{\partial \rho}{\partial \psi_i} \qquad (109)$$

under the condition that all the orbitals are normalized and orthogonal to each other as expressed in Equation (24). The relationship between the density and the orbital is defined as in Equation (106) by equalizing 1 and $1'$. Following the procedure similar to the one in Section 3.1.1, one obtains the following effective one-electron eigenvalue equation:

$$\left(\hat{t} + v + \int \frac{\rho(\vec{r}')}{|\vec{r}-\vec{r}'|}d\vec{r}' + \frac{\partial E_x(\rho)}{\partial \rho} + \frac{\partial E_c(\rho)}{\partial \rho}\right)|\psi_i\rangle = \epsilon_i|\psi_i\rangle \qquad (110)$$

which can be solved by a SCF procedure.

From the practical point of view, the concept of KS orbitals makes DFT similar to the conventional *ab initio* methods. With KS orbitals, one may obtain the kinetic energy T and the Coulomb energy J with an accuracy similar to that of the HF level and leave the necessary adjustments to the exchange and correlation terms. Furthermore, the exchange energy can be obtained almost exactly with the orbitals (with additional computational costs), leaving the needed correction to the correlation term, which is

exactly what the conventional *ab initio* theories are designed to achieve. The difference is the computational cost. Since the correlation energy is parameterized with the density in DFT, it can be computed at the same cost as that of the HF methods. The low computational cost is the main advantage of DFT methods. Therefore, the greatest challenge in DFT is to obtain the correlation functionals $\frac{\partial E_x(\rho)}{\partial \rho}$ and $\frac{\partial E_c(\rho)}{\partial \rho}$.

Finally, it should be noted that a similar method, called the X_α method, was proposed by Slater[37] in the 1950's and has been applied widely in chemistry and physics. The Hohenberg-Kohn theorems put this idea on a solid theoretical foundation and establish the directions for further improvements.

Chapter 4.

Wave Functions for the Spin Density

The electron spin density is the difference between the densities of α and β electrons and can be measured experimentally as the hyperfine structure (HFS). The accurate prediction of the HFS of a radical poses a major challenge to *ab initio* quantum chemistry. Even with today's state-of-the-art theoretical methods and computer power, there are often large discrepancies between theoretical predictions and experimental values. This chapter begins with a discussion of spin density and the experimental measurement of the HFS. A discussion of the current status of theoretical studies of the HFS is followed by the results of the present research which focuses on the study of the requirements placed on the wave functions and basis sets for accurate predictions of the HFS of a radical.

4.1. Spin Density

For a single determinantal wave function such as a UHF or ROHF wave function, the spatial part of each spin orbital which is occupied by an electron is associated with a spin state and the electron density for a particular spin is just the sum of the orbital

densities of the orbitals with that particular spin σ, i.e.[a],

$$\rho^{\sigma}(\bar{r}) = \sum \psi^{\sigma^*}(\bar{r})\psi^{\sigma}(\bar{r}) \tag{111}$$

which can be derived directly from the first-order density matrix (Equation (106)). Analogously, one can obtain the density for the spin σ for a multi-determinantal wave function, such as a CI wave function, in terms of natural spin orbitals (see Equation (81)):

$$\rho^{\sigma}(\bar{r}) = \sum n_i \eta_i^{\sigma}(\bar{r})\eta_i^{\sigma^*}(\bar{r}) \tag{112}$$

Then the spin density becomes:

$$\rho_s(r) = \rho^{\alpha}(r) - \rho^{\beta}(r) \tag{113}$$

In order for the spin density to be an observable, a corresponding Hermitian operator should exist according to the basic principles of quantum mechanics. The following operator serves the purpose:

$$\hat{\rho}_s(\bar{r}) = 2\delta(\bar{r}' - \bar{r})\hat{S}_z \tag{114}$$

where $\hat{S}_z = \sum \hat{S}_{zi}$ and δ is the Kronecker delta which is one when $\bar{r}' = \bar{r}$ and zero

[a] The superscript is used here to emphasize that each orbital in the equation is associated with a spin state.

otherwise.

To show that the $\hat{\rho}_s(\vec{r})$ will yield the spin density, we can use the first-order density matrix expanded in terms of the natural spin orbitals since the $\hat{S}_z$ is a one-electron operator:

$$\begin{aligned}\langle\Psi|\hat{\rho}_s(\vec{r})|\Psi\rangle &= \sum n_i\langle\eta_i^{\alpha}(\vec{r}_1)\alpha|\hat{\rho}_s(\vec{r})|\eta_i^{\alpha}(\vec{r}_1)\alpha\rangle + \sum n_i\langle\eta_i^{\beta}(\vec{r}_1)\beta|\hat{\rho}_s(\vec{r})|\eta_i^{\beta}(\vec{r}_1)\beta\rangle \\ &= \sum n_i\langle\eta_i^{\alpha}(\vec{r}_1)|\delta(\vec{r}-\vec{r}_1)|\eta_i^{\alpha}(\vec{r}_1)\rangle - \sum n_i\langle\eta_i^{\beta}(\vec{r}_1)|\delta(\vec{r}-\vec{r}_1)|\eta_i^{\beta}(\vec{r}_1)\rangle \\ &= \rho_s(r)\end{aligned} \tag{115}$$

More often, a normalized spin density is used, i.e. the spin density divided by the number of unpaired electrons which is equal to $2m_s$.

4.2. Spectroscopic Measurement of Spin Density

Generally speaking, a spectroscopic measurement is an observation of the transitions between the discrete energy levels of a system. When the system changes its state from one energy level to another, it will yield or absorb energy by emission or absorption of light whose frequency ν is determined by the difference between the two energy levels according to the following relationship:

$$h\nu = \Delta E \tag{116}$$

The inter-dependence between spectroscopy and theory is obvious. Theoretical results depend on spectroscopic measurements for verification, as the energy levels and the transition intensity can be calculated theoretically from solving the eigenvalue problem of the Hamiltonian operator. On the other hand, the interpretation of the spectrum replies on theoretical analysis of the interactions among different factors.

4.2.1. Hyperfine interaction

As mentioned in Section 2.5.2, the electronic spin is the intrinsic angular momentum of the electron. This angular momentum generates a magnetic moment μ_e:

$$\hat{\mu}_e = -g_e \beta_e S \tag{117}$$

where S, which is introduced for convenience, is a spin operator whose eigenvalue is the quantum number only, i.e. $S = \frac{1}{\hbar}\hat{S}$. Similarly, a nucleus may have spin and generates the magnetic moment $\mu_N = g_N \beta_N I$. β_e and β_N are called *magnetons*, and g_e and g_N are the g factors, respectively, for electrons and nuclei.

The two magnetic moments produce magnetic fields which interact with each other, resulting in an interaction, called the *hyperfine interaction*. The hyperfine interaction has two parts. One is the so-called *Fermi contact interaction* whose

Hamiltonian is:

$$\hat{H}_{iso} = \frac{8\pi}{3} g_e \beta_e g_N \beta_N \delta(\bar{r} - \bar{r}_N) \boldsymbol{I} \cdot \boldsymbol{S} \tag{118}$$

where $\bar{r}_N$ is the position of the nucleus. The Fermi contact interaction is a pure quantum mechanical effect. The other is the classical dipole-dipole interaction between two magnetic moments:

$$H_{ani} = \frac{\hat{\mu}_N \cdot \hat{\mu}_e}{r^3} - \frac{3(\hat{\mu}_N \cdot \bar{r}) \cdot (\hat{\mu}_e \cdot \bar{r})}{r^5} \tag{119}$$

Since the hyperfine interaction is very small compared to the total energy of the system, it can be treated as a perturbation and the first-order RS perturbation energy can be obtained as in Equation (92). Then the hyperfine interaction Hamiltonian can be written as

$$\hat{H} = \boldsymbol{I} \cdot \boldsymbol{A} \cdot \boldsymbol{S} \tag{120}$$

where $\boldsymbol{A}$ is a matrix or *tensor*. The Fermi contact part of $\boldsymbol{A}$, which is called the *isotropic hyperfine* coupling constant (ICC), is calculated as:

$$A_{iso} = \frac{8\pi}{3} g_e \beta_e g_N \beta_N \rho(\bar{r}_n) \tag{121}$$

where $\rho_s(\vec{r}_n)$ is the normalized spin density at the nucleus. The anisotropic part is calculated as:

$$A_{ani} = g_e\beta_e g_N\beta_N\int(3\vec{r}\vec{r} - r^2)r^{-5}\rho_s(\vec{r})d\vec{r} \qquad (122)$$

and is known as the *anisotropic coupling tensor*. The unit for HFS couplings is gauss (G) or hertz (Hz). 1 G is equal to 2.8025 MHz.

4.2.2. Electron spin resonance

There are only a finite number of electronic and nuclear spin states and the eigenfunctions and eigenvalues of the hyperfine interaction Hamiltonian can be solved easily in the linear space of these states[38]. A simple but useful case is that the anisotropic coupling is zero, which happens when the anisotropic effect is averaged to zero due to molecular motions, and the energy expression becomes:

$$E = A_{iso}m_I m_S \qquad (123)$$

where m_I and m_S are the eigenvalues of I_z and S_z, corresponding to the angular momentum along the z axis. In principle, one could obtain A_{iso} by directly observing the energy change between different m_Is and m_Ss. But this energy change is too small to detect. Instead, they are obtained as the small splittings of other large frequencies.

One of these large frequencies is due to the electronic Zeeman effect.

When an atom or a molecule is placed in a magnetic field $\bar{H}$, the Hamiltonian for the interaction between this external magnetic field and the nuclear and electronic magnetic moments generated from their spins becomes:

$$\hat{H} = g_e \beta_e \bar{H} \cdot S + I \cdot A \cdot S + g_n \beta_n \bar{H} \cdot I \qquad (124)$$

The first term in the above equation is the *Zeeman interaction*, which is the dominant term. The last term corresponds to *nuclear magnetic resonance* (NMR) spectroscopy and is normally too small to be considered here.

The energy expression for the Zeeman interaction is:

$$E = g_e \beta_e H m_S \qquad (125)$$

Not all the transitions between energy levels can be observed. The selection rule is that $\Delta m_S = \pm 1$. Therefore, the observed energy difference is

$$\Delta E = g_e \beta_e H \qquad (126)$$

This transition is the one of interest in *electron spin resonance* (ESR) spectroscopy.

If no other effects are involved, a single energy transition or line would be observed in an ESR experiment which would provide little information other than the electronic g factor. However, from Equation (124), one can see that the transition

between different electronic spin states is coupled with the nuclear spins through the hyperfine interaction. Therefore, the transition energy now depends on the nuclear spin state. For a pure isotropic coupling, for instance, the energy difference becomes:

$$\Delta E = g_e \beta_e H + A_{iso} m_I \tag{127}$$

which means $2I + 1$ different lines evenly spaced with the distance A_{iso} will be observed for m_Is from $-I$ $-I + 1$, to I. This type of spectrum is also called *hyperfine structure*.

4.2.3. Rotational spectroscopy

ESR is not the only spectroscopic method to obtain the HFS. When a molecular rotational spectrum is studied, the splittings due to the hyperfine interactions can also be observed. This is because the rotational angular momentum L will generate a magnetic moment. This magnetic moment will interact with the nuclear magnetic moment. This interaction is further complicated due to the hyperfine interactions between the nuclear spin and the electronic spin. The hyperfine coupling constants are obtained by fitting the experimental data into a coupling model[39].

4.3. Previous Theoretical Calculations of Spin Densities

4.3.1. Simple models

The simplest model to describe the spin density is the ROHF model in which the spin density is decided only by the singly-occupied orbitals since the doubly-occupied orbitals have two electrons with opposite spins. A simple example would be the lithium atom whose electronic configuration is $(1s)^2(2s)^1$ and whose spin density is decided by the singly-occupied ($2s$) orbital. The anisotropic couplings obtained with ROHF are generally in good agreement with experiment, and are not strongly basis set dependent. The ROHF wave function, however, would yield a false zero spin density at the nucleus for the atom nitrogen. The electronic structure of the nitrogen atom is qualitatively described as $(1s)^2(2s)^2(2p_x)^1(2p_y)^1(2p_z)^1$ with each p orbital occupied by one electron with the same spin. Since the spin density is from the three p orbitals that are zero at the nucleus, the ROHF wave function would predict a zero Fermi contact term. From experiment we know, however, that the nitrogen atom has a small isotropic coupling. In order to obtain a nonzero spin density at the nucleus, the s orbitals of the α electrons should be allowed to be different from those of the β electrons. This phenomenon is called *spin polarization*. The simplest wave function to obtain the spin polarization is UHF, in which no restriction is applied to the orbitals with different spins. For the same example, the UHF electronic structure of the nitrogen atom is $(1s)^1(1s)'^1(2s)^1(2s)'^1(2p_x)^1(2p_y)^1(2p_z)^1$. The slight difference between each pair of s

orbitals results in a net spin density at the nucleus.

The UHF model also helps to understand the signs of isotropic coupling constants. For the NH_2 radical, the singly occupied orbital is a nitrogen *p* orbital. From the UHF energy expression (Equation (25)) one can see that the exchange term is favoured when two electrons with the same spin are close to each other. Therefore, when spin polarization happens, the electrons close to the nitrogen tend to have the same spin as that of the unpaired electron in the nitrogen *p* orbital, whereas the electrons around the hydrogens tend to have the opposite spin. This results in a positive sign for the isotropic coupling constant of nitrogen and a negative sign for the hydrogen atoms.

For the open-shell systems whose singly occupied orbital(s) do not possess a nodal plane through the nuclei (that is, *s-type orbitals*), the spin polarization contribution to the Fermi contact term is much smaller than the contribution from the singly occupied orbital(s). The UHF method works well for this type of system quantitatively. An early study on the ground state of lithium[40] showed that the correlation effects were found to be only about 0.5%. For the so-called π *molecules* whose unpaired orbitals have nodal planes through the nuclei (that is, *p-type orbitals*), the UHF method tends to overestimate the spin polarization effect. The amount of overestimation can be very large. For example[41], the A_{iso}(^{13}C) for the planar methyl radical calculated with the UHF method and a contracted [631/41] basis set is 57.8 G, compared with the experimental value 27 G. This is largely due to the fact that a UHF wave function is not an eigenfunction of $\hat{S}^2$, as pointed out in Section 3.1. It is a linear combination of the

current and higher spin states. After the contributions from higher spin states are eliminated, the calculations of the anisotropic coupling constants are improved in many cases but become worse for some other cases[42,43]. It is generally believed that the UHF method cannot give firm theoretical support for the calculation of spin densities[41]. Therefore, higher levels of theory, i.e. those dealing with correlated wave functions, must be used in order to obtain reliable predictions of the spin-polarization effect on the Fermi contact term. The main focus of this chapter is to obtain the Fermi contact term in quantitative agreement with experiment.

4.3.2. MRCISD algorithms

Since most of the rigorous studies on the HFS have been done with the MRCISD method, it is appropriate to introduce the MRCISD algorithms in detail. A sequence of MRCISD wave functions is generated through the following steps: (i) Transform the HF virtual orbital space to K orbitals[44], which are closer to natural orbitals, to improve CI convergence. (ii) Select a list of reference space configurations, starting with the Hartree-Fock configuration. (iii) Generate all single and double excitations from each configuration in the reference space and extract the lowest eigenvector from the resulting Hamiltonian matrix. (iv) Order the configurations in terms of the magnitude of the contributions to the energy or expansion coefficients. (v) From the ordered list choose a set of the most important configurations outside the current reference space to augment the reference space for the next calculation. (vi) Repeat the process until convergence

has been reached. To the extent that this sequence proves efficient in recovering the important correlation contributions to the properties of interest, the enormous number of higher order excitations which compose the bulk of a full CI wave function can be avoided.

Because the number of single and double excitations generated in step (3) may still be too numerous to include the entire set in a variational calculation, second-order, Raleigh-Schrödinger perturbation theory is used to select the energetically most important double excitations[45]. Configurations whose estimated energy contribution to the CI wave functions is greater than some threshold, T_E, are kept and all others are discarded, except that all single excitations from each of the reference configurations are retained in the MRCISD wave function.

4.3.3. Correlated wave functions for the HFS

The simplest ROHF-based wave function to incorporate spin polarization effects is the *CI with single excitations* (CIS). In a CIS wave function, the spin polarization is realized through the configurations in which there are some singly-occupied *s*-type orbitals. It has been found that the CIS method sometimes gives results often in rather good agreement with experiment. For example[41], the $A_{iso}(^{13}C)$ for the planar methyl radical calculated with the CIS method and a [631/41] basis set is 26.6 G, compared with the experimental value 27 G. Its performance, however, is not reliable. A 33% underestimate of the large values at the β-hydrogen has been found in the CIS

calculations of the H_2CN radical[42] although the results at nitrogen and hydrogen are fairly good. Further analysis has shown that the good results at the CIS level are due to a fortuitous cancellation between the effects of double and higher-order CI excitations[46].

One of the first extensive CI calculations on the HFS was carried out in 1983 by Feller and Davidson[47]. They studied ten small radicals for which experimental measurements exist. The levels of theories were CISD and MRCISD with perturbation selection of configurations (see the previous section) with large basis sets. One can see from their results that the CISD results tend to underestimate the Fermi contact term. For example, the CISD $A_{iso}(^{13}C)$ of CH_3 is 16.3 G versus the experimental value 27 G. In order to include excitations higher than doubles, the MRCISD method[48] was used. At the highest level of theory, the calculated ICCs of six radicals are within 10% of the experimental values. For the other four radicals, the results were rather poor. The same authors also reported later some cases for which the agreement with experiment remains poor in spite of considerable efforts at correlation recovery[49]. Apparently, the CI calculations on some molecules done to that date had not converged.

In order to find out how much effort was needed to get converged and, therefore, reliable theoretical results, Feller and Davidson carried out systematic studies[46] on the atoms B-F with respect to the convergence of the expansion of the uncontracted basis functions including polarization functions, the size of the reference space in the MRCISD calculations and the energy threshold T_E for selection of configurations with up to 200,000 configurations selected. From this study, the following conclusions can be drawn: (i) It is possible to get "good" results using small basis sets, or a small reference

space or a large energy threshold T_E or some combination of them. (ii) T_E has to be at least 5×10^{-9} hartree for the results to converge. The best theoretical results for ^{14}N agree very well with the experimental value but differ from experiment by about 10% for ^{17}O and ^{19}F and 50% for ^{11}B. They also studied two difficult molecules B_2 and H_2CO^+ and gave results in poor agreement with experiment. The authors warned[50] that any theoretical HFS studies without extensive recovery of correlation effects will be subject to fortuitous cancellations. Since the HFS is sensitive to geometry, many studies have been done on the effect of vibrational averaging. It is generally agreed that vibrational averaging is negligible for ground states but can be significant for excited states[51].

The reason for the slow convergence of the ICC is not yet completely known. Engels, Peyerimhoff and Davidson[52] made a detailed analysis of the CI calculations of the ICC of nitrogen. Since the ICC is from the *s*-type orbitals, they calculated the contributions from (1*s*) electrons and (2*s*) electrons separately by freezing the electrons in each shell alternatively during CI excitations. The contributions from the two shells are found to be large and opposite in sign to each other (cf. -54 MHz from 1*s* and 58 MHz from 2*s*). The final ICC was a subtle balance between the two. A similar pattern was found later in the study[53] of the HFS of NH.

4.3.4. Recent developments of basis sets

It is evident from the above discussion that the correlation recovery is extremely crucial for obtaining reliable predictions of the ICC. The accuracy of molecular

electronic structure calculations is limited by the truncation of the expansion of the basis set and the expansion of configurations. It is still an art to keep a balance between these two expansions. With increasing computing power, it is getting easier to approach the full-CI limit and the accuracy of ab initio predictions is limited more by the basis sets developed in early years[54].

The most widely used contraction schemes are *segmented contraction schemes* since each contracted basis function contains primitive Gaussians which are different from those used to form each of the other basis functions. Dunning's double zeta plus polarization basis set[15] is an example of a segmented basis set. Segmented basis sets work well for calculations at the HF level as the basis set can be easily saturated at this level of theory. For properties dependent on correlation effects, large primitive sets including high angular momentum polarization functions are often needed to achieve quantitatively good results as evidenced by Feller and Davidson's study of atomic HFSs discussed above. The same authors' study of the electron affinity of the oxygen atom[55] with the same spirit revealed a similar requirement of the basis set. Obviously, such large primitive sets cannot be used for calculations on larger systems and general contraction schemes are desirable to reduce the size of basis sets while minimizing the loss of accuracy.

In contrast with segmented contractions, each basis function of a contracted basis set with a *general contraction scheme* contains almost all the primitive Gaussians. Raffenetti[56] first proposed a general contraction scheme using HF atomic orbitals (AO) as the minimum basis set to which uncontracted primitive Gaussians can be added for

flexibility. Although Raffenetti's approach was shown to be more accurate[57] than the segmented contraction schemes, it was not widely used due to the inefficiency of the AO integral evaluations. With the rapid development of computer hardware and software, the calculations of AO integrals are not the time-determining step any more, at least for molecular property studies, and Raffinetti's idea of general contraction was revisited for the improvement of basis sets for correlation calculations. Almlöf and Taylor[58] suggested using the most populated atomic natural orbitals (ANO) as the basis functions to incorporate correlation effects in the basis functions since natural orbitals tend to give a much shorter CI expansion with the same accuracy (see Section 3.4.2). This approach is especially suitable for reducing the size of a potentially large primitive set and preserving the atomic correlation effect at the same time. It has been shown[59] that ANO-based contractions minimize the total CI energy loss compared with other HF-based contraction schemes, especially at a high degree of contraction. Their atomic HF energy losses are also much less than those obtained with the segmented contraction scheme although the latter uses the atomic HF coefficients.

On the other hand, Dunning maintained[60] that the contraction coefficients based on atomic HF calculations can be used if the exponents of the Gaussian primitives, especially polarization functions, are optimized in atomic correlated calculations. His study led to three observations. (i) Basis sets which include functions with high angular momentum (d,f,g) are required to reduce the error in the correlation energy to 1 kcal/mol or less. (ii) The basis functions could be grouped into sets with each function in the set lowering the correlation energy by an approximately equal amount or falling within a

given range of occupation numbers. (iii) Basis functions optimized to describe correlation effects in atoms also describe molecular correlation effects well. From atomic correlation calculations Dunning found that the incremental energy lowering due to the successive addition of correlation functions falls into distinct groups. Thus, the ($1s1p$) set and the ($1d$) function both decrease the correlation energy by comparable amounts, the incremental lowerings for the ($2s2p$),($2d$),and ($1f$) sets are similar, and so on. Dunning's study emphasized the importance of polarization functions for correlation calculations. For example, a basis set with ($12s6p$) primitives for first-row atoms requires ($3d2f1g$) polarization functions and ($14s8p$) requires ($4d3f2g1h$).

4.3.5. The effect of the basis set on the HFS

It has been realized from very early on that the ICC is greatly dependent on the basis set. One of the potential problems with GTOs could be that they do not possess the right cusp condition. Feller and Davidson[47] compared the total electron density at the nuclei with the exact values for atoms at the HF level and found that an error within 5% percent could be reached by an extended Gaussian basis set. An earlier study using the STO basis set, which has the right cusp showed that the minimum basis set does not give the right Fermi contact term[61]. Therefore, it seems the problems with the basis functions are not due to the cusp condition as the density, not the slope, is desired for the calculations of the ICC. An exact density at a nucleus can be reached when the number of GTOs is sufficiently large.

To find out the requirement of the basis set for the accurate prediction of the ICC, Feller and Davidson[46] made a thorough survey of the dependence of the ICC of nitrogen on the primitive Gaussians. First the (*sp*) space of the primitive Gaussians was saturated by extending the space until the calculated ICC at the MRCISD level does not change any more. Then *d* polarization functions were added until convergence was reached. The convergence of the *f* and *g* polarization functions was also studied in the same fashion. The largest primitive set examined was (19*s*10*p*8*d*4*f*2*g*). They found that the ICC only starts to converge from a primitive set as large as (6*s*4*p*2*d*). When a small set is used, one may get a number in good agreement with experiment for the wrong reason, i.e. by using a large energy threshold and a small reference space. The *d* polarization functions are also found to be essential in order to make a quantitative prediction.

On the other hand, Chipman[41,62,63] has tried to construct a basis set which is as small as possible and yet able to yield reasonably good results. He started out from Huzinaga's (9*s*5*p*) primitive set[64] by contracting it to various degrees. The basis set contractions were segmented and the coefficients were taken from the innermost atomic ROHF orbitals. The correlated wave function used was a small scale MCSCF one developed by choosing carefully the significant configurations on the basis of numerical MCSCF results. He found that semiquantitative results (10% or less difference from numerical values) could be obtained for the first-row atoms except carbon with a contracted set [6*s*3*p*][a] plus a diffuse (*sp*) shell.

The importance of diffuse functions for calculations of HFS was also underscored

---

[a] A pair of square brackets represents the contracted basis set.

by Bauschlicher et al[65] who studied the HFS of the nitrogen atom at high levels of theory including full-CI. They also found that the contraction coefficients taken from ANOs yield the same results as those from HF AOs with a segmented contraction scheme. Other people also studied the basis set effect for the assurance of the quality of the basis sets they chose. For instance, in their study of the HFS of NH, Engels and Peyerimhoff[66] found that a contraction of $(13s8p/8s)^a$ to $[8s5p/5s]$ caused little loss of accuracy of the ICCs of N and H. Feller et al[51] in their study of the HFS of NO investigated the variation of the ICCs as a function of the contraction length for the (*sp*) functions of Dunning's correlation-consistent-polarized-valence-triple-zeta (CC-PVTZ) basis set[60] at the CISD level. They found that further decontraction of the CC-PVTZ set is necessary to increase the flexibility in the core region. Fernández et al[67] carried out a basis set investigation for their calculations of the HFS of B_3. The basis set contractions of all these studies, however, are segmented.

4.4. MRCISD studies of the hyperfine structure of $^{14}NH_2$[68]

The HFS of N, NH, and NH_2 have been subjected to extensive theoretical and experimental studies. With large basis sets and high correlation recovery, the experimental isotropic coupling constant for the nitrogen atom was obtained theoretically by several groups using ab initio methods such as SCF(CASSCF)/MRCISD[65],

[a] A slash "/" in the basis set notation separates the basis sets for each atom. Usually the basis set for the heavy atom appears first.

MRCISD[46,52], and coupled cluster with single and double substitutions (CCSD) including noniterative treatment of triples[69], although the results for other atoms varied and were not as close as for nitrogen. In particular, the study by Feller and Davidson[46] showed that the good numbers from previous theoretical studies of atomic and molecular HFS arose from a largely fortuitous cancellation of errors due to insufficient correlation recovery and inadequate basis sets. The HFS of the molecule NH was studied with the many-body perturbation theory (MBPT)[70], numerical multiconfiguration self-consistent field (MCSCF)[63] and MRCISD[66] methods. The MRCISD study by Engels and Peyerimhoff[53] showed a deviation of a few MHz from experiment for the isotropic coupling constants on both N and H.

Among the studies of the HFS of NH_2[71,72,73], the most systematic study on NH_2 was carried out by Funken, Engels, Peyerimhoff and Grein[73]. They used a contracted basis set (13*s*8*p*2*d* contracted to 8*s*5*p*2*d*) and a reference space of up to 23 configurations in their MRCISD calculations, with an energy threshold of 2×10^{-7} hartree. Their calculated hyperfine couplings (24.1 MHz for N and -63.4 MHz for H) are in good agreement with the microwave rotational spectroscopic experiment[74] (27.9 MHz for N and -67.2 MHz for H). Their results were, however, not converged with respect to the energy threshold for the multireference calculations. A further study by the same research group[75] revealed that the effect of vibrational motion is negligible. A more recent study[76] used STO-expanded GTOs for the CI calculations and then obtained the Fermi contact terms with the original STOs. The numbers were not as close to the experimental ones as those in the study by Funken *et al*[73].

The question addressed in this section relates to the previous MRCISD work by Funken *et al*[73] and Engels *et al*[75]: can convergence of the HFS of NH_2 be achieved in the MRCISD calculations, and if so, does the converged result still differ from experiment. The problem is explored in three dimensions: the basis set, the size of the reference space and the energy threshold T_E for selecting configurations. The Gaussian primitives were left uncontracted as it has been shown in previous studies that the impact of basis set contraction can be very strong.

4.4.1. Methodology

The calculated HFS is sensitive to the wave function form and the basis set. Various correlation recovery techniques such as CCSD including noniterative treatment of triples, MRCISD, MCSCF, Møller-Plesset perturbation theory with orders from second to fifth, quadratic single and double CI and MBPT have previously been used with varying degrees of success. Feller *et al*[51] compared different correlation recovery algorithms based on ROHF and UHF. In this work ROHF based MRCISD is used because its wave function has the right symmetry and provides a systematic way to improve the accuracy to the full-CI limit[46,77,78]. Since one cannot include all the singly and doubly excited configurations generated with a certain reference space, the strategy is to reach converged results for a certain size of the reference space with respect to the energy threshold for configuration selection. This is taken as a good estimate of the limit in which all single and double excitations are included. The size of the reference space

is increased until the results converge with respect to both the size of the reference space and T_E, which is assumed to be a good estimate of the full CI limit for the given basis set. The same procedure is repeated for a larger basis set to see if improvement can be achieved. The calculations were carried out by using the MELDF-X program[48]. The geometry of NH_2 was optimized at the MP2/6-31G** level, yielding a bond length of 1.023Å and a bond angle 102.7° (experimentally 1.024Å and 103.3° [79]).

Since correlation recovery is extremely important to spin polarization, there have been some studies[67,80] of HFS using Dunning's correlation-consistent basis sets[60,81] which were designed to yield a good description of valence correlation. Recently Feller et al[51] used Dunning's triple zeta basis set augmented with (*1s1p1d1f*) diffuse functions to study the HFS of the molecule NO. The best results obtained with more than two million configurations included in the variational step were about 4 MHz too small for ^{14}N and 2 MHz too large for ^{17}O compared with experiment. In the same study, no converged results could be obtained with respect to the reference space, due to too many configurations. It is believed that more configurations have to be included to achieve convergence with respect to the energy threshold and/or the size of the reference space. On the other hand, atomic HFS calculations[46] with uncontracted primitive Gaussians show that polarization functions with angular momentum higher than d functions have only a marginal effect on the result, e.g. about 0.2 MHz for nitrogen, and it is reasonable to expect that they have even less effect in molecular calculations, as the basis functions on the other atoms will automatically be used for polarization. Besides, the core electrons were frozen when Dunning's basis set was obtained and this may be a further source of

error, since it is well-known that the Fermi contact term is the cancellation between core correlation and valence correlation. In his development of semi-quantitative basis sets for HFS calculations, Chipman[41,62] also showed the fluctuation of the HFS with respect to the contraction scheme. In the present study, the sets of primitive Gaussians derived from atomic SCF calculations are left uncontracted and two sets of d-type polarization functions are used on nitrogen and two sets of p-type polarization functions on hydrogen from Dunning's basis set[60]. The *s* and *p* primitives are from atomic SCF calculations by van Duijneveldt[82] and one more diffuse *s* and a set of *p* functions are add. d as they are known to be important for HFS.

4.4.2. Results and discussion

Figure 4.1 displays the change of the isotropic constant A_{iso} (^{14}N) with respect to the size of the reference space and the energy threshold T_E for selecting configurations with the (11*s*7*p*2*d*/7*s*2*p*) basis set. The size of the reference space is denoted by the number of spin-adapted configurations in that space. The sizes of the reference spaces are 10, 20, 30, 40 and 50, respectively, before spin-adaption. The corresponding numbers are given in Table 4.1. It can be seen that A_{iso} (^{14}N) converges with T_E, after T_E is smaller than 10^{-7} hartree and converges with respect to the size of the reference space if a sufficiently small T_E is used. If a large T_E is used, however, one might get the wrong conclusion about the effect of the increase of the size of the reference space. This is illustrated in Figure 4.2 which describes the A_{iso} (^{14}N) versus the size of the

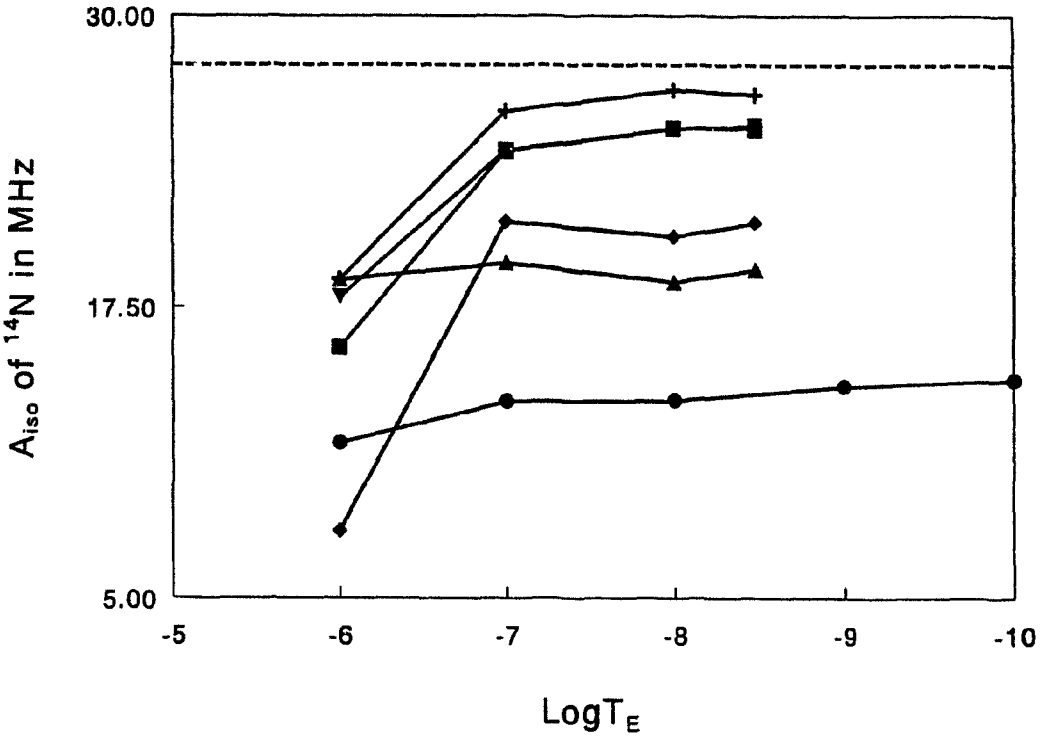

Figure 4.1. $A_{iso}(^{14}N)$ versus the energy threshold T_E with the (11*s*7*p*2*d*/7*s*2*p*) basis set. The number of reference configurations is denoted by 1 (•), 27 (▲), 50 (◆), 83 (■), 111 (+) and 126 (▼). The experimental value is indicated by the dashed line. The line denoted by ▼ coincides with the one denoted by ■ with T_E smaller than 10^{-7} hartree.

reference space at $T_E=10^{-6}$ hartree (which has been widely used, mainly because of hardware limitations) and $T_E=3.3\times10^{-9}$ hartree. From Figure 4.2 one might conclude that a reference space of 27 configurations is better than the one with 50 or more configurations because the former is closer to the experimental one. Only when T_E is smaller than 10^{-7} hartree, does A_{iso} show a steady trend as illustrated in Figure 4.3 and approach the experimental value. As pointed out by Feller and Davidson[46], a sufficiently small T_E is thus essential to obtain meaningful results, and a multireference approach may not make sense without taking this into consideration. Unlike the NO case studied

Table 4.1. Isotropic couplings, A_{iso}, (in MHz) of ^{14}N and H in NH_2 as a function of the energy threshold T_E (in hartrees) and the size of the reference space with the (11*s*7*p*2*d*/7*s*2*p*) basis set.

	Number of reference configurations						
Log T_E	1	27	50	83	111	126	Expt'l[a]
^{14}N							27.9
-6.0	11.66	18.69	7.87	15.78	18.71	17.96	
-7.0	13.43	19.[illegible]	21.18	24.20	25.92	24.25	
-8.0	13.48	18.57	20.53	25.19	26.83	25.19	
-8.48	14.36[b]	19.11	21.12	25.16	26.64	25.30	
H							-67.2
-6.0	-55.56	-60.63	-61.31	-62.83	-63.96	-64.15	
-7.0	-55.38	-62.17	-62.82	-63.71	-64.84	-65.03	
-8.0	-55.09	-62.52	-63.62	-64.51	-65.51	-65.61	
-8.48	-55.12[b]	-62.51	-63.09	-64.79	-65.79	-65.90	

[a] Ref. 74.

[b] All single and double excitations from the single reference are included.

by Feller *et al*[51], an exponential fit does not work in the present case for the curves with 50, 83 or 111 reference configurations. Therefore, caution should be taken when introducing this kind of fitting.

Similar to ^{14}N, the A_{iso} of hydrogen converges at $T_E=10^{-7}$ hartree given a certain size of reference space. Its behaviour is, however, more predictable in the sense that it decreases steadily with respect to a decrease of T_E, and with an increase in the number of reference configurations, as shown in Figures 4.3 and 4.4 (the counterparts to Figures 4.1 and 4.2 for ^{14}N). It is also easier to obtain a semi-quantitative result for H than for

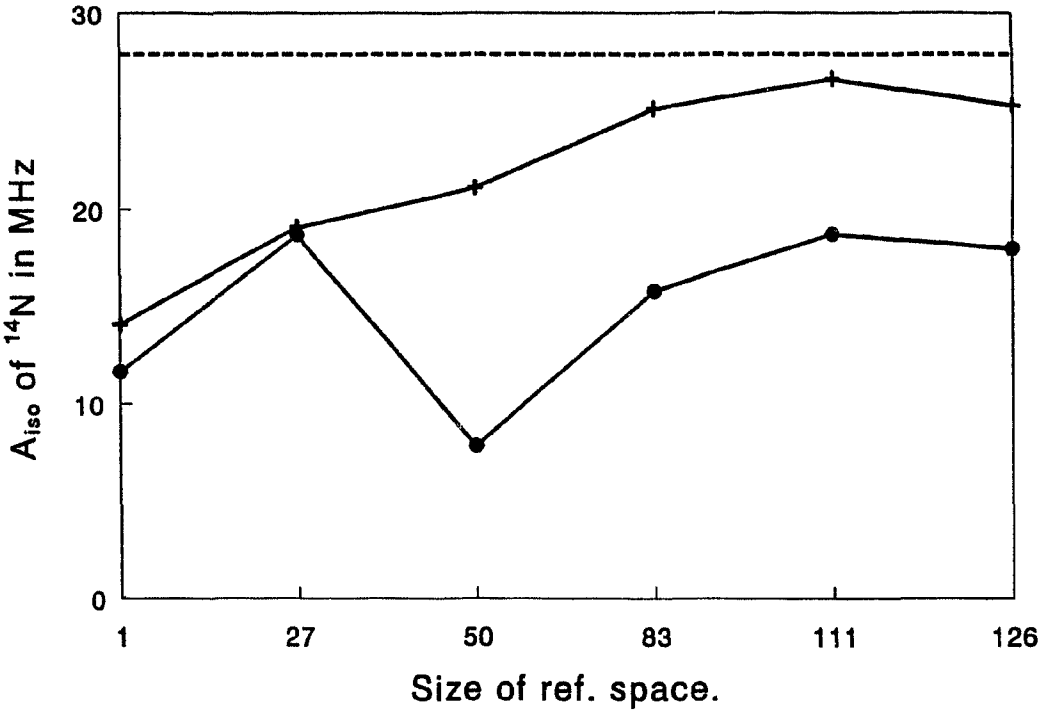

Figure 4.2. Plot of A_{iso} (^{14}N) as a function of the size of the reference space by use of the (11*s*7*p*2*d*/7*s*2*p*) basis set. The energy threshold T_E is denoted by 10^{-6} hartree (•) and 3.3×10^{-9} hartree (+). The experimental value is indicated by the dashed line.

^{14}N and even a single-reference CISD calculation recovers 80% of the experimental value.

The best theoretical predictions of the isotropic couplings with this basis set are 25.30 MHz for ^{14}N and -65.90 MHz for the proton, which are slightly different from the experimental results of 27.88 to 28.11 MHz and -67.22 to -67.59 MHz, respectively, and somewhat better than the results of Funken *et al*[73].

The basis set was extended by adding two *s* and one set of *p* functions to nitrogen and one *s* to hydrogen to see whether better agreement can be achieved. From Figures 4.5 and 4.6 (the counterparts of Figures 4.1 and 4.2) it can be seen that similar to the

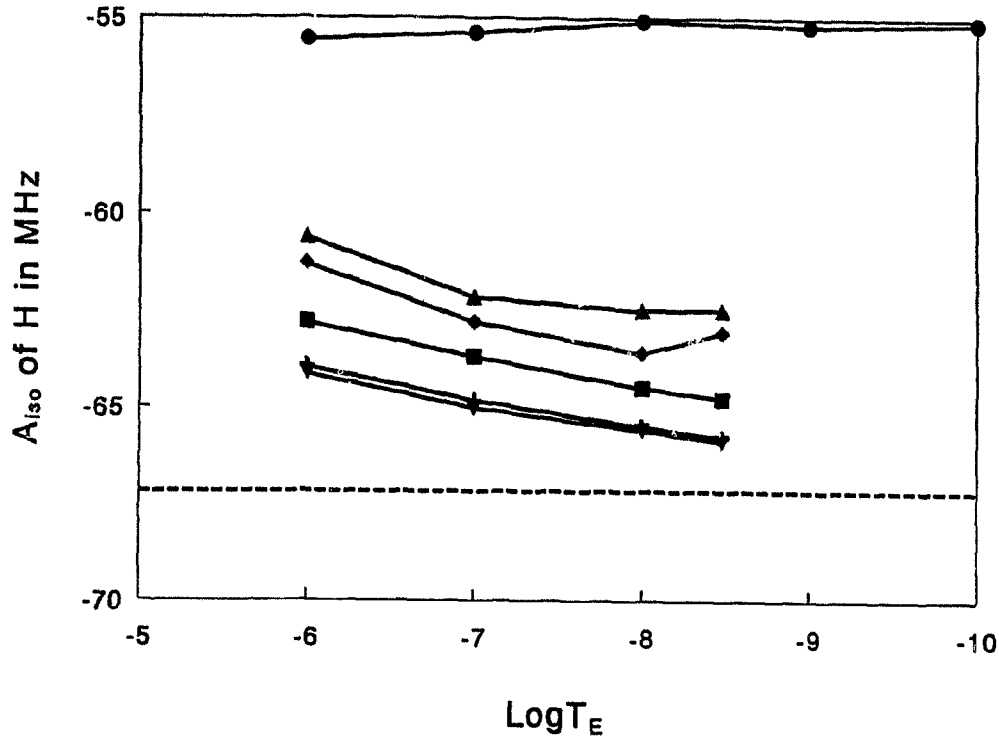

Figure 4.3. Plot of A_{iso} (H) as a function of the energy threshold T_E by use of the (11*s*7*p*2*d*/7*s*2*p*) basis set. The number of reference configurations is denoted by 1 (•), 27 (▲), 50 (◆), 83 (■), 111 (+) and 126 (▼). The experimental value is indicated by the dashed line.

situation with the smaller basis set, A_{iso} (^{14}N) converges after including more than 83 configurations in the reference space and using a T_E smaller than 10^{-7} hartree. This time, however, the converged number is more than 1 MHz higher and essentially the same as the experimental one, considering experimental uncertainty which may be as large as 1 MHz for an accurate measurement. The best theoretical number is between 28.45 MHz (111 reference configurations, $T_E=3.3\times10^{-9}$ hartree) and 27.44 MHz (126 reference configurations, $T_E=10^{-8}$ hartree).

A numerically large T_E ($> 10^{-7}$ hartree) still does not make sense. For example, one may conclude (cf. Figures 4.7 and 4.8) that one reference CISD is a very good

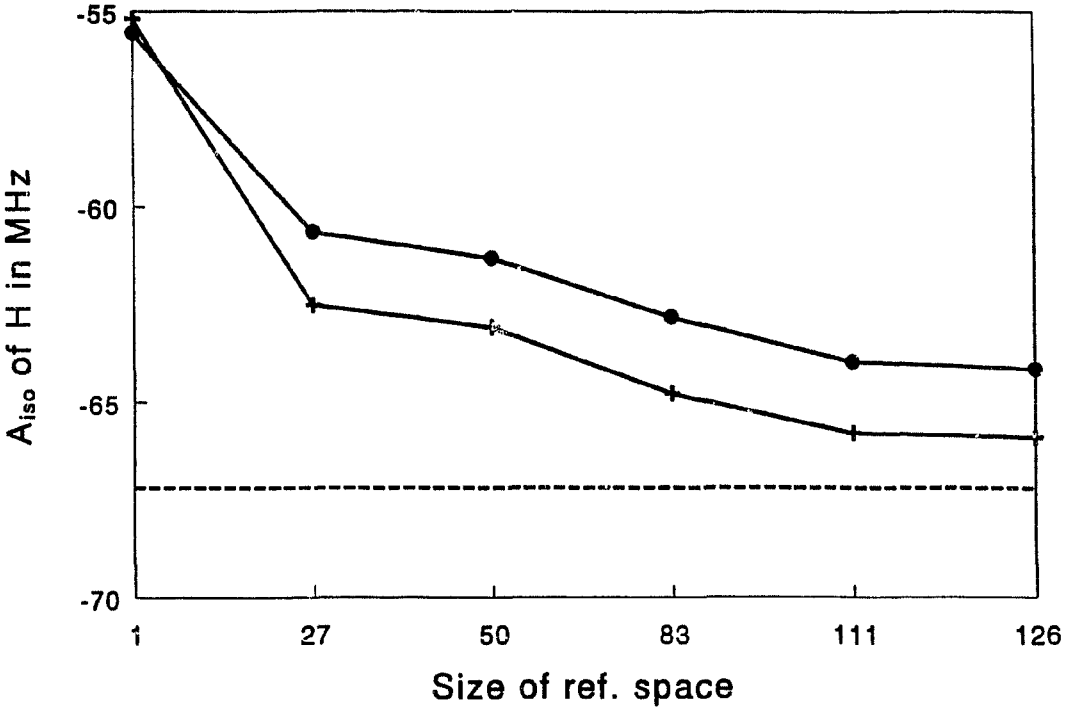

Figure 4.4. Plot of A_{iso} (H) as a function of the size of the reference space by use of the (11s7p2d/7s2p) basis set. The energy threshold T_E is denoted by 10^{-6} hartree (•) and 3.3×10^{-9} hartree (+). The experimental value is indicated by the dashed line.

simple model which recovers 75% of the experimental result, but it is actually due to fortuitous cancellation.

From Figures 4.7 and 4.8 it can be seen that the A_{iso} for hydrogen is also converged to the experimental value and the best theoretical number is between -65.57 MHz (111 reference configurations, $T_E=3.3\times10^{-9}$ hartree) and -68.47 MHz (126 reference configurations, $T_E=10^{-8}$ hartree). The number of configurations in the variational step is above 350,000.

In contrast to the requirement of high correlation recovery for isotropic couplings, anisotropic couplings are very stable throughout all the correlation levels, as shown in

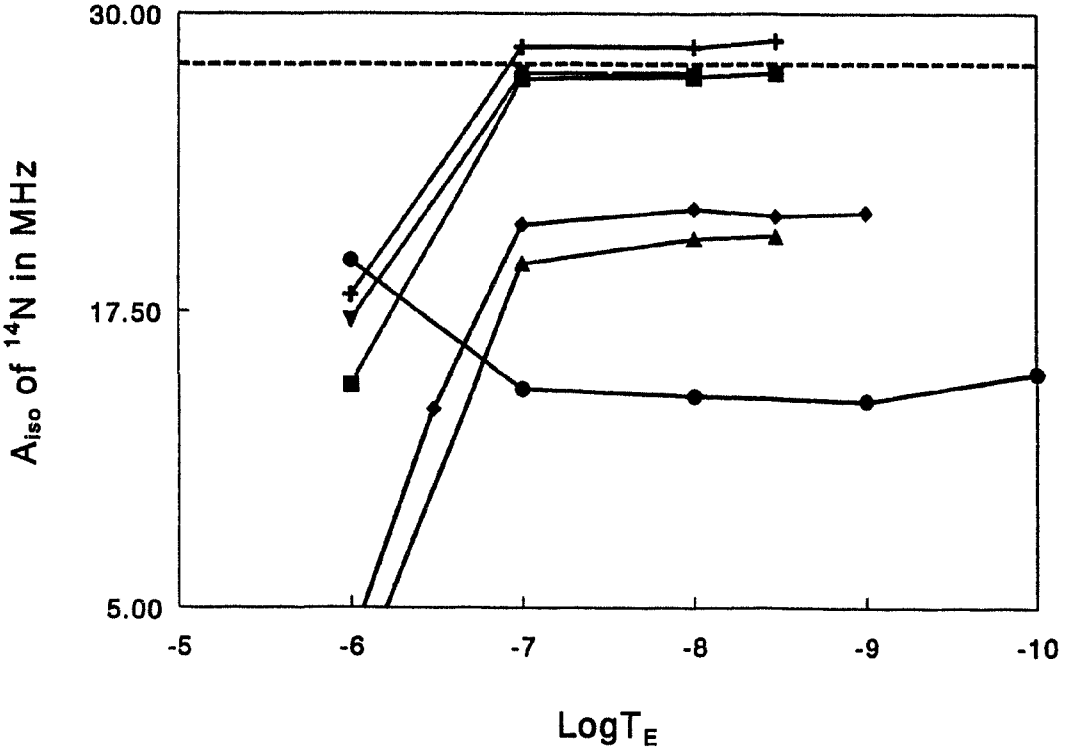

Figure 4.5. Plot of A_{iso} (^{14}N) as a function of the energy threshold T_E by use of the (13s8p2d/8s2p) basis set. The number of reference configurations is denoted by 1 (•), 27 (▲), 50 (◆), 83 (■), 111 (+) and 126 (▼). The experimental value is indicated by the dashed line. The line denoted by ▼ coincides with the one denoted by ■ with T_E smaller than 10^{-7} hartree.

Table 4.2. The insensitivity of the anisotropic tensor with respect to basis set and form of correlation treatment has also been explored for NH_2 in the DFT study which will be presented in Section 4.6, giving very similar results and conclusions.

The convergence of the correlation energy, CI total energy - ROHF energy, and the sum of the squares of the expansion coefficients of configurations in the reference space are shown in Figure 4.9 for comparison. It is immediately apparent that both quantities converge more smoothly than the isotropic coupling constants. Therefore, the effect of a larger T_E and smaller reference space is less predictable for the isotropic

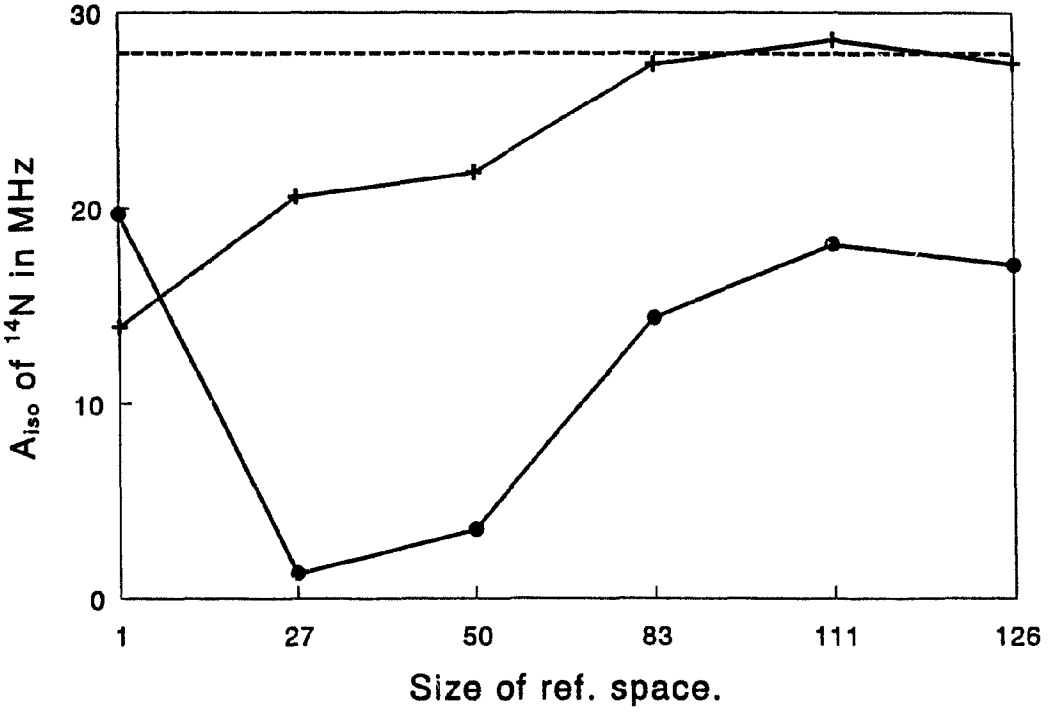

Figure 4.6. Plot of A_{iso} (^{14}N) as a function of the size of the reference space by use of the (13s8p2d/8s2p) basis set. The energy threshold T_E is denoted by 10^{-6} hartree (•) and 3.3×10^{-9} hartree (+). The experimental value is indicated by the dashed line.

Table 4.2. The anisotropic coupling constant, A_{dip}, (in MHz) of ^{14}N calculated with the CISD and MRCISD (50 reference configurations) methods for different basis sets and configuration selection thresholds.

	CISD	MRCISD			Expt'l[a]
Basis set		10^{-6}	10^{-7}	10^{-8}	
(11*s*7*p*2*d*/7*s*2*p*)	42.52	42.38	42.27	42.23	43.85
(13*s*8*p*2*d*/8*s*2*p*)	42.76	42.56	42.51	42.46	

[a] Ref. 74.

coupling constants than for the recovery of the correlation energy.

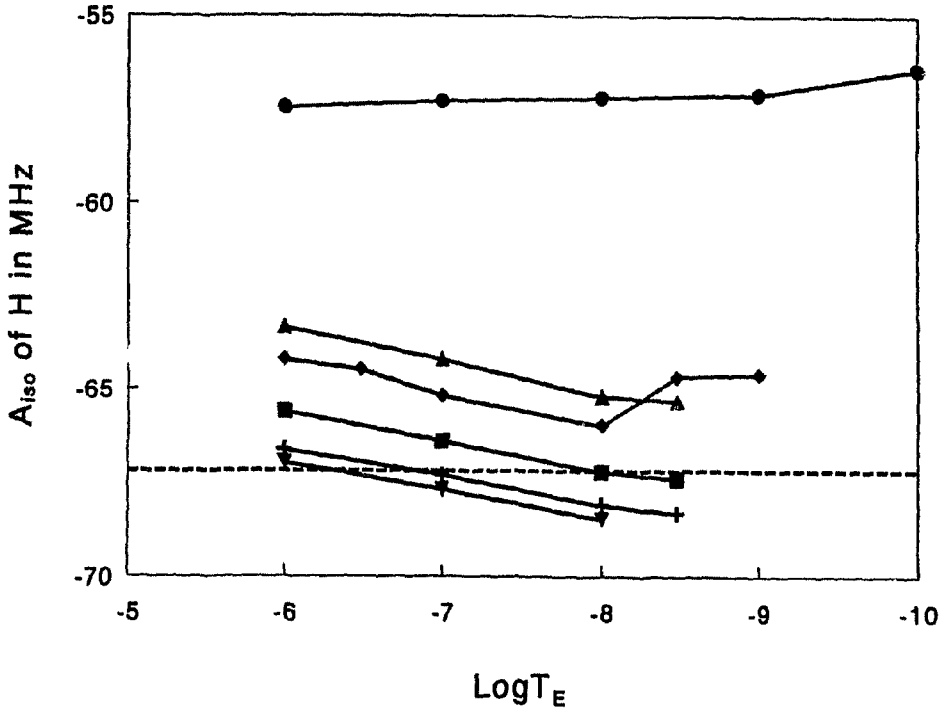

Figure 4.7. Plot of A_{iso} (H) as a function of the energy threshold T_E by use of the (13*s*8*p*2*d*/8*s*2*p*) basis set. The number of reference configurations is denoted by 1 (•), 27 (▲), 50 (◆), 83 (■), 111 (+) and 126 (▼). The experimental value is indicated by the dashed line.

4.5. The convergence of basis set contractions

In this section, comparison is made among the effects of the segmented and two general contraction approaches (HF and ANO) on the calculations of the molecular hyperfine structure of NH_2. More specifically, the isotropic hyperfine coupling constant of ^{14}N in NH_2 has been calculated at the MRCISD level with basis sets contracted at various degrees with the three contraction schemes. As it has been shown in the last section, an accurate prediction of the ICC can be obtained at the extended CI level. The

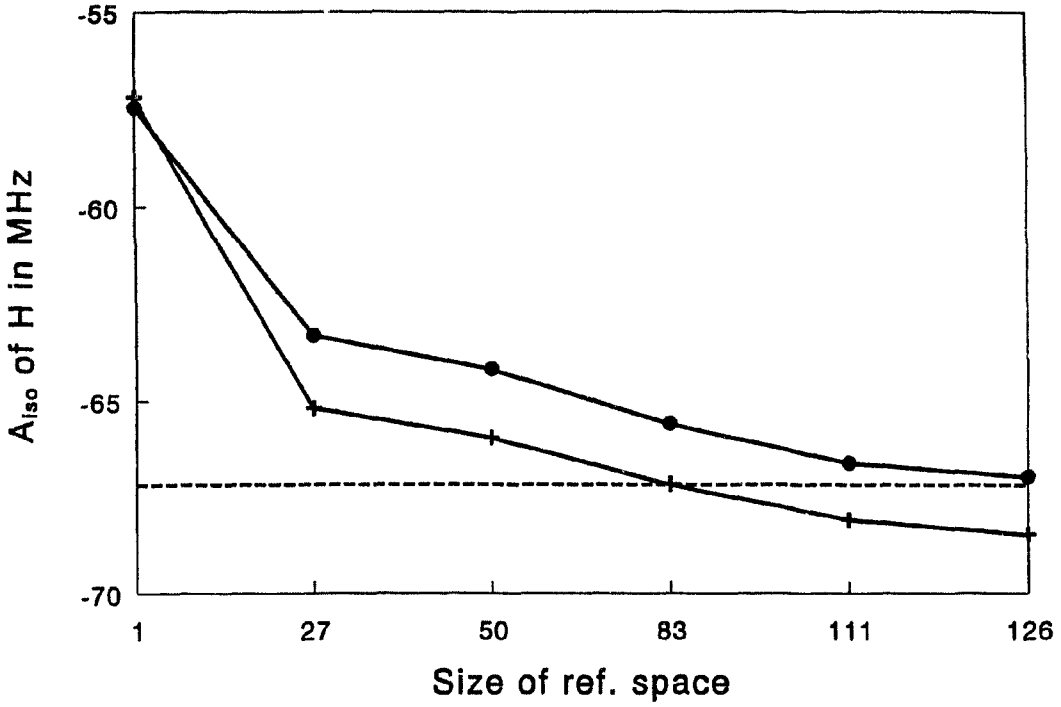

Figure 4.8. Plot of A_{iso} (H) as a function of the size of the reference space by use of the (13s8p2d/8s2p) basis set. The energy threshold T_E is denoted by 10^{-6} hartree (•) and 3.3×10^{-9} hartree (+). The experimental value is indicated by the dashed line.

approach used in the last section, however, would be very difficult to extend to a larger system. The problem is the computational cost. From the calculations, it has been found that the number of selected configurations grows linearly with respect to the decrease of the energy threshold. The largest single job includes about 350,000 configurations in the final variational procedure, which takes all of the 3 gigabyte disk space available on the IBM RS/6000 Model 500 workstation. For the calculation with the energy threshold 10^{-7} hartree, reference size of 83 and (13*s*8*p*2*d*/8*s*2*p*), at which the result starts to converge, the number of selected configurations is about 70,000. Davidson[83] has argued that the computational cost grows like $N!$ with respect to the number of atoms at a fixed

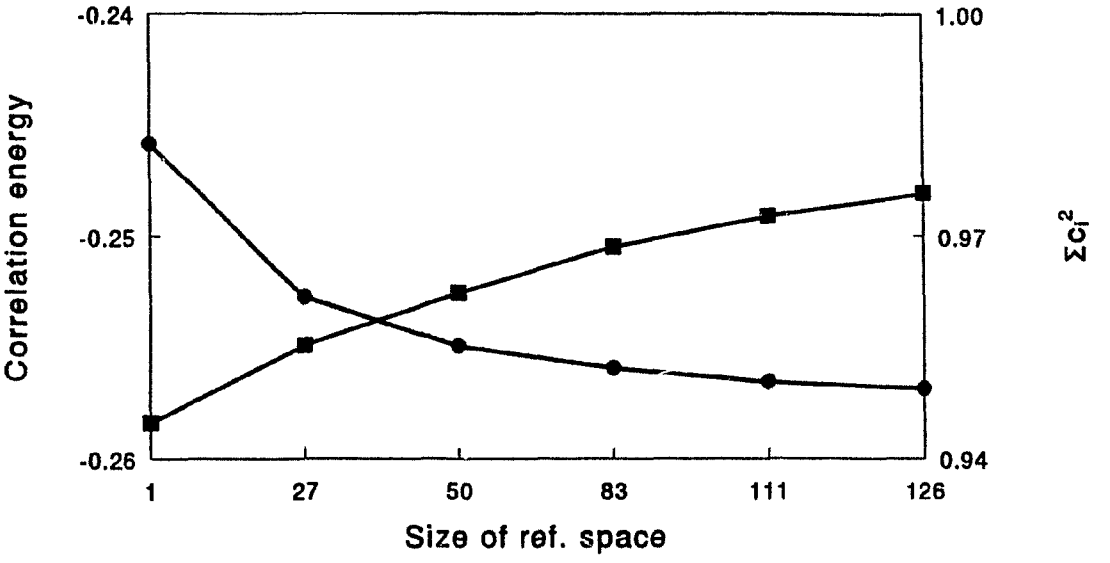

Figure 4.9. Plot of the correlation energy (in hartrees) (•) and the sum of the squares of the coefficients in the reference space $\sum c_i^2$ (■) as a function of the size of the reference space by use of the (11s7p2d/7s2p) basis set. The energy threshold for selecting configurations is 10^{-7} hartree.

accuracy. Thus, the workstations used for this research, which are probably more powerful than the most powerful supercomputer several years ago, cannot handle a system with even just one more hydrogen atom. The motivation of this study is to find a way of contracting the primitive basis set used in the last section such that the ICC can be predicted reliably and the computing cost can reduced substantially.

In contrast to the previous ANO contraction studies which froze core electrons for CI calculations, full-electron correlation is essential for the calculation of the HFS and is included here in the construction of ANO basis functions. The ICC of ^{14}N in NH_2 is totally due to correlation effects because of the π symmetry of the singly occupied orbital of the ROHF wave function. It has been realized[52,63,66,84] that the contribution of the core

electron correlation has the opposite sign to that of the valence electron correlation and that the ICC depends on a subtle balance between them. Therefore, the HFS provides a good test for the effectiveness of the ANO approach for the inclusion of the core-electron correlation.

4.5.1. Methodology

As in the previous section, the MRCISD method has been used for all the hyperfine structure calculations on NH_2. It has been shown in that study that the isotropic coupling constant of nitrogen converges with a reference space of 30 configurations (83 spin-adapted configurations) and an energy threshold of 10^{-7} hartree. In this study, the same energy threshold and the 31 configurations (before spin-adaption) with the highest coefficient contributions are used as the reference configurations for the calculations of the HFS of NH_2. The larger set of the two primitive sets used in Section 4.4, (13*s*8*p*2*d*/8*s*2*p*), is used as the uncontracted basis set, with the set of *d* functions being five instead of six.

Since the ICC of hydrogen is much less sensitive to the change of basis functions, as shown in Section 4.4, the basis set for hydrogen has been contracted to [4*s*2*p*] for all the calculations except those with uncontracted basis sets. For the sake of conciseness, only the basis set for nitrogen will be mentioned in the discussion.

4.5.2. Results and discussion

Table 4.3. The CISD populations of the atomic natural orbitals of the nitrogen atom.

ANO	*s*	*p*
1	1.998825	0.995599
2	1.982731	0.005586
3	0.012236	0.000372
4	0.000812	0.000124
5	0.000219	0.000024
6	0.000026	0.000006
7	0.000006	0.000001
8	0.000002	$< 10^{-6}$
9 - 13	$< 10^{-6}$	

The two general contraction schemes and one segmented scheme are compared in this section. The scheme denoted as ANO uses ANOs from an all-electron atomic CISD calculation, (the two sets of *d* polarization functions are not included in the atomic calculations). The ANOs are ordered by their populations and listed in Table 4.3. Unless noted otherwise, the contracted basis functions are the first few orbitals, i.e. the ones with the highest populations in the *s* and *p* spaces.

The contraction scheme denoted as HFGen is the Raffenetti approach[56] which uses all the occupied atomic HF orbitals, plus the most diffuse primitive Gaussians to add flexibility. HFSeg is the segmented contraction scheme used in Chipman's basis set

study[62]. A contracted HFSeg basis set consists of the inner parts of the atomic 1*s* and 2*p* HF orbitals plus the remaining primitives.

Table 4.4. The MRCISD ICC (in MHz) of ^{14}N in NH_2 with different contraction schemes for the nitrogen atom[a].

Basis set	ANO	HFGen	HFSeg
[4*s*3*p*2*d*]	8.22	59.32	72.63
[5*s*3*p*2*d*]	15.82	66.09	82.52
[6*s*3*p*2*d*]	20.21	14.10	29.26
[7*s*3*p*2*d*]	22.71	25.77	26.86
[8*s*3*p*2*d*]	20.88	25.69	25.89
[7*s*3*p*2*d*]	22.71	25.77	26.86
[7*s*4*p*2*d*]	21.64	23.64	24.67
[7*s*5*p*2*d*]	20.48	21.91	22.75
[7*s*6*p*2*d*]	21.51	21.30	22.16

[a] The (13*s*8*p*2*d*) uncontracted basis set yields 21.57 MHz; the experimental value is 27.9 MHz.

Table 4.4 lists the ICC of ^{14}N in NH_2 with various basis set contractions. The basis functions for nitrogen are enlarged first in the *s* space from [4*s*3*p*2*d*] to [8*s*3*p*2*d*]. It can been seen that the ANO ICC starts to converge at [6*s*3*p*2*d*], a triple-zeta plus polarization (TZP) basis set, and the ICC of the HF contraction schemes starts to converge at [7*s*3*p*2*d*]. The results of the HF-based approaches are consistent with Feller and Davidson's conclusion[46] that at least a TZP basis set is needed to achieve meaningful results. Chipman also found that the result of the [6*s*3*p*] contraction of Huzinaga's (9*s*5*p*) primitive set[64] leads to better results than the [5*s*3*p*] contraction. The converged

results of the two HF-based schemes lead to closer agreement with the experimental value than the uncontracted, indicating that one could obtain better agreement with experiment for the HFS using a contracted basis set rather than an uncontracted set of primitive Gaussians due to a fortuitous cancellation of errors. Expansion of the *p* space from [7*s*3*p*2*d*] to [7*s*6*p*2*d*] has a stronger effect on the HF-based schemes. The results of the ANO and the two HF-based approaches and that of ANO converge to the uncontracted one. Overall, the ANO scheme seems to converge faster, especially in the *p* space, and more smoothly than the other two schemes. For the basis sets with a higher degree of contraction, [4*s*3*p*2*d*] and [5*s*3*p*2*d*], the errors of the HF-based contractions are too large for them to be useful even for qualitative analysis.

The different convergence behaviour of the ANO and HF approaches shows the differences in their abilities to recover the correlation effect of the core electrons relative to the correlation effect of the valence electrons. It has been shown[52,63,66,84] that the contributions from these two correlation effects to the ICC have opposite signs and large magnitudes. The ICC is the result of the subtle compromise between them. The contribution from the valence electrons for ^{14}N in NH_2 with the uncontracted basis set is positive (65 MHz), suggesting that the contribution from the core electrons is negative, similar to the situation for N[46,84] and NH[63,66]. At a high degree of basis set contraction ([4*s*3*p*2*d*] or [5*s*3*p*2*d*]), the ANO scheme yields a small ICC, indicating that more core-electron correlations are recovered than those of the valence-electrons. In contrast, the two HF based approaches recover more valence-electron correlation than core-electron correlation. A balanced description starts only after a contraction of [6*s*3*p*2*d*].

The difference can be understood in terms of the basis set diffuseness.

Chipman's[62] and Bauschlicher et al's[65] atomic HFS studies have shown that the core correlation effect is always enhanced (the ICC is increased in the case of N) when a set of diffuse (*sp*) functions is added to either an uncontracted or a contracted basis set. The reason that the HF-based approaches at the high degree of contraction yield large ICC values is that the occupied HF AOs that are used as the basis functions are not sufficiently tight. Chipman[62] found that only the first four innermost primitives of the (9*s*6*p*) set could be contracted in order to get a balanced description between the core and valance electron correlations. On the other hand, the ANOs are the eigenvectors of the atomic electronic density which decreases exponentially away from the nucleus. Therefore, they are less sensitive to the outer part of an atom and are considered tight. When only the first few ANOs are taken as basis functions, the basis set is not sufficiently diffuse and the correlation of the valence electrons is under-represented as indicated by the small ICC at the high degree of contraction.

The insufficient recovery of valence-electron correlation for a small ANO basis set is contrary to the speculation[58,59] about a possible full-electron ANO basis set. It is generally believed that the valence orbitals correlate mostly with the first few virtual orbitals whereas the core orbitals correlate with the outermost virtual orbitals. Similarly, the ANOs needed for core-electron correlations may have very small occupancies which are not included in a high-degree contraction, resulting in an insufficient description of the core-electron correlations. It is one of the reasons that the full-electron correlation has been avoided in previous studies of the ANO contraction approach. It has been thought that the desired orbitals for correlating core electrons are either most populated (corresponding to occupied core orbitals) or the nearly least populated (corresponding to

virtual orbitals for core electrons). The latter will be excluded in a procedure in which the most populated natural orbitals are chosen (as in the calculations of Table 4.3).

Table 4.5. The effect of replacing the 5th *s* ANO (the outermost one) of the contracted [5*s*3*p*2*d*] basis set with *s* ANOs 6 to 13.

Replacement ANO	ICC (in MHz)	Energy loss (in mhartree)
5	15.82	0.000
6	20.89	0.950
7	17.56	3.344
8	12.11	3.567
9	9.42	3.732
10	8.74	3.806
11	8.54	3.833
12	8.39	3.840
13	8.31	3.841

To study further the effect of the less populated ANOs versus that of the more populated ANOs, the 5th *s* ANO, the least populated orbital of the five most populated *s* ANOs used in the basis set [5*s*3*p*2*d*] has been replaced with each of the rest of the six ANOs, the 6th to the 13th. Table 4.5 lists the ICC of ^{14}N and the total energy relative to that of the [5*s*3*p*2*d*] basis set for each replacement. Replacement with the 6th and the 7th ANO shifts the balance more towards valence-electron correlation with the former having the strongest effect, raising the ICC by 5 MHz. This is hardly surprising since

the replacement orbitals are more diffuse. The replacements with the further less populated ANOs (8th - 13th) lower the ICC. The replacement with the 6th ANO also yields much less energy loss than that with others. The increase and then decrease of the ICC also shows that valence electron correlation will be under-represented if the outermost basis function is too diffuse.

Table 4.6. The effect of replacing the 7th *s* ANO (the outermost one) of the contracted [7*s*3*p*2*d*] basis set with *s* ANOs 8 to 13.

Replacement ANO	ICC (in MHz)	Energy loss (in mhartree)
7	21.64	0.000
8	19.76	-0.058
9	19.74	0.210
10	20.28	0.283
11	20.05	0.309
12	19.85	0.313
13	19.73	0.314

A similar replacement study was also carried out for the basis set [7*s*3*p*2*d*] and the results are listed in Table 4.6. Since the 6th and the 7th ANOs are included as basis functions, the replacement of a less populated ANO has much less effect on the ICC. One can see that the ICC is around 20 MHz, about 1 MHz smaller than the uncontracted and the contracted [7*s*3*p*2*d*] results. There are energy losses too except for the first

replacement which yields a slight energy gain. This indicates that the balance of the correlations of the core electrons and valence electrons is well represented by the first seven *s* ANOs.

Table 4.7. The effect of using the outermost primitive Gaussian as the diffuse function.

Basis set	ICC	Energy loss[a] (in mhartree)
[3+1*s*, 2+1*p*, 2*d*]	33.48	23.278
[4+1*s*, 2+1*p*, 2*d*]	12.83	20.742
[5+1*s*, 2+1*p*, 2*d*]	19.95	15.624
[6+1*s*, 2+1*p*, 2*d*]	23.49	18.861
[7+1*s*, 2+1*p*, 2*d*]	23.33	18.742

[a] The energy difference between the total energy with the basis sets in this table and that with the basis set in Table 4.4 at the same size.

Another way of increasing the diffuseness and the flexibility of a basis set, as done by Almlöf and Taylor in their study[58] of the ANO basis set, is to use the outermost primitives as basis functions. Thus, the [4+1*s*, 2+1*p*] basis set includes the first four *s* ANOs, first two *p* ANOs and the outermost *s* and *p* primitives. Table 4.7 lists the effect of using one set of the diffuse (*sp*) primitive Gaussians. The energy loss in the table is the difference between the energy with the current primitive-added basis set and that with the basis set in Table 4.4 of the same size, e.g. the energy with the [4+1*s*, 2+1*p*] basis set minus the energy with the [5*s*3*p*] basis set in Table 4.4.

Apparently, due to the diffuseness of the basis set, the ICC increases at both the low and high degrees of basis set contraction, especially for the small basis set [3+1*s*,

2+1*p*, 2*d*] where the ICC is four times that of [4*s*3*p*2*d*]. In fact, the pattern of the numbers shifts towards the results of the HF-based ones, although the fluctuation is much less drastic. The ICC with the segmented contraction scheme and ANO coefficients is calculated and the results are very similar to those with the two HF-based contractions, analogous to the finding of Bauschlicher et al[65]. The energy loss found here is very large. In fact, the total energy with this revised ANO scheme is larger than that with the smallest size of the normal ANO approach. The energy loss is also much larger than that reported by Almlöf and Taylor[58]. This may be due to two reasons: they decontracted the *d* and *f* polarization functions and they used valence CISD only. As pointed out by Almlöf et al[85], the good performance of the ANO basis set is due to its correct nodal structure and the errors introduced by compromising the nodal structure are several orders of magnitude larger than those due to inadequacies of the primitive set. A primitive Gaussian does not possess any nodal structure of the final natural orbital and, thus, bears much less correlation effect than an ANO. It may therefore not be advisable to add primitive Gaussians for the calculations of HFS.

Finally, the numbers of configurations generated at the MRCISD level with and without perturbation selections are listed in Table 4.8. One can see that the numbers of configurations selected with the two HF contraction schemes are smaller than the ANO one and grow somewhat slower than the latter with the increase of contraction degree. This is especially obvious when the expansion is in the *p* space. It can also be seen that the number with a contracted basis set is not so much smaller than that with the uncontracted basis set whereas the number of configurations with the contracted basis sets before perturbation selection are three times smaller than that with the uncontracted basis

Table 4.8. The number of configurations selected versus the degrees of basis set contraction and contraction scheme[a].

Basis set	Total	ANO	HFGen	HFSeg
[4*s*3*p*2*d*]	491	52	43	40
[5*s*3*p*2*d*]	564	31	44	45
[6*s*3*p*2*d*]	600	34	46	46
[7*s*3*p*2*d*]	662	60	48	48
[8*s*3*p*2*d*]	660	58	50	50
[7*s*4*p*2*d*]	699	62	49	50
(13*s*8*p*2*d*)	2077	74		

[a] The total number of configurations is the number before perturbation selection which is similar among the three contraction schemes.

set. It is a little surprising because one would expect a similar degree of reduction of the number of configurations. It seems that the basis set contraction is not as helpful as expected when a fixed accuracy is desired. But further studies are needed before such a conclusion can be made.

4.6. Density Functional Theory as a Possible Alternative for HFS Studies[86]

The MRCISD method and other *ab initio* correlation methods are so computationally demanding that they are not practical for the calculation of the HFS of the vast majority of the molecules of interest to chemists. It is therefore sensible to look

at the DFT method which is computationally more efficient. The linear combination of Gaussian-type orbitals version of DFT (LCGTO-DFT), may be a practical alternative because it yields results comparable to those obtained with conventional correlated *ab initio* treatments at a much lower computational cost. The DFT results for the hyperfine structures (HFS) of a large variety of molecules are similar to those calculated at the MRCISD level of theory[87]. This prompted us to examine the performance of the LCGTO-DFT approach to the prediction of HFS in terms of the dependence of the results on basis sets and functional forms. Atomic calculations have the advantage that no geometry effects, which are important in molecular HFS calculations, are involved. In the present study, calculations were also done on NH_2 and NH_3^+ to reveal the difference in behaviour between atoms and molecules, and that between the isotropic and the anisotropic couplings. NH_2 and NH_3^+ are selected because the HFSs of these radicals have been carefully determined experimentally and studied thoroughly with conventional correlation methods.

4.6.1. Methodology

The LCGTO-DFT package deMon[88] was used for the present study. There are two major variables in DFT: the functional form and the basis set. In addition to the local spin density approximation (LDA) (Dirac exchange term, and correlation correction by Vosko, Wilk and Nusair[89]), two widely employed correction algorithms to the exchange and correlation potential are used: Becke's exchange potential[90] with Perdew's correlation functional[91] (denoted BP), and the Perdew and Wang exchange

functional[92] with the correlation correction by Perdew[91] (PWP). The orbital basis set used here is the DFT modified Huzinaga (11*s*,7*p*) basis set[93] with a contraction scheme designed for NMR calculations[94], and to which two *d*-functions with exponents 0.35 and 1.4 have been added. This basis set is denoted by IGLO-III. A similar, but smaller, basis set with the contraction (9*s*5*p*1*d*)/[6*s*4*p*1*d*], denoted IGLO-II, is also used for comparison. Furthermore, auxiliary basis sets are utilized for the fitting of the Coulomb potential and the exchange and correlation potentials. Of the auxiliary basis sets available in deMon, the (4,4;4,4), (4,3;4,3) and (5,2;5,2) ones[95] are used. The numbers before the semi-colon denote the auxiliary basis set used for the fitting of the Coulomb potentials and those after the semi-colon for the exchange and correlation potentials. The notation '4,4' means there are four *s*-type Gaussians and another four shells of *s*, *p*, *d* functions sharing the same exponents. The fitting of the Coulomb potential is done analytically, whereas for exchange and correlation potentials a numerical fitting procedure is used. For each atom, a grid is thereby constructed, consisting of 32 radial shells with 6, 12, 26 or 194 angular points per shell (see below). Unless indicated, the grid used consists of 26 angular points per randomly oriented shell.

4.6.2. Results and discussion

The results of the atomic calculations, listed in Table 4.9, depend very strongly on the functional form. Changing the functional changes not only the magnitudes but also the signs of the atomic ICCs. This may be compared with *ab initio* calculations at different choices of theoretical models and basis sets (see the discussion in Section

Table 4.9. Atomic isotropic coupling constants (MHz).

Functional	Basis sets		^{11}B	^{13}C	^{14}N	^{17}O
	Orbital	Auxiliary				
LDA	IGLO-III	(4,4;4,4)	-6.23	-1.65	-0.91	2.45
LDA	IGLO-II	(4,4;4,4)	-20.73	-44.43	-27.37	55.47
LDA	(11s,7p,2d)	(4,4;4,4)	-7.18	-7.79	-3.44	8.11
LDA	IGLO-III	(4,3;4,3)	-15.80	-4.10	-2.14	0.35
LDA	IGLO-III	(5,2;5,2)	a	-9.10	-5.16	7.56
BP	IGLO-III	(4,4;4,4)	-29.93	-23.84	-4.73	-1.20
BP	IGLO-II	(4,4;4,4)	-43.54	-52.35	-23.54	1.89
BP	(11s,7p,2d)	(4,4;4,4)	-32.61	-28.05	-6.64	-3.52
BP	IGLO-III	(4,3;4,3)	-7.24	-29.73	-8.87	10.15
BP	IGLO-III	(5,2;5,2)	a	-25.15	-9.67	14.03
PWP	IGLO-III	(4,4;4,4)	-56.73	-37.46	7.71	-46.12
PWP	IGLO-II	(4,4;4,4)	-68.48	-47.82	-8.81	-36.25
PWP	(11s,7p,2d)	(4,4;4,4)	-70.10	-47.40	0.39	-50.00
PWP	IGLO-III	(4,3;4,3)	-32.37	1.45	15.70	-17.77
PWP	IGLO-III	(5,2;5,2)	a	12.66	23.29	-43.20
Expt'l[b]			11.6		10.45	-34.5
Numerical UHF[c]			24.3	86.6	60.4	-118.2
Numerical MCSCF[d]			22.5	26.6	10.9	-27.6
MRCISD[e]			6.4	17.8	10.1	-30.2

[a] The (5,2;5,2) auxiliary basis set is not available for boron.

[b] Boron - ref. 96, nitrogen - ref. 97, oxygen - ref. 98.

[c] Ref. 99.

[d] Ref. 84.

[e] Ref. 46.

4.3.3), which also show dramatic fluctuations. The values for boron, carbon and oxygen

generally decrease in the series LDA-RP-PWP when the (4,4;4,4) auxiliary basis set is employed. Using the (4,3;4,3) and the (5,2;5,2) auxiliary bases, the PWP calculations seem to generate results relatively close to experiment for carbon, nitrogen and oxygen. Similar observations have also been made for most molecular hyperfine structure calculations to date[87].

When the smaller basis set IGLO-II is used with the (4,4;4,4) auxiliary basis set, the values for B, C and N decrease by between 10 and 43 MHz, and that for O increases by between 2 and 53 MHz. With this choice of basis set, the value for oxygen obtained at the PWP level is very close to the experimental one, whereas the others become worse.

A common practice among molecular orbital theories is to use contracted basis sets instead of Gaussian primitives to lower the computational demands and to assume that the error introduced is acceptably small. This approach is generally valid for most properties. The basis set (11s,7p,2d) listed in Table 4.9 is the uncontracted form of IGLO-III. We can see that when the uncontracted basis is employed, the values generally decrease somewhat, with the one exception of oxygen. The largest changes are observed using the PWP correction scheme.

It should be emphasized that the observed changes in HFS parameters with the size of basis set and contraction are not unusual, and that *ab initio* calculations suffer the same problem. For an example, see Table 2 of ref. 62.

It has been found that molecular geometries and vibrational frequencies do not change significantly with auxiliary basis sets[88]. For atomic HFS calculations there is, however, a strong dependence on the size of the auxiliary basis set. The results in Table 4.9 show that removing one shell from (4,4;4,4) to (4,3;4,3) gives large fluctuations in

isotropic couplings, especially when used in conjunction with the PWP functional. The third auxiliary basis set (5,2;5,2) further enhances the results. This time, the values for carbon are improved to be close to the MRCISD results, and that for oxygen is fairly close to the experimental number.

Overall, the results obtained at the PWP/IGLO-III level with the (4,3;4,3) and (5,2;5,2) auxiliary basis sets are in fairly good agreement with experiment[96,97,98] and previous MRCISD values[46] and compare favourably with the UHF method[99]. The effects of the non-local gradient corrections have, e.g., been investigated by Ziegler et al[100]. They found that the main difference relative to LDA is a removal of density from the core tail and valence tail regions, and an increase of the core density. This has also been observed directly in terms of densities and HFS couplings in other studies[87]. In particular it has been found that the PWP correction enhances this effect to a higher degree than does the correction scheme by Becke and Perdew. The fact that Gaussian functions do not satisfy the correct cusp condition at the nuclei can, at a high degree, be overcome by using a sufficiently large basis set with large core-region orbital coefficients.

In Tables 4.10 and 4.11 the results for NH_2 and NH_3^+ are listed (MP2/6-31G** optimized geometries with C_{2v} symmetry with bond length 1.023 Å and bond angle 102.7°, and D_{3h} symmetry with bond length 1.020 Å, respectively). It can be seen that the results, in particular for the isotropic coupling constants of ^{14}N, still vary with the functionals, but the changes are much more damped than in the atomic studies. The change of basis sets also has a much smaller effect on the ICC for the molecules than for the atoms, as does decontraction of the IGLO-III basis set. For the two molecules under

Table 4.10. Isotropic coupling constants (MHz) of $^{14}NH_2$ and $^{14}NH_3^+$.

Functional	Basis sets		$^{14}NH_2$		$^{14}NH_3^+$	
	Orbital	Auxiliary	N	H	N	H
LDA	IGLO-III	(4,4;4,4)	7.91	-48.91	16.57	-56.14
BP	IGLO-III	(4,4;4,4)	17.23	-51.91	29.40	-63.47
PWP	IGLO-III	(4,4;4,4)	23.21	-46.85	35.82	-59.18
PWP	IGLO-II	(4,4;4,4)	18.12	-57.01	30.57	-69.88
PWP	(11s,7p,2d)	(4,4;4,4)	21.11	-50.84	33.40	-64.73
PWP	IGLO-III	(4,3;4,3)	25.57	-42.62	35.92	-56.52
PWP	IGLO-III	(5,2;5,2)	27.38	-50.50	41.38	-63.44
expt'l[a]			27.9	-67.2	54.6	-76.8
UHF[b]			42.0	-101.6	86.0	-135.5
MRCISD[c]				24.1	-63.4	50.12-79.58

[a] Ref. 74 for NH_2 and ref. 101 for NH_3^+.

[b] Ref. 102 for NH_2 and ref. 103 for NH_3^+.

[c] Ref. 73 for NH_2 and ref. 104 for NH_3^+.

study, the combination of the PWP functional and the IGLO-III + (5,2;5,2) basis set gives overall HFS in closest agreement with experiment[74,101,102,103] and MRCISD values[73,104], especially for NH_2.

The anisotropic coupling tensors for the nitrogen and hydrogen atoms of the two molecules have also been calculated and listed in Table 4.11. For the orientation of the principal elements for the nitrogen, X is the symmetry axis and Z is perpendicular to the molecular plane. Since the singly occupied nitrogen *p* orbital is along Z, a large magnitude is found. For the hydrogens, the picture is different. The smallest principal

Table 4.11. Anisotropic coupling constants (MHz) of $^{14}NH_2$ and $^{14}NH_3^+$. X,Y,Z are the eigenvalues of the anisotropic coupling tensors.

Functional	Basis sets			$^{14}NH_2$		$^{14}NH_3^+$	
	Orbital	Auxiliary		N	H	N	H
LDA	IGLO-III	(4,4;4,4)	X	-43.40	-54.87	-48.13	-56.05
			Y	-43.36	-8.66	-48.13	-13.30
			Z	86.75	63.54	96.26	69.35
BP	IGLO-III	(4,4;4,4)	X	-44.99	-54.65	-49.13	-56.58
			Y	-43.94	-7.54	-49.13	-12.24
			Z	88.93	62.19	98.25	68.81
PWP	IGLO-III	(4,4;4,4)	X	-45.64	-54.19	-49.59	-56.05
			Y	-44.30	-7.54	-49.59	-12.19
			Z	89.94	61.73	99.18	68.24
PWP	IGLO-II	(4,4;4,4)	X	-45.17	-54.24	-48.53	54.90
			Y	-43.55	-9.27	-48.53	-13.70
			Z	88.72	63.51	97.05	68.60
PWP	(11s,7p,2d)	(4,4;4,4)	X	-45.17	-54.24	-49.52	-56.15
			Y	-43.55	-9.27	-49.52	-12.17
			Z	88.72	63.51	-99.85	68.31
PWP	IGLO-III	(4,3;4,3)	X	-45.45	-53.57	-49.16	-55.44
			Y	-44.20	-6.83	-49.16	-11.48
			Z	89.65	60.40	98.31	66.92
PWP	IGLO-III	(5,2;5,2)	X	-45.09	-54.02	-49.23	-55.81
			Y	-43.95	-7.17	-49.23	-12.28

	Z	89.04	61.20	98.46	68.09
expt'l[a]	X	-44.6	-55.4	-42.42	-54.88
	Y	-43.1	-5.2	-42.42	-7.00
	Z	87.7	65.8	84.84	61.88
UHF[b]	X	-36.0	-60.6	-43.54	-59.92
	Y	-32.0	-5.0	-43.54	-16.24
	Z	70.0	86.6	87.08	76.16
MRCISD[c]	X	-42.9	-54.5	-46.38	-49.45
	Y	-42.4	-7.3	-46.38	-14.28
	Z	85.3	61.7	92.76	63.73

[a] Ref. 90 for NH_2 and ref. 121 for NH_3^+.

[b] Ref. 102 for NH_2 and ref. 103 for NH_3^+.

[c] Ref. 73 for NH_2 and ref. 104 for NH_3^+

element, Y, is perpendicular to the molecular plane, similar to the situation of the CH_3[105] radical.

One can see from Table 4.11 that they change very little with functional form and basis set, and are in very good agreement with experiment[74,106] and MRCISD[73,104] values. This is promising since anisotropic coupling constants are much harder to obtain experimentally, and since the DFT methods can handle much larger molecules than conventional *ab initio* CI methods.

The final variable tested in the present communication is the size of the grid used in the fitting of the exchange-correlation functional. The computer code presently used

Table 4.12. The effects of varying the grid size on the HFS of ^{14}N and NH_3^+ [a].

			Functional Form		
Nucleus	N_{grid} [b]	HFS	LDA	BP	PWP
		Atomic Nitrogen			
^{14}N	6	iso	-5 16	-9 67	23 29
	12	iso	-5 16	-9 67	23.29
	26	iso	-5 16	-9.67	23.29
	194	iso	-5 16	-9 66	23 29
		NH_3^+			
^{14}N	6	iso	15 76	26 89	33.37
		X	-48 19	-49.14	-49.78
		Y	-48 19	-49 14	-49 78
		Z	96 38	98.28	99.56
^{1}H		iso	-54 83	-59.91	-55.84
		X	-55 86	-56 01	-55 61
		Y	-13 14	-11.91	-11.88
		Z	68 99	67 92	67 49
^{14}N	194	iso	16 52	29.43	35.75
		X	-48 13	-49 13	-49 59
		Y	-48 13	-49 13	-49 59
		Z	96 26	98 25	99 18
^{1}H		iso	-56 14	-63 63	-58.86
		X	-56 06	-56.43	-56 00
		Y	-13 29	-12 17	-12 09
		Z	69 35	68.60	68.08

[a] In the atomic calculations, the (5,2,5,2) auxiliary basis set is used, and for NH_3^+ the (4,4;4,4) and (4,2,4,2) auxiliary basis sets for N and H, respectively, are used Throughout, the IGLO-III orbital basis set is employed All results are in MHz

[b] N_{grid} indicates the number of angular points employed in the fitting of the exchange correlation functional in each of the 32 radial shells

in this study allows for a variation of the grid as described in Section 4.6.1. Table 4.12

lists the results from the grid calculations on ^{14}N and $^{14}NH_3^+$, using 6, 12, 26 or 194 angular points each in 32 radial shells. In the atomic calculations, it is apparent that the present choice of grids has very little influence on the computed HFSs. A small effect is first observed in the BP calculations when the finest grid is employed. In the case of the NH_3 radical cation, the effect is stronger, in particular when going from the coarsest grid (N_{grid}=6) to the finer ones. For the isotropic terms, the effects of changing the functional form are far greater than the effects of varying the grid size. For the anisotropic hyperfine couplings, the functional form has very little influence, and the effects are more comparable in magnitude.

4.7. Conclusions

In this chapter, the convergence of the spin polarization in terms of the ICC calculated with quantum chemistry methods is explored.

First, the problem of obtaining a converged set of hyperfine parameters of the NH_2 radical from MRCISD theory is addressed in terms of the size of the reference space and the configuration selection energy threshold T_E. The reference space is varied from one (CISD) to 126 spin-adapted reference configurations, and the energy threshold is lowered as far as 3.3×10^{-9} hartree. The effect of basis set is also explored by using two uncontracted basis sets (11*s*7*p*2*d*/7*s*2*p*) and (13*s*8*p*2*d*/8*s*2*p*). The number of spin-adapted configurations included in the calculations varies from a few thousand for the CISD

calculations up to 350,000 for the largest efforts. As expected from previous work, the anisotropic coupling constants show very little variation with the various parameters, and are in very good agreement with experiment. Convergence is basically observed already at the CISD level for this part of the hyperfine tensor. For the isotropic couplings large variations are found as a function of T_E and reference space, and it is concluded that converged solutions cannot be reached unless a selection threshold below 10^{-7} hartree coupled with a reference space of at least 80 spin-adapted configurations is used. The best theoretical predictions of the hyperfine couplings lie well within the error bars (1 MHz) of the experimental data.

Secondly, the convergence of basis set contraction schemes to the ICC has been examined on the basis of the above MRCISD study. The contraction schemes tested here include the atomic natural orbital method, Raffenetti's general contraction method and the segmented method. The contraction coefficients for Raffenetti's and the segmented methods are taken from atomic HF orbitals. The primitive set for nitrogen is (13*s*8*p*) and is contracted to a series of basis sets, first from [4*s*3*p*2*d*] to [8*s*3*p*2*d*] in the *s* space and from [7*s*3*p*2*d*] to [7*s*6*p*2*d*] in the *p* space. It has been found that all three methods converge to the result with the uncontracted primitive set and that the ANO approach leads to a smoother and somewhat faster convergence than the other two HF-based methods. Therefore, at a moderate degree of contraction such as (13*s*8*p*2*d*) to [7*s*6*p*2*d*], all three contraction schemes are expected to yield similar results whereas the ANO approach is able to yield semi-quantitative results at a higher degree of contraction. The different behaviours of the contraction schemes at small basis set sizes are interpreted in terms of the diffuseness of the basis set. Thus, the small ICC with the ANO scheme is

due to the tightness of the ANOs and the large ICC with the two HF-based approaches is due to the diffuseness of the HF AOs.

We also examined the recovery of the core electron correlation effect with the ANO approach using the sensitivity of HFS to the balance between the core electron and valence electron correlations. In contrast to the previous speculation, it is found here that the core-electron correlation is recovered well with the simple choice of the ANOs according to the populations. In addition, it has also been found that adding the outermost primitive Gaussians to an ANO set to increase the diffuseness is not advisable for the calculations of HFS.

Thirdly, the potential of the application of DFT to HFS study is explored. A survey of exchange and correlation functionals and basis sets has been conducted using the first-row atoms and the molecules NH_2 and NH_3^+. It has been found that the calculated anistropic couplings for the molecules do not change much and are in good agreement with *ab initio* and experimental values. The ICC changes dramatically with different combinations of functionals and basis sets, although the calculated molecular ICCs change much less than the atomic values. For NH_2 and NH_3^+, the computed PWP/IGLO-III + (5,2;5,2) values are in excellent agreement with experiment and MRCISD data.

Chapter 5.

Isomers of the Alkaline-Earth Hydroxides

Reliable predictions of new molecular structures and properties is one of the ultimate goals of theoretical studies. In this chapter, the CI and MCSCF methods presented in Chapter 3 will be used to predict the existence of a new isomer of each of the alkaline-earth hydroxides with particular attention paid to their structures and vibrational frequencies. Qualitative analysis of the bonding will also be made in order to understand the new structures. Since the experimental data referred in this work consist mainly of geometries and vibrational frequencies, the basics of the experimental measurements are introduced first, followed by a summary of previous studies on the same systems and then the results of the present research.

5.1. Spectroscopic Measurement of Molecular Structures and Vibrations

The geometry of a molecule can be calculated theoretically. Within the Bohr-Oppenheimer approximation, the motion of electrons and nuclei are separable. Since the Hamiltonian is dependent on the positions of nuclei $\bar{R}$ (Equation (4)), the wave function and total energy are functions of $\bar{R}$. The calculated geometric structure $\bar{R}_0$ of a

molecule then corresponds to the lowest energy with respect to $\bar{R}$, i.e.

$$\left(\frac{\partial E(\bar{R})}{\partial \bar{R}}\right)_{\bar{R}-\bar{R}_0} = 0 \tag{128}$$

The above structure is often referred to as the *equilibrium structure*, around which the nuclei vibrate.

A molecular structure can also be measured experimentally through molecular rotational spectroscopy in the gas phase. The rotational Hamiltonian operator can be written as:

$$\hat{H}_r = \frac{\hat{L}_x^2}{2I_x} + \frac{\hat{L}_y^2}{2I_y} + \frac{\hat{L}_z^2}{2I_z} \tag{129}$$

where the I_i are the *moments of inertia* defined in the principal axis system and the $\hat{L}_i$ are the angular momentum operators with respect to the nuclei. The moments of inertia are simple functions of the nuclear coordinates. The moments of inertia can be obtained from the transitions between rotational energy levels and, thus, the geometry of the molecule can be determined.

The simplest example is a homonuclear diatomic molecule. Its Hamiltonian operator is:

$$\hat{H}_r = \frac{\hat{L}^2}{2I} \tag{130}$$

where I is calculated in terms of the internuclear distance R and the nuclear mass m:

$$I = \frac{1}{2}mR^2 \tag{131}$$

From Section 2.5.1 we know that the eigenvalue for $\hat{L}^2$ is $L(L+1)\hbar^2$ and the energy difference between level $(L-1)$ and L thus becomes:

$$\Delta E = \frac{L\hbar}{I} \tag{132}$$

By experimentally observing ΔE, the internuclear distance can be obtained.

In addition to rotation, the nuclei have another type of motion - vibration around the equilibrium position of the nuclei. The Hamiltonian for the molecular vibration is:

$$\hat{H}_v = -\frac{1}{2m_i}\sum \nabla_i^2 + \sum_{i<j} V(i,j) \tag{133}$$

where m_i is the mass of the ith nucleus and $V(i,j)$ is the interatomic potential. Usually

the displacements of the nuclei around the equilibrium position are very small. This equation is separable if the potential is written as a harmonic force:

$$\hat{H}_v = -\frac{1}{2}\sum\left(\frac{\partial^2}{\partial\xi_i^2} + k_i\xi_i^2\right) \tag{134}$$

where the ξ_i are the mass weighted Cartesian displacement coordinates and the k_i are the force constants which can be derived theoretically from the second derivatives of the energy with respect to the displacements. For the vibrational mode i, the vibrational energy is:

$$E_i = \hbar\sqrt{k_i}\left(v_i + \frac{1}{2}\right) \tag{135}$$

where v_i is the *vibrational quantum number*. The energy difference between two adjacent energy levels becomes:

$$\Delta E_i = h\nu_i \tag{136}$$

where ν_i is the *harmonic vibrational frequency*, which can be calculated as $\frac{1}{2\pi}\sqrt{k_i}$, and thus the theoretical predictions of the force constants can be verified experimentally.

5.2. Previous work on alkaline-earth hydroxides

The gas-phase alkaline earth monohydroxides are of considerable astrophysical interest. Tsuji[107] has predicted that these compounds are important species in stellar atmospheres. This interesting class of free radicals provides a number of ideal candidates for optical studies since they are readily produced in the laboratory and their low-lying electronic states are located in a convenient region for dye laser excitations. In 1983, Harris and co-workers performed the first rotational analysis of CaOH/CaOD[108] and SrOH/SrOD[109] and established the linear geometry of these molecules. They used a molecular source operating at low temperature and low pressure which greatly reduced the spectral density. Since then, spectroscopic investigations of MOH (M = Mg, Ca, Sr and Ba) molecules[110,111,112,113,114,115,116,117,118,119,120] have progressed rapidly. In particular, extensive and high precision data for CaOH and SrOH have been recorded in several laboratories, yielding important physical quantities such as permanent electric dipole moments[114], and the Renner-Teller and Fermi resonance parameters[116,119,120]. The simultaneous study of the two isotopomers, CaOH and CaOD, has led to accurate determination of the equilibrium bond lengths, valence force constants and Coriolis coupling parameters for the ground state[120].

The geometries and electronic structures of CaOH and other alkaline earth monohydroxides have also been subject to various theoretical studies. It has been well established that like the molecules consisting of alkaline earth metals and other electronegative ligands (L), they are essentially ionically bonded as $M^+(OH)^-$. The metal gives one *s* electron to the ligand and the two parts are held together

electrostatically. This picture is consistent with the experimental observations and the theoretical studies which indicate that all of these molecules are linear or quasilinear. The linearity suggests that the bonding is ionic, for if the bonding were covalent the lone−pairs on oxygen would force the molecules to bend. The low−lying electronic states are formed by promoting the unpaired electron from the n*s* orbital of the metal to the n*p*(n−1)*d* and the (n+1)*s* orbitals. Based on this model, a substantial amount of theoretical work with ab initio and semi-empirical methods has been done.

Assuming that the molecules will dissociate into ions, Bauschlicher and Partridge[121] calculated the dissociation energy of CaOH and LiOH using the ROHF method with a large basis set of at least triple−zeta plus double polarization quality. Their result (4.08 eV, zero-point energy corrected) is close to the experimental value[122] of 4.23±0.04 eV. Bauschlicher et al[123] studied the structures and energetics of the ground states of the alkali and alkaline−earth monohydroxides (including CaOH) at the CISD level with the same basis set. In addition to the equilibrium distance between the metal and the ligand and the dissociation energy, vibrational frequencies and bending potentials were calculated. The CISD dissociation energy (4.15 eV, zero-point energy corrected) is closer to the experimental value than the ROHF value. The calculated bond lengths are less than 0.02 Å different from the experimental values. The calculated Ca-O stretch frequency is very close to the experimental value whereas the calculated Mg-O stretch frequency is 50 cm^{-1} less than the experimental value. The permanent dipole moments of the $X^2\Sigma^+$, $A^2\Pi$ and $B^2\Sigma^+$ states of CaOH were calculated at the computed equilibrium geometries with the coupled−pair functional (CPF) and modified CPF methods[124]. Large discrepancies are found among the predictions of the dipole moment

at different theoretical levels. The geometries and bending potentials of BeOH and MgOH were also studied using unrestricted–Hartree–Fock fourth–order Møller–Plesset perturbation theory by Palke and Kirtman[125]. This bending potential and Bauschlicher et al's[123] are quite different from the experimental result, which is not surprising, given the flat nature of the bending potential. Ortiz studied the ground and excited states of CaL (L = CH_3, NH_2, OH and F) by means of electron propagator calculations[126]. Semi-empirical models were proposed[127,128,129,130] to calculate the binding energies, excitation energies and dipole moments of these ionic molecules M^+L^- including L = OH^-. The models were based on the classic electrostatic interaction plus the polarization of M^+ and L^- and the excited states were treated in a fashion closely related to ligand field theory. The predictions compared well to experimental and ab initio data.

5.3. The Second Structure of CaOH: HCaO[131]

During the study of the energy surface of CaOH another minimum was found with an electronic state of $^2\Sigma^+$ symmetry. It has the form HCaO with a linear structure, analogous to HBO and HAlO. In this section, the energy surface around the minimum at both the Hartree–Fock and the CISD levels is described. Also included are the O-H stretching frequency and the bending frequency of CaOH, which were omitted from previous theoretical studies. The ground state of this system, $^2\Pi$, will be discussed in Section 5.5.

5.3.1. Computational methods

The basis set used for most of the calculations is fairly complete: (15*s*13*p*7*d*2*f*/9*s*9*p*6*d*2*f*) for Ca, (11*s*7*p*3*d*1*f*/6*s*4*p*3*d*1*f*) for O and (8*s*4*p*/5*s*3*p*) for H. The *s* and *p* functions of the Ca basis set start from the 14*s*9*p* basis set of Wachters'[132] with the addition of his two diffuse, 4*p*-like functions, as well as two additional *p* functions and a diffuse *s* function. The exponents and contraction coefficients for the *d* and *f* polarization functions are from the literature[123]. The O basis set uses the (11*s*6*p*) primitive set of van Duijneveldt[82] contracted to [6*s*3*p*]. This is supplemented with a diffuse set of *p* functions optimized for the negative ion, three sets of *d* functions and one set of *f* functions, resulting in (11*s*7*p*3*d*1*f*/6*s*4*p*3*d*1*f*). The H basis set is the (6*s*) set of van Duijneveldt[82] contracted to [3*s*] to which two diffuse *s* functions and four sets of *p* functions are added; the *p* functions are further contracted[123], resulting in (8*s*4*p*/5*s*3*p*).

The calculations were first done at the ROHF level, followed by the CISD calculations to include the correlation effects for the valence−shell electrons on all the atoms, plus the outer-core $(3s)^2(3p)^6$ electrons of Ca. The study on alkaline-earth monohalides[133] has shown that the pair-pair terms, the double excitations where one electron is excited from a M^+ outer-core orbital and the other from a L^- valence orbital, are increasingly important when the M-L distance is small and tends to make the bond short. Including the outer-core shell electrons (17 electrons in total) in correlation calculations compensates for the correlation effect of valence electrons, which tends to make the bond too long and yields results in better agreement with experiment for the M-L bond length, frequency and dissociation energy. In the CI calculations, the

contributions of all configurations from double excitations were estimated by means of perturbation theory and those that are predicted to make contributions below a threshold (10^{-7} hartree for bond stretching modes) were eliminated from the diagonalization of the Hamiltonian matrix to save disk space and computing time[77,78]. The estimated contribution from the discarded configurations changed little during optimization for bond-stretching modes.

For the CISD bending potential scan, the estimated contribution from the discarded configurations changes with the angle and becomes increasingly significant. Because of hardware limitations a somewhat smaller basis set was used. It is basically a triple-zeta valence (TZV) basis set augmented with diffuse and polarization functions. The basis functions for H are from Dunning's TZV basis set[134] augmented with a diffuse *s* function and three sets of *p* polarization functions, resulting in a basis set (6*s*3*p*/4*s*3*p*). The (11*s*7*p*3*d*/6*s*4*p*3*d*) set for O is composed of Dunning's TZV[134], a diffuse *s*, a diffuse set of *p* and three sets of *d* polarization functions. The Ca set starts from Wachters' (14*s*9*p*) set[132] contracted to (8*s*4*p*), augmented with three *p* functions to describe the subshell (4*p*), and three *d* polarization functions, resulting in (14*s*12*p*3*d*/8*s*7*p*3*d*). The energy threshold for selecting configurations included in the Hamiltonian diagonalization was also decreased to 5.0×10^{-8} hartree. With this basis set, the estimated contribution from the discarded configurations was less than 10^{-5} hartree and had little effect on the geometry optimization.

The equilibrium bond distances and harmonic frequencies were obtained by a parabolic fit to the energy curves with step intervals less than 0.03 Å. The bending angle was scanned up to 15° from the linear structure. The calculations were done with

the Gaussian 92/DFT[135] and MELDF-X[48] programs.

5.3.2. Results and discussion

ROHF

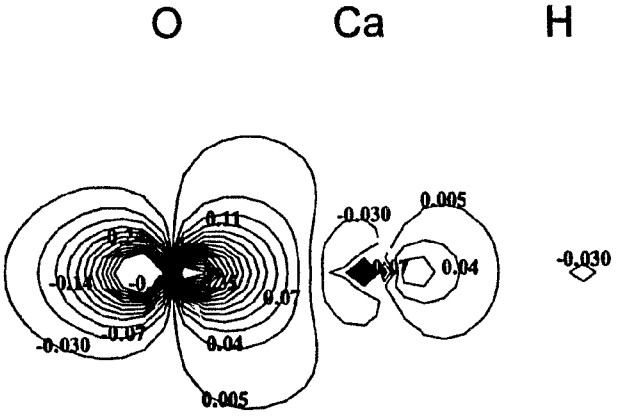

Figure 5.1. Contour plot of the singly occupied orbital of HCaO.

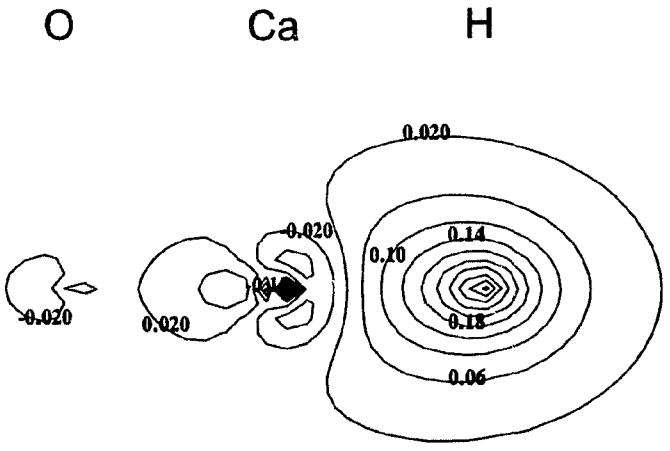

Figure 5.2. Contour plot of the bonding orbital between H and Ca.

Optimization of linear HCaO yielded 2.073 Å for H-Ca and 2.028 Å for Ca-O at the ROHF level. SCF convergence failure with Gaussian 92 prevented characterization of the stationary point by frequency analysis. A potential scan of the bond angle using MELDF-X at the optimized bond lengths of the linear structure confirmed that the linear structure is a minimum. The H-Ca and Ca-O harmonic stretching frequencies and the unscaled harmonic bending frequency were computed to be 1324 cm^{-1}, 560 cm^{-1} and 108 cm^{-1}, respectively. CaOH was also calculated at the ROHF level for comparison. In contrast to CaOH where the unpaired electron is on Ca, the unpaired electron of HCaO is mainly of oxygen $2p_z$ character, which is also the bonding orbital between Ca and O. The contours of the singly occupied orbital of HCaO corresponding to the bonding between Ca and O are depicted in Figure 5.1. The Mulliken population analysis gave -0.69, 1.47 and -0.77, respectively, for H, Ca and O, showing that the amount of negative charge hydrogen gains is quite large, close to what the oxygen does, although one might expect a larger difference as the latter is much more electronegative. Since the number of electrons lost by Ca in HCaO is close to twice that (0.79) in CaOH, one can argue that Ca in HCaO loses two electrons, one each to hydrogen and oxygen.

Figure 5.2 shows the doubly occupied molecular orbital corresponding to the bonding between H and Ca. The molecular orbital is dominated by the contribution of the hydrogen s basis functions. The calculation also shows that the negative charges on both hydrogen and oxygen increase as the bond lengths increase. Therefore, the H−Ca and Ca−O bonds are largely ionic. The overall HF electronic structure can be symbolized as $H(1s)^2Ca(4s)^0O((2s)^2(2p_x)^2(2p_y)^2(2p_z)^1)$ or $H^-Ca^{2+}O^-$.

CISD

Table 5.1. The total CISD energies, equilibrium bond lengths, and harmonic frequencies of HCaO and CaOH.

HCaO (theory)	CaOH (theory)	CaOH (experiment, ref. 116)
E_{total} = -752.41773 hartrees	-752.52027 hartrees[a]	
R(H−Ca) = 2.021 Å	R(O−H) = 0.948 Å	0.954 Å
R(Ca−O) = 2.002 Å	1.988 Å (ref. 123)	1.975 Å
ω(H−Ca) = 1288 cm^{-1}		
ω(Ca−O) = 515 cm^{-1}	629 cm^{-1} (ref. 123)	617 cm^{-1}
ω(H-Ca−O) = 170 cm^{-1}	ω(Ca−O-H) = 405 cm^{-1}	354 cm^{-1}
ω(H-Ca−O) = 146 cm^{-1}	ω(Ca−O-H) = 380 cm^{-1} (9 electrons[b])	
	ω(O-H) = 4040 cm^{-1}	

[a] Calculated at the geometry as of ref. 123.

[b] The CISD result includes 17 electrons unless noted otherwise.

The geometries and harmonic frequencies of HCaO and CaOH at the CISD level along with the experimental results for CaOH are listed in Table 5.1. Compared with the ROHF results, the H-Ca bond length is shortened by 0.052 Å, and the Ca-O bond length by 0.026 Å. This is similar to the CaOH case where the Ca-O bond length was shortened by 0.018 Å when electron correlation was included[123]. Relative to the Ca-O bond in CaOH, the Ca-O bond in HCaO is slightly longer and has a lower frequency, indicating that the latter is weaker (since hydrogen is very light, the Ca-O stretching frequency can be used to compare the Ca-O bond strengths of HCaO and CaOH).

In order to understand the H-Ca bond, it is helpful to compare the results with the bond length and frequency of the CaH molecule. The experimental values[136] for CaH are 2.0025 Å and 1298.34 cm^{-1}, respectively, which are comparable with those of the H-Ca bond in HCaO, 2.021 Å and 1288 cm^{-1} respectively, suggesting a similarity between the two.

A potential energy scan of the H-Ca-O bond angle confirmed that the linear structure is a minimum at the CISD level, which reinforces the conclusion at the ROHF level that the linear structure is energetically favoured. In fact, the curvature at the CISD level is greater than at the HF level, indicated by the greater bending frequency (170 cm^{-1} vs. 151 cm^{-1} with the TZV basis set) at the CISD level.

The previous theoretical studies of MOH have been focused on characterizing the Ca-O bond with the O-H bond length fixed at its value in free OH^-. In this work, the potential curve for the O-H stretching mode has been calculated. The optimized bond length is slightly (0.006 Å) shorter than the experimental result, and the frequency is much higher than that of free OH or OH^{-1}, which is around 3700 cm^{-1} [137]. The increase of the O-H frequency from a free anion to a ligand in MOH should not be surprising as M^+ would make OH^- more polarized.

Since the experimental value of the CaOH bending frequency is available[116], theoretical calculations were carried out for comparison. It is found that the bending frequency of CaOH calculated, with 17 electrons included in the CISD procedure was about 50 cm^{-1} higher than the experimental value (354 cm^{-1}). The CISD value (380 cm^{-1}) including only valence shell electrons (9 electrons), however, has been found to be in better agreement with experiment. The energy difference between the two structures

HCaO and CaOH is large (269 kJ/mol), which may help to explain why HCaO has not been observed experimentally.

5.4. The $^2\Sigma^+$ states of HBeO, HMgO and HCaO

From the last section, it has been learned that a second structure, HCaO with a $^2\Sigma^+$ state, exists on the hypersurface of CaOH. It is linear and the H−Ca and Ca−O bond lengths are 2.021 Å and 2.002 Å respectively. The overall electronic structure is largely ionic and can be described as $H(1s)^2Ca(4s)^0O((2s)^22(p_x)^22(p_y)^2(2p_z)^1$. The H-Ca bond is similar to that of the HCa molecule as indicated by the similar bond length and frequency. The Ca-O bond in HCaO is longer and has a lower frequency than that in CaOH, suggesting that the former is weaker.

The finding of this new structure provided the motivation to explore the possibility of HBeO and HMgO and to try to understand the bonding of these new structures. Thus, extensive ab initio CASSCF calculations for HMO (M=Be, Mg and Ca) were carried out for the $^2\Sigma^+$ state, which is the ground state of MOH.

5.4.1. Methodology

In this study, the complete-active-space-self-consistent-field (CASSCF) method was chosen because the availability of CASSCF analytical gradients makes the full geometry optimization feasible. Moreover, a multiconfiguration approach is required for the study of the isomerization of HMO/MOH, one of the objectives of this research. The

CASSCF method can potentially perform better than the single reference CISD method. For example, in their benchmark study of the radical OH, Bauschlicher and Langhoff[138] found that CASSCF gives spectroscopic constants, such as the equilibrium bond length, frequency, dipole moment and dissociation energy, closer to the full-CI result than the single reference CISD method, when oxygen virtual *p* orbitals with π symmetry are included in the active space. The multiconfiguration method has also been used for the studies of similar systems[139,140,141,142].

In addition to the bonding and antibonding σ orbitals, the occupied and virtual orbitals pertaining to the O 2*s* electrons were also included, resulting in six a_1 orbitals in the CASSCF active space. In addition, the occupied and virtual *p* orbitals of oxygen, two b_1 orbitals and two b_2 orbitals, are also included in the active space. The final active space is composed of 9 electrons and 10 orbitals and can be denoted as (622). Although including the (n - 1) shell of metal atoms might lead to better quantitative results, it would be prohibitively expensive. CISD calculations with a single reference are also carried out for comparison. The GAMESS program[143] was used for all the calculations in this section.

The extensive basis sets used are the same as those in the Bauschlicher et al[123] study of MOH. The Be (11*s*5*p*2*d*/6*s*3*p*2*d*) contracted basis set was formed from the 11*s* primitive set of van Duijneveldt[82] to which five sets of *p* functions[144] and two sets of *d* functions[145] were added. The Mg (12*s*9*p*5*d*/6*s*5*p*4*d*) contracted basis set was extracted from McLean and Chandler's[146] modification of the original Huzinaga (12*s*9*p*) basis set[147], to which five sets of *d* functions[123] were added. The basis sets for Ca, O and H are the same as those in Section 5.3.

5.4.2. Calculated spectroscopic parameters and energetics

The CASSCF optimized spectroscopic parameters - bond lengths, stretching and bending harmonic frequencies and dipole moments - of Hbeo, Hmgo and Hcao are listed in Table 5.2. All of these molecules favour the linear structure. In contrast with the hydroxides in which the central oxygen atom has lone pairs, linearity is expected even if the bonds are covalent. The CASSCF spectroscopic parameters of MOH are listed in Table 5.2 for comparison. It can be seen that the M-O bond length of HMO is slightly longer than that of MOH, by amounts ranging from 0.01 Å for BeOH to 0.05 Å for MgOH. The M-O bond stretching frequency of HMO does not differ much from that of MOH except for M = Be where the former is more than 100 cm^{-1} lower than the latter. The implication of this observation will be discussed in the next section.

The SCF (ROHF) results are also listed in Table 5.2 (in parentheses) for comparison. From Bauschlicher et al's study[123] of MOH, the difference between the SCF and CISD optimized M-O bond lengths (at a fixed O-H bond length of 0.947 Å) are 0.001 Å for both Be and Mg and 0.018 Å for Ca. The M-O stretching frequency also differs by only 7 cm^{-1} at most. Considering the numbers were obtained with a parabolic fit, the differences are trivial. The CASSCF M-O stretching frequencies calculated here for both MOH and HMO show the same trend as they are only slightly smaller than the SCF frequencies. On the other hand, the CASSCF stretching frequencies for the covalent O-H bonds differ significantly from the SCF results. The CASSCF M-O bond lengths are longer by approximately 0.02 - 0.03 Å.

Compared with the experimental results of CaOH[120], the CASSCF M-O is 0.05 Å

Table 5.2. The bond lengths r_e (in Å), frequencies ω_e (in cm^{-1}) and dipole moments μ (in debyes) of HMO and MOH at the CASSCF and SCF (in parentheses) levels.

	H - M		M - O		O - H		bending	μ
	r_e	ω_e	r_e	ω_e	r_e	ω_e	ω_e	
HBeO	1.324(1.324)	2258(2261)	1.425(1.405)	1120(1163)			579(583)	0.637
HMgO	1.723(1.692)	1592(1751)	1.851(1.823)	652(663)			197(227)	2.318
HCaO	2.102(2.072)	1210(1314)	2.043(2.027)	543(564)			163(156)	0.107
BeOH(bent)			1.415(1.391)	1257(1327)	0.955(0.934)	3975(4280)	422(409)	1.260
BeOH(linear)			1.390(1.372)	1311(1367)	0.949(0.929)	4056(4346)	109i(222i)	1.802
MgOH			1.802(1.774)	676(688)	0.951(0.931)	4012(4311)	516(601)	1.754
CaOH			2.027(2.004)	597(620)	0.956(0.934)	3925(4240)	407(418)	0.605

too long and the CASSCF M-O frequency is 19 cm^{-1} too low whereas the O-H bond length is in excellent agreement with experiment (0.956 vs. 0.954 Å). In fact, the SCF Ca-O bond length is closer to experiment than the CASSCF one. This is because the (n-1) shell of the metal atoms is not included in the current correlation calculations. A previous study of the alkaline-earth monohalides[148] has shown that the pair-pair terms, the double excitations where one electron is excited from a M^+ orbital and the other from a L^- orbital, are increasingly important when M and L are getting close and tend to make the bond short. All the CASSCF bending frequencies are smaller than the SCF ones except for Hcao which is consistent with the CISD results in Section 5.3 where the CISD bending frequency is larger than the SCF one. Overall, SCF is a good zero-order approximation. The SCF method was also found to be effective for understanding the polarization of Ca^+ in CaOH[124].

Since there is no experimental O-H stretching frequency for OH^- as a ligand, an estimate based on the experimental frequencies of OH and OH^- is usually made for the processing of experimental data. The experimental bond lengths and harmonic frequencies are available [136,149,150] for these two molecules (0.970 Å and 3739 cm^{-1} for OH, 0.964 Å and 3738 cm^{-1} for OH^-) and agree remarkably well with the theoretical predictions[151]. In their theoretical study of the alkaline hydroxides, Bauschlicher et al[123] used 3700 cm^{-1} as the O-H stretching frequency in MOH and the O-H bond length was fixed at 0.947Å. Although the CASSCF calculated values of the O-H bond length are in agreement with their representative CISD value of 0.95 $\pm$ 0.01 Å, our stretching frequency of 4000 cm^{-1} is much larger than that of OH and OH^-. In order to determine the accuracy of the O-H frequency obtained here, the frequency of free OH^- has also

been calculated with the (322) active space in the CASSCF calculation. The harmonic frequency (3728 cm^{-1}) and the bond length (0.969 Å) are in excellent agreement with experiment. The increase of the O-H frequency from a free anion to a ligand in MOH is probably due to the polarization effect of M^+ on OH^-. It is believed that the previous estimates of the O-H stretching frequency are too small, although this error will probably not have much effect on calculations of other stretching frequencies.

By the means of the MCPF method Bauschlicher et al[124] predicted the permanent dipole moment of CaOH to be 0.980 D with an estimated uncertainty of 0.2 D, which is smaller than the experimental value (1.465(61) D) obtained from a supersonic molecular beam optical Stark effect study[114]. The CASSCF prediction of 0.605 D is smaller than the Bauschlicher MCPF value but better than the CISD result[124] of 0.449 D. Therefore, the CASSCF dipole moments can only be used for qualitative comparison. The CASSCF dipole moment of MgOH (1.75 D) is larger than that of CaOH, and larger than a semiempirical prediction[130] (1.2 D). The same study also predicted an identical dipole moment for CaOH. It would be reasonable to expect MgOH to have a larger dipole moment because Mg^+ is smaller than Ca^+ and less polarizable. The dipole moments of HMO reach a maximum at M = Mg. This will be discussed further in the next section.

Table 5.3 lists the energy difference ΔE between HMO and MOH at various levels of theory. It can been seen that all energy differences are around 0.1 hartree, or more than 240 kJ/mol after correction for the zero-point energy. This large energy difference may explain why no experimental observation of HMO has been reported. The situation is quite different for the Group III(IUPAC XIII) elements. For the latter, HBO is more

Table 5.3. The energy differences ΔE (in hartree) between HMO and MOH (M = Be, Mg and Ca) at various theoretical levels. The energy differences with zero-point energy correction (in kJ/mol) are given in parentheses.

	ΔE_{SCF}	ΔE_{CASSCF}	ΔE_{CISD}[a]
HBeO/BeOH	0.08685 (220)	0.10789 (278)	0.10080
HMgO/MgOH	0.10336 (251)	0.09998 (244)	0.11775
HCaO/CaOH	0.09489 (229)	0.11333 (278)	0.10254

[a] Zero-point energy is not available for the CISD results because CISD frequencies were not calculated.

stable than BOH, whereas AlOH is more stable than HAlO[152].

5.4.3. Discussion

The focus of past theoretical studies of alkaline earth hydroxides has been on their similarity with the alkali hydroxides as both of them are ionic compounds. The possible existence of HMO makes it desirable to compare with Group III elements, which have occupied *p* orbitals and can be trivalent when the *s* and *p* orbitals are hybridized, or monovalent when only a *p* orbital is used for bonding. For example, the Lewis structures of HBO and BOH can be easily drawn. In the recent ab initio studies[152,153] of the isomerization of HBO/BOH and HAlO/AlOH, it has been noticed that monovalent species become more stable when moving down the Group III elements. This has been attributed to the lower efficiency of *sp* hybridization due to the presence of both *s* and *p* core orbitals and used to explain why HBO is more stable than BOH, whereas AlOH

is more stable than HAlO.

Group II elements have empty valence *p* orbitals and therefore *sp* hybridization is even less efficient than for the Group III elements. Any possible bivalency of these elements can only be understood with at least one ionic bond (except, perhaps, Be which does not have a core *p* shell) because the valence *p* orbital will be too diffuse to hybridize with the valence *s* orbital. Since the SCF wavefunction is a good zeroth-order approximation for describing HMO/MOH, a generalized bond order analysis based on it, as proposed by Mayer (see Section 3.3), will be used to assist the analysis of the bonding. This bond-order analysis method can be used to indicate the degree of ionic character of a bond, e.g., the bond order for a complete ionic bond will be zero, whereas the bond order for a nonpolarized covalent single bond will be 1. Since H is much lighter than all the other elements involved, the H-M and M-O stretching frequencies will be used for comparison of the bond strengths of these two bonds.

In order to understand the bonding of the HMO molecules, it is helpful to compare the H-M and M-O bonds in MH and MO in addition to those in MOH. Table 5.4 lists the CASSCF bond lengths and stretching frequencies, as well as the SCF bond orders in the Σ^+ states of HMO, MOH, MH, MH^+, MO and MO^+ for the following discussion. The cations are included due to the possibility of ionic bonds.

HBeO

The relationship between Be and the rest of the Group II elements is similar to that of B to the rest of the Group III elements. Since there are no inner *p* orbitals, the empty

Table 5.4. The CASSCF bond lengths (in Å), frequencies (in cm^{-1}) and SCF bond orders of HMO, MOH, MH, MH^+, MO, and MO^+ in their lowest Σ^+ states.

	H - M bond				M - O bond		
	r_e	ω_e	Bond order		r_e	ω_e	Bond order
HBeO	1.324	2258	0.94		1.425	1120	0.97
BeOH					1.390	1311	1.26
BeH	1.358	2016	1.02	BeO	1.335	1534	2.13
BeH^+	1.344	2073	1.01	BeO^+	1.349	1434	1.43
HMgO	1.723	1592	0.91		1.851	652	0.13
MgOH					1.802	676	<0.05
MgH	1.788	1461	0.84	MgO	1.788	664	1.12
MgH^+	1.695	1644	0.86	MgO^+	1.734	699	0.29
HCaO	2.102	1210	0.50		2.043	543	0.48
CaOH					2.027	597	0.47
CaH	2.073	1531	0.61	CaO	1.852	732	1.48
CaH^+	1.963	1393	0.81	CaO^+	1.927	670	0.68

p orbitals of Be are relatively compact and can be used for hybrid orbitals to form covalent bonds. For instance, both BeOH and BOH are bent whereas the hydroxides of the other elements in both groups are linear; the Be_4 cluster is strongly bonded due to the efficiency of sp hybridization, whereas Mg_4 and Ca_4 are only weakly bonded at the correlated level (CISD)[145].

The calculations for the $^2\Sigma^+$ state of HBeO show that Be forms two *sp* hybrid orbitals, one of which is used to form the covalent bond (doubly occupied molecular orbital) with H 1s and the other to form a covalent bond (singly occupied molecular

orbital) with the empty O $2p_z$. The two doubly occupied π orbitals (O p_x and p_y) overlap with the empty Be p_x and p_y and form two weak π bonds to give a Be-O bond order of about 1 rather than the 0.5 expected from the Lewis structure. This bond order is also the same as the Be-O bond in BeOH, which also indicates that the Be-O bond in HBeO is covalent, similar to that in BeOH.

It is interesting to compare HBeO with BeH and BeO. In BeH, Be forms two *sp* hybrid orbitals, one of which forms a covalent bond with H. The other sp hybrid orbital is singly occupied, remains localized on Be and is slightly antibonding. When the unpaired electron is removed to form BeH^+, the bonding is strengthened a little.

The bonding in BeO can be understood as a covalent bond between Be^+ ($(2s)^1$) and O^- ($(p_x)^2(p_y)^2(p_z)^1$). The two doubly occupied π orbitals (O^- p_x and p_y) overlap with the empty Be^+ p_x and p_y to form two weak conjugate π bonds, so that the overall bond order is 2. A similar conjugation effect also occurs in HBO and makes the B-O bond length shorter than a normal B-O double bond[152]. When one electron is removed from the σ bonding orbital, the bonding is weakened, as shown by a decrease in the frequency, the increase of the bond length and the decrease of the bond order by 0.5. Table 5.4 shows that the H-Be bond in HBeO is more similar to that in BeH and BeH^+ than the Be-O bond in HBeO is related to BeO and BeO^+. The reason for this is that the *sp* hybrid orbitals used for bonding in HBeO are more diffuse than the Be 2*s* orbital used in BeO and BeO^+ and, therefore, the Be-O bond in HBeO is significantly weaker and longer. The Be-O bond order is also smaller, as the longer bond length makes the conjugate π bonds weaker.

HMgO

In contrast to BeOH, MgOH has been recognised as being ionic due to its linear structure. The near-zero bond order of the Mg-O bond in MgOH is consistent with this argument. Similar to BeH and BeH^+, the bonding of MgH and MgH^+ is still mainly covalent but more polarized, as indicated by a bond order somewhat smaller than 1.0. The bond length and frequency of H-Mg in HMgO lie between MgH and MgH^+, but closer to the latter. Similar to BeO, MgO can still be described as being covalently bonded between Mg^+ and O^-, but its bond order is smaller than that of BeO and close to that of a single bond (1.0) due to the lower efficiency of π conjugation since the Mg *p* orbitals are more diffuse. MgO^+ is ionic and similar to $Mg^{2+}O^-$, as the small bond order and large SCF Mulliken charges of Mg (1.58) and O (-0.58) indicate. These results also show the tendency of Mg to form an ionic bond with oxygen. The Mg-O bond in HMgO has a very small bond order, suggesting that it is ionic, as in MgOH and MgO^+, but a little weaker. Therefore, the molecule looks like $(HMg)^+O^-$. This viewpoint is also consistent with the large negative Mulliken charge on O (-0.75) compared to H (-0.33) and the much larger dipole moment of HMgO relative to HBeO.

HCaO

Since Ca is further down the periodic table, it has a lower ionization energy than Be and Mg, and therefore, it has a greater tendency to form ionic bonds. The H-M bond in CaH and CaH^+ is much more ionic than its Mg counterparts, as indicated by the large

Mulliken charges (-0.41 on H and 1.41 on Ca for CaH^+), as well as the smaller bond order. The H-Ca bond in HCaO is weaker than that of CaH and CaH^+, and more ionic than the H-Mg bond in HMgO, as shown by the large magnitude of the Mulliken charge on H (-0.69). The similarity of the Ca-O frequency and bond order in HCaO and to those of CaOH suggests that the Ca-O bond in HCaO is ionic. Al. 'he bond orders involving Ca, however, are larger than those of Mg, contrary to what one would expect for a more ionic bond. This is consistent with the argument of the polarization of Ca^+ in CaOH, which was used to explain why the dipole moment of CaOH is extraordinarily small[124]. Part of the reason is the compactness of the inner unoccupied 3*d* orbitals of Ca, which can hybridize efficiently with Ca 4*s* orbitals. One indication of this is the high Mulliken population of the *d* orbitals (0.2). The properties of Ca are often closer to those of Be than to Mg. For example, MgOH has the lowest dissociation energy among alkaline earth monohydroxides[123] and the dissociation energy of MgH is smaller than that of BeH and CaH[136]. HCaO is ionic and resembles $H^-Ca^{2+}O^-$.

5.5. The $^2\Pi$ State of HMO

In the last two sections, it has been established that the alkaline earth hydroxides have another linear isomer with the form HMO. Its two bonds are increasingly ionic with the increase of the atomic number. The instability of the $^2\Sigma^+$ state of HMO relative to MOH remains more or less the same for all the alkaline earth elements studied. The unpaired electron is largely on oxygen, occupying the M-O bonding orbital to maintain $^2\Sigma^+$ symmetry.

Linear HMO does not necessarily have to adopt a $^2\Sigma^+$ ground state. If the bonding orbital is doubly occupied, i.e., forming $^2\Pi$, the molecule may be more stable. With such a state, the unpaired electron shares two oxygen *p* orbitals perpendicular to the molecular axis with the other two electrons. Calculations have been carried out to explore this possibility at the same level (CASSCF) as in the last section and $^2\Pi$ has been found to be the ground state of HMO.

Table 5.5. The energy[a] difference between the $^2\Pi$ and $^2\Sigma^+$ states of HMO.

	ΔE_{SCF}	ΔE_{CASSCF}	ΔE_{CASSCF} (in kJ/mol)
HBeO	0.06437	0.04561	119
HMgO	0.02156	0.02196	58
HCaO	0.00226	0.00272	7

[a] The unit is hartree except for the data in the last column which is in kJ/mol.

Table 5.5 lists the energy difference between the $^2\Pi$ and $^2\Sigma^+$ states. It can be seen that the excitation energy decreases dramatically with an increase in atomic number. This observation is in excellent agreement with the argument made in the last section about the bonding characters between M and O. For HBeO, the Be-O bond is mainly covalent and the change from a half bond to a full bond increases the strength of the bonding greatly, reducing the energy difference between the ground state ($^2\Pi$) of HBeO and that of BeOH by half. For HCaO, on the other hand, the Ca-O bond is largely ionic and the singly occupied orbital is mostly on oxygen for both the $^2\Pi$ and $^2\Sigma^+$ states. The move of the unpaired electron from the σ orbital to the π orbitals happens locally and does not significantly affect the bonding. Also, the two states are nearly degenerate,

close to the case of a separated O^-. The ionic character of Mg-O bond in HMgO is between Ca-O and Be-O and therefore, the excitation energy is between those of the latter as well.

Table 5.6. The CASSCF bond lengths (in Å), frequencies (in cm^{-1}) of HMO in their $^2\Sigma^+$ and $^2\Pi$ states.

		H - M bond		M - O bond	
		r_e	ω_e	r_e	ω_e
HBeO	$^2\Sigma^+$	1.324	225	1.425	1120
	$^2\Pi$	1.327	218	1.480	1143
HMgO[a]	$^2\Sigma^+$	1.723	1751	1.851	663
	$^2\Pi$	1.739	1714	1.928	701
HCaO	$^2\Sigma^+$	2.102	1210	2.043	543
	$^2\Pi$	2.123	1177	2.171	501

[a] The frequencies of HMgO are HF results. CASSCF frequencies for the $^2\Pi$ state of HMgO have not been obtained due to the difficulty of convergence.

The bond lengths and harmonic stretching frequencies of the $^2\Pi$ states are listed in Table 5.6 along with those of the $^2\Sigma^+$ states for comparison. The stronger M-O σ bond increases the repulsion to the H-M σ bond and causes the H-M bond length and stretching frequency of the $^2\Pi$ state to become longer and smaller than those of the $^2\Sigma^+$ state. The M-O frequency of the $^2\Pi$ state is only slightly larger than that of the $^2\Sigma^+$ state for Be and Mg and smaller for Ca.

5.6. Conclusion

The alkaline-earth metal monohydroxides MOH have long been considered to be simple ionic compounds, similar to the alkali metal monohydroxides. The present calculations show that they also have isomers with the formula HMO. The $^2\Sigma^+$ and $^2\Pi$ states of HBeO, HMgO and HCaO have been studied at the CISD and CASSCF level with basis sets of at least triple-zeta plus double polarization quality. The correlation includes all the valence electrons, resulting in a CASSCF active space denoted by (622). The optimized structures are all linear. The M-O bond distance in HMO is slightly longer than that in MOH with similar stretching frequencies. The H-M bond length in HMO is comparable with that in MH with similar stretching frequencies. The bond lengths of the $^2\Pi$ state of HMO are longer than those of the $^2\Sigma^+$ state whereas the stretching frequencies are similar for the both states.

The existence of HMO for alkaline earth metals makes it interesting to compare with Group III elements for which both HMO and MOH structures exist. Group III elements have both covalent and ionic characters and the bonding of HMO can be easily understood as being covalent (*sp* hybrids) with increasing ionic character and instability as the atomic number increases. MOH becomes progressively more stable than HMO as the atomic number increases. Since Group II elements have empty *p* orbitals, the *sp* hybrids will be less efficient and the bonding of HMO for Group II elements will be expected to be more ionic. The ionic character increases with atomic number: HBeO has two polarized covalent bonds formed from the *sp* hybrids of Be, HMgO has one covalent bond (between H and Mg) and one ionic bond (between Mg and O) and can be viewed as $(HMg)^+O^-$, and HCaO has two ionic bonds represented by $H^-Ca^{2+}O^-$. This point of view is supported by comparison with the bonding in MOH, MH, MH^+, MO and MO^+

in the $^2\Sigma^+$ state. The picture also implies that the unpaired electron is increasingly localized on oxygen, which explains why the energy difference between the $^2\Sigma^+$ and $^2\Pi$ states of HMO decreases with an increase in atomic number.

The geometries and spectroscopic parameters of MOH for the alkaline-earth elements have also been calculated for the purpose of comparison. It is worthwhile to note that the OH^- stretching frequency in MOH is much larger than in free OH^-, in contrast to the assumption in previous publications.

Chapter 6.

A general linear scaling orbital-optimization method

Efficient orbital optimization, or matrix diagonalization within the self-consistent-field (SCF) method, is critical to the application of quantum chemistry methods to large molecular systems, as a method is now available to evaluate Coulomb integrals with a near-linear scaling with respect to the size of the molecule[154]. One notable development in the study of diagonalization is the density-matrix divide-and-conquer method proposed by Yang and Lee[35]. In their method, the density matrix is divided according to the Mulliken population analysis and each piece of the divided density matrix is approximated by a set of local eigenfunctions and eigenvalues. Since the local environment is independent of the size of the molecule, a linear scaling is achieved for the diagonalization step. This method is an extension of Yang's earlier divide-and-conquer approach within the context of density functional theory (DFT)[155]. Other DFT linear-scaling approaches[156,157,158,159,160,161,162] have been proposed with different local approximations of the density matrix.

Within the framework of the conventional SCF molecular orbital theory, Stewart[163] wrote a semiempirical program which is capable of optimizing orbitals at a near-linear scaling. With his method, one starts with a set of localized molecular orbitals (LMO) chosen on the basis of Lewis structure. Since minimal basis sets are used in semiempirical methods, the occupied and virtual LMOs can be identified. The

optimization is then done by annihilating the interactions between the occupied LMOs and their neighbouring virtual LMOs. This method, in principle, scales linearly for the optimization part because the number of neighbouring LMOs depends only on the local environment.

We propose a general approach based on the localization of molecular orbitals, which enables a formal linear scaling of the orbital optimization for large molecular systems.

With a single-determinant wave function, a set of spin orbitals is obtained by solving the following equation by the means of the variation principle:

$$\hat{F}|\psi_i\rangle = \sum_j \epsilon_{ij}|\psi_j\rangle \qquad (137)$$

where $\hat{F}$ is a one-electron operator derived from an energy expression. The ϵ_{ij} are the Lagrange undetermined multipliers introduced due to the orthogonality constraint between the orbitals with the same spin:

$$\langle\psi_i|\psi_j\rangle = 0 \qquad (138)$$

In the conventional SCF approach, a diagonal form of Equation (137) is assumed and the orbitals are expanded in the space of all the basis functions, resulting in $O(N^3)$ scaling for diagonalization where N is the size of the molecule. The orbitals obtained this way, called canonical orbitals, are not the only set of orbitals satisfying Equation (137). Since a Slater determinant is invariant under a unitary transformation,

methods[164,165,166] of transforming the canonical orbitals were proposed many years ago to obtain a set of localized orbitals to account for the observed localization of chemical bonds. Each LMO corresponds to a chemical bond.

The localization of the chemical bonds is a general phenomenon and LMOs can always be obtained through transformation. If the LMOs in a molecule are *optimized directly*, it is only necessary to expand each of the LMOs in a set of basis functions located close to it, i.e. the variational space for each LMO is localized. To a LMO ψ_i, the other orbitals can be divided into three groups: (i) ψ_j whose variational space is the same as ψ_i; (ii) neighbouring orbitals ψ_k whose variational spaces overlap with that of ψ_i; and (iii) ψ_l whose variational spaces have effective zero-overlap with that of ψ_i. The zero-overlap is equivalent to the orthogonality between ψ_l and ψ_i, i.e.

$$\langle \psi_l | \psi_i \rangle = 0 \tag{139}$$

The effective zero-overlap between basis functions in two local variational spaces separated by a large distance can be generally assumed because the overlap integral decays exponentially with respect to the inter-LMO distance.

Equation (137) can be written as:

$$\hat{F}|\psi_i\rangle = \sum_j \epsilon_{ij}|\psi_j\rangle + \sum_k \epsilon_{ik}|\psi_k\rangle + \sum_l \epsilon_{il}|\psi_l\rangle \tag{140}$$

Since the orthogonality between ψ_l and ψ_i always holds due to the effective zero-

overlap (Equation (139)), the third term in the above equation may be removed. The first term, which includes ψ_i, may be assumed to be diagonalized due to the invariance of the Slater determinant. Equation (140) then becomes:

$$\hat{F}|\psi_i\rangle - e_{ii}|\psi_i\rangle + \sum_k e_{ik}|\psi_k\rangle \qquad (141)$$

e_{ik} in the second term of the above equation cannot be assumed to be zero as in the conventional approach because ψ_i and ψ_k have different variational spaces. But it can be absorbed into a new operator, similar to the solution of the restricted open-shell Hartree-Fock (ROHF) equations[167]:

$$[\hat{F} - \sum_k (\hat{F}|\psi_k\rangle\langle\psi_k| + |\psi_k\rangle\langle\psi_k|\hat{F})]|\psi_i\rangle = e_{ii}|\psi_i\rangle \qquad (142)$$

The ψ_k remain unchanged while the ψ_i are optimized.

By expanding the above equation in a local variational space, the LMOs ψ_i are optimized following the conventional SCF procedure in each local variational space. When each of the LMOs does not change any more, the convergence is reached. With the assumptions that the size of a local variational space and that the number of neighbouring orbitals are independent of the size of the molecule, this iterative procedure scales linearly with respect to the size of the molecule. The method, which closely resembles the conventional Hartree-Fock method, is general and applicable to *ab initio*

Hartree-Fock, DFT and semiempirical methods. It can be integrated into the current quantum chemistry programs because Equation (141) is solvable using the conventional SCF procedure.

The localization of molecular orbitals can be generally assumed for most molecular systems. Although no spin-restriction is applied in the above formulation, spin-restriction for a closed-shell system can be achieved with a proper initial guess or when the interatomic distances are small. As a simple example, the dissociation of H_2 can be described qualitatively correctly by two spin orbitals, one localized on each H. The spin-restriction automatically results when two H atoms are close[22]. An extreme example of the *de*localized orbital would be a singly occupied conjugated π orbital ranging across the molecule.

Stewart's method[163] can be viewed as a special case of the above formulation. The use of the projection operator $\sum_k |\psi_k\rangle\langle\psi_k|$ in Equation (141) excludes neighbouring occupied LMOs from the actual variational space, which is equivalent to Stewart's approach when a minimal basis set is used. The implementation of the current approach should also be easier because the only requirement for the initial set of orbitals is that the occupied orbitals must be localized.

The similarity between the density-matrix divide-and-conquer approach[35] and the method presented here is that both of them apply the variation principle locally. The major difference is that the former yields an optimized first-order density matrix whereas the latter yields a set of optimized orbitals. The use of localized orbitals has the following advantages: (i) Localized correlation treatments such as the multiconfiguration

SCF method can be incorporated into the current approach in a straightforward way. (ii) The orbital-based concepts or models developed with small molecules could be directly extended to the interesting parts of large molecules. The drawback is that not all the orbitals can be localized, although most chemical systems do not possess this problem. The scheme presented here also allows one part of a molecule to be treated more accurately than other parts through use of a larger basis set or a localized correlation treatment. Finally, it should be noted that most of the multicentre integrals do not need to be calculated because the density-matrix elements between the basis functions belonging to zero-overlap variational spaces are zero. In fact, the number of these integrals scales formally as $O(N^2)$ instead of $O(N^4)$ as in the conventional approach.

Chapter 7.

Concluding Remarks and Future Outlook

Various aspects of the theoretical calculations of the hyperfine structure have been investigated in Chapter 4. The hyperfine structure of the $^{14}NH_2$ radical has been investigated by means of multireference single and double configuration interaction techniques and the results presented in Section 4.4. Particular attention has been paid to the dependence of the coupling constants on the reference space, the configuration selection energy threshold and the basis set. It has been found that convergence can be obtained only if more than 83 spin-adapted reference configurations are included with an energy threshold of at least 10^{-7} hartree. With up to 126 reference configurations, an energy threshold smaller than 10^{-8} hartree and an uncontracted (13s8p2d/8s2p) basis set, the MRCISD isotropic couplings (27.44 and -68.47 MHz for N and H, respectively) are in very good agreement with experimental data (27.9 MHz and -67.2 MHz, respectively).

The above level of theory is hardly applicable even to a slightly larger system. A smaller set of basis functions would be desirable to reduce the number of possible configurations so that the MRCISD approach can be used for larger systems. The applicability of basis set contractions has been explored using the same molecule as an example in Section 4.5. Three contraction schemes are examined: the segmented Hartree-Fock, the general Hartree-Fock and the atomic natural orbital. It has been found

that all three contraction schemes yield convergence to the uncontracted one with a basis set which is a little more than one half the size of the uncontracted basis set, or equivalent to a triple-zeta basis set, whereas the ANO approach provides the smoothest and fastest convergence. If a smaller basis set is desirable, the ANO approach is recommended because the other two approaches do not have a predictable trend at a high degree of contraction. It has also been found that selecting the most populated ANOs works for the correlation of core-electrons too, which is contrary to some earlier speculations.

Even with a basis set with a reduced size, the conventional correlation methods such as MRCISD cannot be carried far enough to treat most of the molecular systems of interest to chemists. An alternative correlation method is based on density functional theory. In Section 4.6 some of the exchange and correlation functionals and basis sets have been surveyed for calculations of the spin polarization of atoms and molecules. It has been shown that the atomic isotropic coupling constants are very dependent on the functional form, the auxiliary basis set and the orbital basis set. The calculations on the molecular systems NH_2 and NH_3^+ show less dependence for isotropic couplings and almost independence for anisotropic couplings. It is found that the combination of Perdew and Wang's non-local exchange functional and Perdew's correlation correction functional with a [7*s*6*p*2*d*]/(5,2;5,2) orbital/auxiliary basis set gives results in semiquantitative agreement with experiment and MRCISD calculations.

From the present studies and related reports in the literature, one can see that more effort must be made to search for the conditions under which a reliable prediction of the spin polarization can be made. Other studies[46] have shown that a large primitive set with

polarization functions of high angular momentum may be needed to obtain converged results. The future study of the basis set contraction should, therefore, include the contractions of polarization functions, along with larger sets of primitive Gaussians. It has also been found from the present studies that the reduction of effective configurations included in the variational step due to the basis set contraction is not as large as one might expect from the great deal of reduction for the total number of configurations generated at the same MRCISD level. This phenomenon has not been observed before and should be pursued further. The application of DFT to the calculation of the spin polarization is relatively new. More surveys on the effects of exchange and correlation functionals and basis sets are needed before a clear conclusion can be drawn about the applicability of the current DFT methods. The experience gained from the basis set studies with the conventional methods suggests that similar studies should also be tried with the DFT methods. In contrast to the conventional methods, there is no systematic way to obtain the correlation effects with more and more accuracy. Eventually it may be necessary to obtain functionals specifically adapted for the spin polarization studies.

In Chapter 5, a new isomer of the alkaline-earth hydroxides has been predicted. A great deal of attention has been paid to alkaline-earth hydroxides experimentally and theoretically. Previous studies have stressed the ionic bonding between the metal and the hydroxide group as a ligand. Through theoretical calculations, we have found that another structure, HMO, exists. It has two low-lying electronic states - $^2\Pi$ and $^2\Sigma^+$. The studies have been carried out at the ROHF, CISD and CASSCF levels with a basis set of at least triple-zeta plus double polarization quality. The correlation treatment of CASSCF includes the nine valence electrons and ten orbitals resulting in an active space

denoted by (622). The optimized structures of HMO (M = Be, Mg and Ca) are all linear and the energy of HMO lies from 159 kJ/mol for HBeO to 271 kJ/mol for HCaO above that of MOH. The M-O bond length in HMO is predicted to be longer than that in the corresponding MOH. The M-O stretching frequencies are very similar for the two structures. The H-M bond lengths and stretching frequencies in HMO are very similar to the same properties in the corresponding diatomic molecule (MH). Analysis of the electronic structures suggests that HBeO has two polarized covalent bonds formed from the *sp* hybrids of Be; HMgO has one covalent bond (between H and Mg) and one ionic bond and can be viewed as $(HMg)^{+}O^{-}$; HCaO has two ionic bonds represented by $H^{-}Ca^{2+}O^{-}$.

The future investigation of this system should include the isomerization from MOH to HMO. It would be interesting to know how the low-lying states of the two structures correlate with each other and to compare with the Group VI elements. The isomerization may happen in two ways - unimolecular and intermolecular. For a unimolecular isomerization, difficulty may arise because more than one state must be included in the reaction path search and care should be taken. It would also be interesting to make predictions about some other properties which are observable experimentally such as spin-orbit interactions.

A general self-consistent-field (SCF) approach, whose matrix diagonalization scales linearly with respect to the size of the molecule, is proposed in Chapter 6. In contrast to the density-matrix divide-and-conquer approach, localized molecular orbitals are optimized directly. The method closely resembles the conventional SCF method. The implementation and test of this method should be carried out in the near future.

References

1. P.A.M. Dirac, *The Principles of Quantum Mechanics*, Oxford University Press, London, 1930.

2. J.C. Slater, *Phys. Rev.* **34**, 1293 (1929); **35**, 509 (1930).

3. D.R. Hartree, *Proc. Cambridge Phil. Soc.*, **24**, 89, 111 (1928).

4. V. Fock, *Z. Physik*, **61**, 126 (1930).

5. J.C. Slater, *Phys. Rev.*, **35**, 210 (1930).

6. T.A. Koopmans, *Physica*, **1**, 104 (1933).

7. C. Møller and M.S. Plesset, *Phys. Rev.*, **46**, 618 (1934).

8. J.A. Pople and R.K. Nesbet, *J. Chem. Phys.* **22**, 571 (1954).

9. C.C.J. Roothaan, *Rev. Mod. Phys.* **32**, 179 (1960).

10. E.R. Davidson, *Chem. Phys. Lett.* **21**, 565 (1973).

11. R. Carbo and J.M. Riera, *A general SCF theory*, Springer-Verlag, Berlin, 1978.

12. C.F. Jackels and E.R. Davidson, *Int. J. Quant. Chem.*, **8**, 707 (1974).

13. C.C.J. Roothaan, *Rev. Mod. Phys.* **23**, 69 (1951).

14. S.F. Boys, *Proc. Roy. Soc (London)* **A 200**, 542 (1950).

15. T.H. Dunning, *J. Chem. Phys.* **53**, 2823 (1970).

16. I. Mayer, *Chem. Phys. Lett.* **97**, 270 (1983).

17. R.K. Nesbet, *J. Chem. Phys.* **43**, 311 (1965).

18. E.R. Davidson, *J. Comput. Phys.* **17**, 87 (1975).

19. B.O. Roos, *Chem. Phys. Lett.* **15**, 153 (1972).

20. B.O. Roos and P.E.M. Siegbahn, in Modern Theoretical Chemistry, Vol III, pp 277, edited by H.F. Schaefer III, Plenum Press, New York, 1977.

21. I. Shavitt, *Int. J. Quantum Chem. Symp.* **11**, 131 (1977).

22. A. Szabo and N.S. Ostlund, *Modern Quantum Chemistry*, MacMillan, New York, 1982.

23. H. Shull and P.O. Löwdin, *J. Chem. Phys.* **23**, 1565 (1955).

24. C.F. Bender and E.R. Davidson, *J. Phys. Chem.* **70**, 2675 (1966).

25. (a) W. Meyer, *Int. J. Quantum Chem. Symp.* **5**, 341 (1971); (b) W. Meyer, *J. Chem. Phys.* **58**, 1017 (1973); (c) R. Ahlrichs, H. Lischka, V. Staemmler and W. Kutzelnigg, *J. Chem. Phys.* **62**, 1225 (1975).

26. F.W. Bobrowicz and W.A. Goddard III, in *Methods of Electronic Structure Theory*, Vol. 3, edited by H.F. Schaefer III, Plenum Press, New York, 1977, pp 79.

27. G. Das and A.C. Wahl, *J. Chem. Phys.* **44**, 87 (1966).

28. A.C. Wahl and G. Das, In *Methods of Electronic Structure Theory*, Vol. 3, edited by H.F. Schaefer III, Plenum Press, New York, 1977, pp 51.

29. B.O. Roos, P.R. Taylor and P.E.M. Siegbahn, *Chem. Phys.* **48**, 157 (1980).

30. K. Ruedenberg, M.W. Schmidt, M.M. Gilbert and S.T. Elbert, *Chem. Phys.* **71**, 41 (1982).

31. P. Hohenberg and W. Kohn, *Phys. Rev.* **B 136**, 864 (1964).

32. L.H. Thomas, *Proc. Camb. Phil. Soc.* **23**, 542 (1927).

33. E. Fermi, *Z. Phys.* **48**, 73 (1928).

34. P.A.M. Dirac, *Proc. Camb. Phil. Soc.* **26**, 376 (1930).

35. W. Yang and S.-T. Lee, *J. Chem. Phys.* **103**, 5674 (1995).

36. W. Kohn and L.J. Sham, *Phys. Rev.* **A 140**, 1133 (1965).

37. J.C. Slater, *Phys. Rev.* **81**, 385 (1951).

38. W. Weltner, Jr., *Magnetic Atoms and Molecules*, Scientific and Academic Editions, New York, 1983.

39. C.H. Townes and A.L. Schawlow, "*Microwave Spectroscopy*", McGraw-Hill, New York, 1955.

40. S. Larsson and V.H. Smith, Jr., *Phys. Rev.* **178**, 137 (1969).

41. D.M. Chipman, *Theor. Chim. Acta* **82**, 93 (1992).

42. D.M. Chipman, I. Carmichael and D. Feller, *J. Phys. Chem.* **95**, 4702 (1991).

43. D.M. Chipman, *J. Chem. Phys.* **94**, 6632 (1991).

44. D. Feller and E.R. Davidson, *J. Chem. Phys.* **74**, 3977 (1981).

45. E.R. Davidson and C.F. Bender, *Chem. Phys. Lett.* **59**, 369 (1978); D. Rawlings and E.R. Davidson, *Chem. Phys. Lett.* **98**, 424 (1983).

46. D. Feller and E.R. Davidson, *J. Chem. Phys.* **88**, 7580 (1988).

47. D. Feller and E.R. Davidson, *J. Chem. Phys.* **80**, 1006 (1984).

48. MELDF-X, L. McMurchie, S. Elbert, S. Langhoff, and E.R. Davidson, The University of Washington, Indiana University, and the Molecular Science Research Centre (1993).

49. D. Feller and E.R. Davidson, *Theor. Chim. Acta* **68**, 57 (1985).

50. D. Feller and E.R. Davidson, in "Theoretical Models of Chemical Bonding, Part 3", Z.B. Maksic Ed., Springer-Verlag, Berlin, Heidelberg, 1991.

51. D. Feller, E.D. Clendening, E.A. Mcullough, Jr. and R.J. Miller, *J. Chem. Phys.* **99**, 2829 (1993).

52. B. Engels and S.D. Peyerimhoff and E.R. Davidson, *Mol. Phys.* **62**, 109 (1987).

53. B. Engels and S.D. Peyerimhoff, *Mol. Phys.* **67**, 583 (1989).

54. C.W. Bauschlicher, Jr. and P.R. Taylor, *J. Chem. Phys.* **85**, 2779 (1986).

55. D. Feller and E.R. Davidson, *J. Chem. Phys.* **90**, 1024 (1989)

56. R.C. Raffenetti, *J. Chem. Phys.* **58**, 4452 (1973).

57. R.D. Bardo and K. Ruedenberg, *J. Chem. Phys.* **60**, 918 (1974).

58. J. Almlöf and P.R. Taylor, *J. Chem. Phys.* **86**, 4070 (1987).

59. J. Almlöf and P.R. Taylor, *Adv. Quant. Chem.* **22**, 301 (1991) and references therein for other variations of ANO approaches and applications.

60. T.H. Dunning, Jr., *J. Chem. Phys.* **90**, 1007 (1989).

61. S.M. Poling, E.R. Davidson and G. Vincow, *J. Chem. Phys.* **54**, 3005 (1971).

62. D.M. Chipman, *Theor. Chim. Acta* **76**, 73 (1989).

63. D.M. Chipman, *J. Chem. Phys.* **91**, 5455 (1989).

64. S. Huzinaga, *J. Chem. Phys.* **42**, 1293 (1965).

65. C.W. Bauschlicher, S.R. Langhoff, H. Partridge, and D.P. Chong, *J. Chem. Phys.* **89**, 2985 (1988).

66. B. Engels and S.D. Peyerimhoff, *Mol. Phys.* **67**, 583 (1989).

67. B. Fernández, P. Jørgensen, and J. Simons, *J. Chem. Phys.* **98**, 3060 (1993).

68. J. Kong and R.J. Boyd, *J. Chem. Phys.* **102**, 3674 (1995).

69. S.A Perera, J.D. Watts and R.J. Bartlett, J. Chem. Phys. 100, 1425 (1994)

70. P. Kristiansen and L. Veseth, J. Chem. Phys. 84, 6336 (1986).

71. K. Ohta, H. Nakatsuji, K. Hirao and T. Yonezawa, *J. Chem. Phys.*, **73**, 1770 (1980).

72. H. Sekino and R.J. Bartlett, J. Chem. Phys. 82, 4225 (1985).

73. K. Funken, B. Engels, S.D. Peyerimhoff and F. Grein, Chem. Phys. Lett. 172, 180 (1990).

74. G.W. Hills and J.M. Cook, *J. Mol. Spectrosc.*, **94**, 456 (1982).

75. B. Engels, M. Peric, W. Reuter, S.D. Peyerimhoff, and F. Grein, *J. Chem. Phys.*, **96**, 4526 (1992).

76. H. Nakatsuji and M. Izawa, J. Chem. Phys., 97, 435 (1992).

77. R.J. Cave, S.S. Xantheas, and D. Feller, *Theor. Chim. Acta* **83**, 31 (1992).

78. D. Feller, *J. Chem. Phys.* **98**, 7059 (1993).

79. (i) K. Dressler and D.A. Ramsay, *Phil. Trans. R. Soc. London*, A **251**, 553 (1959); (ii) R.D. Brown, F.R. Burden, P.D. Godfrey, and J.R. Gillard, *J. Mol. Spectrosc.*, **25**, 301 (1974); (iii) R.N. Dixon, G. Duxbury, and D.A. Ramsay, *Proc. R. Soc. London*, A **296**, 137 (1967).

80. B. Fernandez, P. Jorgensen and J. Simons, *J. Chem. Phys.*, **98**, 7012 (1993).

81. R.A. Kendall, T.H. Dunning, Jr., and R.J. Harrison, *J. Chem. Phys.*, **96**, 6796 (1992).

82. F.B. van Duijneveldt, *IBM, Res. J.*, 945 (#16437) (1971).

83. E.R. Davidson, in *Reviews in Computational Chemistry*, Ed. K.B Lipkowitz and D.B. Boyd, VCH, New York, 1990, pp 373.

84. D.M. Chipman, *Phys. Rev.* **A 39**, 475 (1989).

85. J. Almlöf, T. Helgaker, and P.R. Taylor, *J. Chem. Phys.* **92**, 3029 (1988).

86. J. Kong, LA. Eriksson and R.J. Boyd, *Chem. Phys. Lett.* **217**, 24 (1994).

87. (i) L.A. Eriksson, V.G. Malkin, O.L. Malkina and D.R. Salahub, *J. Chem. Phys.* **99**, 9756 (1993); (ii) L.A. Eriksson, O.L. Malkina, V.G. Malkin and D.R. Salahub, *J. Chem. Phys.* **100**, 5066 (1994); (iii) L.A. Eriksson, J. Wang and R.J. Boyd, *Chem. Phys. Lett.* **211**, 88 (1993); (iv) L.A. Eriksson, J. Wang, R.J. Boyd and S. Lunell, *J. Phys. Chem.* **98**, 792 (1994); (v) M.A. Austen, L.A. Eriksson and R.J. Boyd, *Can. J. Chem.* **72**, 695 (1994).

88. (i) A. St-Amant and D.R. Salahub, *Chem. Phys. Lett.* **169**, 387 (1990); (ii) A. St-Amant, Ph.D. Thesis, Université de Montréal, 1991; (iii) D.R. Salahub, R. Fournier, P. Mlynarski, I.Papai, A. St-Amant and J. Ushio, in *Density Functional Methods in Chemistry*, J.K. Labanowski and J.W. Andzelm, Eds., Springer-Verlag, New York 1991.

89. S.H. Vosko, L. Wilk and M. Nusair, *Can. J. Phys.* **58**, 1200 (1980).

90. A.D. Becke, *Phys. Rev.* **A 38**, 3098 (1988).

91. (i) J.P. Perdew, *Phys Rev.* **B 33** 8822 (1986); (ii) *idem ibid*, **B 34**, 7406 (1986).

92. J.P. Perdew and Y. Wang, *Phys Rev.* **B 33**, 8800 (1986).

93. (i) S. Huzinaga, *J. Chem. Phys.* **42**, 1293 (1965); (ii) S. Huzinaga and Y. Sakai, *J. Chem. Phys.* **50**, 1371 (1969).

94. W. Kutzelnigg, U. Fleischer and M. Schindler, in *NMR - Basic Principles and Progress*, Vol. 23, Springer-Verlag, Heidelberg, 1990, pp 165.

95. F. Sim, D.R. Salahub, S. Chin and M. Dupuis, *J. Chem. Phys.* **95**, 4317 (1991).

96. J.S.M. Harvey, L. Evans, and H. Lew, *Can. J. Phys.* **50**, 1719 (1972).

97. (i) W.W. Holloway, Jr. and R. Novick, *Phys. Rev. Lett.*, **1**, 367 (1958); (ii) W.W. Holloway, Jr., F. Luscher and R. Novick, *Phys. Rev.* **126**, 2109 (1962).

98. (i) J.S.M. Harvey, *Proc. R. Soc. London* **A 285**, 581 (1961); (ii) J.M. Hirsch, G.H. Zimmerman, D.H.Larson, and N.F.Ramsey, *Phys. Rev.* **A 16**, 484 (1977).

99. P.S. Bagus, B. Liu, and H.F. Schaefer III, *Phys. Rev.* **A 2**, 555 (1970).

100. (i) V. Tschinke and T. Ziegler, *Can. J. Chem.* **67**, 480 (1988); (ii) L. Fan and T. Ziegler, *J. Chem. Phys.* **94**, 6057 (1991).

101. A.J. McKinley and J. Michl, *J. Phys. Chem.*, **95**, 2674 (1991).

102. J.M.Cook and G.W.Hills, *J. Chem. Phys.* **78**, 2144 (1983).

103. L. Bonazzola, N. Leray, J. Roncin, and Y. Ellinger, *J. Phys. Chem.*, **90**, 5573 (1986)

104. Uncontracted (18*s*,13*p*,2*d*/10*s*,7*p*) MRCISD calculations with 50 reference determinants, author's unpublished results.

105. J.E. Wertz and James R. Bolton, *Electron Spin Resonance - Elementary Theory and Practical Applications*, Chapman and Hall, New York, 1986.

106. J.P. Michaut, and J. Roncin, *Nouv. J. Chim.*, **2**, 129 (1977).

107. T. Tsuji, *Astron. Astrophys.* **23**, 411 (1973).

108. R.C. Hilborn, Zhu Qingshi and D.O. Harris, *J. Mol. Spectrosc.* **97**, 73 (1983).

109. J. Nakagawa, R.F. Wormsbecher and D.O. Harris, *J. Mol. Spectrosc.* **97**, 37 (1983).

110. W.T.M.L. Fernando, M. Douay and P.F. Bernath, *J. Mol. Spectrosc.* **144**, 344 (1990).

111. W.L. Barclay, Jr., M.A. Anderson and L.M. Ziurys, *Chem. Phys. Lett.* **196**, 225 (1992).

112. J.A. Coxon, M. Li, and P.I. Presunka, *Mol. Phys.* **76**, 1463 (1992).

113. L.M.Ziurys, W.L. Barclay, Jr. and M.A. Anderson, *Astrophys. J.* **384**, L63 (1992).

114. T.C.Steimle, D.A. Fletcher, K.Y. Jung, and C.T. Scurlock, *J. Chem. Phys.* **96**, 2556 (1992).

115. C.N. Jarman and P.F. Bernath, *J. Chem. Phys.* **97**,1711 (1992).

116. M. Li and J.A. Coxon, *J. Chem. Phys.* **97**, 8961 (1992).

117. P.I. Presunka and J.A. Coxon, *Can. J. Chem.* **71**, 1689 (1993).

118. C.T. Scurlock, D.A. Fletcher, and T.C. Steimle, *J. Mol. Spectrosc.* **159**, 350 (1993).

119. P.I. Presunka and J.A. Coxon, *J. Chem. Phys.* **101**, 201 (1994).

120. M. Li and J.A. Coxon, *J. Chem. Phys.* **102**, 2663 (1995).

121. C.W. Bauschlicher, Jr. and H. Partridge, *Chem. Phys. Lett.* **106**, 65 (1984) .

122. M.W. Chase, J.L. Curnutt, R.A. McDonald and A.N. Syverud, *JANAF tables, J. Phys. Chem. Ref. Data* **7**, 793 (1978).

123. C.W. Bauschlicher, Jr., S.R. Langhoff and H. Partridge, *J. Chem. Phys.* **84**, 901 (1986).

124. C.W. Bauschlicher,Jr., S.R. Langhoff, T.C. Steimle and J.E. Shirley, *J. Chem. Phys.* **93**, 4179 (1990).

125. W.E. Palke and B. Kirtman, *Chem. Phys. Lett.* **117**, 424 (1985).

126. J.V. Ortiz, *J. Chem. Phys.* **92**, 6728 (1990).

127. E.S. Rittner, *J. Chem. Phys.* **19**, 1030 (1951).

128. T. Törring, W.E. Ernst and S. Kindt, *J. Chem. Phys.* **81**, 4614 (1984).

129. T. Törring, W.E. Ernst and J. Kändler, *J. Chem. Phys.* **90**, 4927 (1989).

130. J.M. Mestdagh and J.P. Visticot, *Chem. Phys.* **155**, 79 (1991).

131. J. Kong and R.J. Boyd, *J. Chem. Phys.* **103**, 10070 (1995).

132. A.J.H. Wachters, *J. Chem. Phys.* **52**, 1033 (1970).

133. S.R. Langhoff and C.W. Bauschlicher, Jr., *J. Chem. Phys.* **84**, 1687 (1986).

134. T.H. Dunning, *J.Chem.Phys.* **55**, 716 (1971).

135. M.J. Frisch, G.W. Trucks, H.B. Schlegel, P.M.W. Gill, B.G. Johnson, M.W. Wong, J.B. Foresman, M.A. Robb, M. Head−Gordon, E.S. Repogle, R. Gomperts, J.L. Andres, K. Raghavachari, J.S. Binkley, C. Gonzalez, R.L. Martin, D.J. Fox, D.J. DeFrees, J. Baker, J.J.P. Stewart and J.A. Pople, *Gaussian 92/DFT*, Gaussian Inc. Pittsburgh PA, 1993.

136. K.P. Huber and G. Herzberg, *Molecular Spectra and Molecular Structure*, Vol. IV, Van Nostrand Reinhold Co , New York, 1979.

137. N.H. Rosenbaum, J.C. Owrutsky, L.M. Tack and R.J. Saykally, *J. Chem. Phys.* **84**, 5308 (1986).

138. C.W. Bauschlicher and S.R. Langhoff, *Chem. Rev.* **91**, 701(1991).

139. M. Kolbuszewski and J.S. Wright, *Chem. Phys. Lett.* **98**, 338 (1994).

140. P.J. Bruna, B. Meng and J.S. Wright, *J. Mol. Spectrosc.* **159**, 79 (1993).

141. B. Meng, P.J. Bruna and J.S. Wright, *Mol. Phys.* **79**, 1305 (1993).

142. M. Kolbuszewski and J.S. Wright, *Can. J. Chem.* **71**, 1562 (1993).

143. M.W. Schmidt, K.K. Baldridge, J.A. Boatz, S.T. Elbert, M.S. Gordon, J.J. Jensen, S. Koseki, N. Matsunaga, K.A. Nguyen, S. Su, T.L. Windus, M. Dupuis, J.A. Montgomery, *J. Comput. Chem.* **14**, 1347 (1993).

145. C.W. Bauschlicher, P.S. Bagus, and B.N. Cox, *J. Chem. Phys.* **77**, 4032 (1982).

146. A.D. McLean and G.S. Chandler, *J. Chem. Phys.* **72**, 5639 (1980).

147. S. Huzinaga, Approximate Atomic Functions II, Department of Chemistry Report, University of Alberta, Edmonton, Alberta, Canada (1971).

148. S.R. Langhoff and C.W. Bauschlicher, Jr., *J. Chem. Phys.* **84**, 1687 (1986).

149. J.P. Maillard, J. Chauville, and A.W. Mantz, *J. Mol. Spectrosc.* **63**, 120 (1976).

150. N.H. Rosenbaum, J.C. Owrutsky, L.M. Tack and R.J. Saykally, *J. Chem. Phys.* **84**, 5308 (1986).

151. H.-J. Werner, P. Rosmus, and E.-A. Reinsch, *J. Chem. Phys.* **79**, 905 (1983).

152. Y. Yamaguchi, B.J. DeLeeuw, G. Vacek, C.A. Richards and H.F. Schaefer III, *J. Chem. Phys.* **101**, 3006 (1994).

153. G. Vacek, B.J. DeLeeuw, and H.F. Schaefer III, *J. Chem. Phys.* **98**, 8704 (1993).

154. C.A. White, B.G. Johnson, P.M.W. Gill and M. Head-Gordon, *Chem. Phys. Lett.* **230**, 8 (1994).

155. W. Yang, *Phys. Rev. A* **44**, 7823 (1991).

156. W. Kohn, *Chem. Phys. Lett.* **208**, 167 (1993).

157. X.-P. Li, R.W. Nunes, and D. Vanderbilt, *Phys. Rev. B* **47**, 10891 (1993).

158. P. Ordejón, D.A. Drabold, M.P. Grumbach and R.M. Martin, *Phys. Rev. B* **48**, 14646 (1993).

159. E.B. Stechel, A.R. Williams and P.J. Feibelman, *Phys. Rev. B* **49**, 10088 (1994).

160. F. Mauri and G. Galli, *Phys. Rev. B* **50**, 4316 (1994).

161. P.D. Walker and P.G. Mezey, *J. Am. Chem. Soc.* **115**, 12423 (1993).

162. D.C. Allan and M.P. Teter, *J. Am. Ceram. Soc.* **73**, 3247 (1990).

163. J.J.P. Stewart, *Int. J. Quantum. Chem.* **58**, 133 (1996).

164. J.E. Lennard-Jones and J.A. Pople, *Proc. Roy. Soc. (London)* **A 202**, 166 (1950).

165. S.F. Boys, *Rev. Mod. Phys.* **32**, 296 (1960).

166. C. Edmiston and K. Ruedenberg, *Rev. Mod. Phys.* **35**, 457 (1963).

167. C.C.J. Roothaan, *Rev. Mod. Phys.* **32**, 179 (1960).